

**EFFICIENT AND SELECTIVE GENE TRANSFER DIRECTED TO MUSCLE BY  
TROPISM-MODIFIED ADENO-ASSOCIATED VIRUS VECTOR**

by

Chi-Yi Yu

BS, Kaohsiung Medical University, Taiwan R.O.C., 1997

MS, National Yang-Ming University, Taiwan R.O.C., 1999

Submitted to the Graduate Faculty of  
Graduate School of Public Health in partial fulfillment  
of the requirements for the degree of  
Doctor of Philosophy

University of Pittsburgh

2007

UNIVERSITY OF PITTSBURGH  
GRADUATE SCHOOL OF PUBLIC HEALTH

This dissertation was presented

by

**Chi-Yi Yu**

It was defended on

**January 25, 2007**

and approved by

Dissertation Advisor:

**Xiao Xiao, PhD**

Associate Professor

Department of Orthopaedic Surgery

School of Medicine

University of Pittsburgh

Committee Chair and Dissertation Co-Advisor:

**Phalguni Gupta, PhD**

Professor

Department of Infectious Diseases and Microbiology

Graduate School of Public Health

University of Pittsburgh

Committee Member:

**Paula R. Clemens, MD**

Associate Professor

Department of Neurology

School of Medicine

University of Pittsburgh

Committee Member:

**Frank J. Jenkins, PhD**

Associate Professor

Department of Pathology

School of Medicine

University of Pittsburgh

Committee Member:

**Simon M. Barratt-Boyes, PhD**

Associate Professor

Department of Infectious Diseases and Microbiology

Graduate School of Public Health

University of Pittsburgh

Copyright © by Chi-Yi Yu

2007

**EFFICIENT AND SELECTIVE GENE TRANSFER DIRECTED TO MUSCLE BY  
TROPISM-MODIFIED ADENO-ASSOCIATED VIRUS VECTOR**

Chi-Yi Yu, PhD

University of Pittsburgh, 2007

Gene therapy offers a promise for treating inherited muscle disorders. The advantages of recombinant adeno-associated virus (rAAV) gene delivery vector include nonpathogenicity and long-term gene expression after a single administered dose. However, rAAV predominantly transduces the liver after systemic administration, reducing its efficiency for gene transfer to the heart and skeletal muscle. The question of how to deliver the therapeutic genes into most of the diseased myofibers becomes a challenge. The goal of this project is to develop an efficient and muscle-specific AAV vector for systemic delivery. Here, the muscle-targeting peptide ASSLNIA was incorporated into AAV2 capsid after residue 587 without heparin-binding motif (587 TG MTP vector) or with heparin-binding motif (588 HB MTP vector) since heparan sulfate is the primary cellular receptor of AAV2. The efficiencies and selectivities of muscle targeting of modified rAAVs were evaluated *in vitro* and *in vivo*.

This study demonstrated that the peptide-modified vectors maintained their myotube transduction ability. Peptide-engineered AAVs decreased their transductions in non-muscle cell lines. In addition, the 587 TG MTP vector did not require the heparin-dependent mechanism for muscular targeting. The C2C12 myotube transductions of 587 TG MTP and 588 HB MTP vectors were inhibited 47%~58% in the presence of free ASSLNIA peptide while unmodified rAAV2 transduction was only suppressed by 25%. To explore the muscle-

targeting abilities of modified rAAVs *in vivo*, mice were injected intravenously via a tail vein with a viral dose containing  $9 \times 10^{11}$  genomic particles. After four weeks, mouse organs were harvested for the luciferase assay. The 587 TG MTP vector demonstrated enhanced muscle and heart transduction compared to unmodified rAAV2. Importantly, the 587 TG MTP virus significantly reduced its transduction of liver, lungs, and spleen. The vector biodistribution in organs was also determined by real-time PCR and peptide-modified vectors showed similar targeting effects. Moreover, this study found that both 587 TG MTP and 588 HB MTP vectors were resistant to antibody neutralization.

These results indicate that this muscle-targeting peptide facilitates the generation of an efficient and muscle-specific AAV vector for systemic gene delivery in the treatment of muscle diseases to provide clinical and public health benefits.

## TABLE OF CONTENTS

<b>ACKNOWLEDGMENT .....</b>	<b>XIII</b>
<b>1. INTRODUCTION.....</b>	<b>1</b>
<b>1.1 Muscular dystrophy.....</b>	<b>1</b>
<b>1.1.1 Clinical definition and classification .....</b>	<b>1</b>
<b>1.1.2 Epidemiology .....</b>	<b>2</b>
<b>1.1.3 Pathogenesis.....</b>	<b>2</b>
<b>1.1.4 Therapeutic approaches .....</b>	<b>12</b>
<b>1.1.4.1 Pharmacological therapy.....</b>	<b>13</b>
<b>1.1.4.2 Cell-based therapy .....</b>	<b>15</b>
<b>1.1.4.3 Gene therapy .....</b>	<b>17</b>
<b>1.2 Adeno-associated virus.....</b>	<b>20</b>
<b>1.2.1 Discovery.....</b>	<b>20</b>
<b>1.2.2 AAV genome.....</b>	<b>21</b>
<b>1.2.3 AAV life cycle .....</b>	<b>24</b>
<b>1.2.4 AAV receptor .....</b>	<b>25</b>
<b>1.2.5 AAV intracellular trafficking .....</b>	<b>26</b>
<b>1.2.6 AAV capsid structure .....</b>	<b>29</b>
<b>1.2.7 rAAV production in gene therapy.....</b>	<b>30</b>

1.2.8	rAAV integration .....	34
1.2.9	Immune responses to rAAV .....	35
1.3	Engineering AAV tropisms.....	37
1.3.1	Ligand-directed targeting .....	39
1.3.2	Combinatorial AAV library.....	40
1.3.3	Chimeric AAV vectors.....	41
1.3.4	Mosaic AAV vectors .....	42
1.3.5	Two-component system. ....	44
1.4	Specific aims.....	45
2.	<b>MODIFICATIONS OF AAV2 CAPSID MEDIATE SELECTIVE VECTOR TARGETING TO MYOTUBES AND CONFER VIRAL RESISTANCE TO NEUTRALIZATION.....</b>	<b>47</b>
2.1	Introduction.....	47
2.2	Material and methods.....	49
2.2.1	Cell culture .....	49
2.2.2	Plasmid construction .....	50
2.2.3	Molecular modeling .....	51
2.2.4	rAAV vector production.....	51
2.2.5	<i>In vitro</i> transduction assay .....	53
2.2.6	<i>In vitro</i> neutralization assay .....	54
2.2.7	Luciferase assay .....	55
2.2.8	Statistical analysis .....	55
2.3	Results.....	56

2.3.1	Generation of AAV2 capsid mutants .....	56
2.3.2	Transduction efficiencies of modified vectors in cultured myotubes.....	66
2.3.3	Targeting selectivities of modified vectors.....	70
2.3.4	Neutralization profiles of peptide-modified rAAV vectors.....	78
2.4	Discussion .....	85
3.	<b>DEPENDENCE OF HSPG-BINDING OF MODIFIED AAV2 VECTORS IN MYOTUBE TARGETING .....</b>	<b>94</b>
3.1	Introduction.....	94
3.2	Material and methods.....	95
3.2.1	<i>In vitro</i> heparin competition assay.....	95
3.2.2	Heparin-binding assay.....	96
3.2.3	<i>In vitro</i> peptide blocking experiment.....	96
3.2.4	Statistical analysis.....	96
3.3	Results.....	97
3.3.1	HSPG-binding dependence for peptide-modified rAAV transduction..	97
3.3.2	Heparin-binding affinity of modified rAAV vectors .....	99
3.3.3	Influence of synthesized blocking peptide in rAAV transduction.....	102
3.4	Discussion .....	104
4.	<b>INCORPORATION OF MUSCLE-SPECIFIC LIGAND INTO CAPSID RETARGETS AAV2 TO STRIATED MUSCLE AFTER SYSTEMIC DELIVERY .....</b>	<b>109</b>
4.1	Introduction.....	109
4.2	Material and methods.....	110
4.2.1	<i>In vivo</i> characterization of vectors via intramuscular delivery .....	110



4.2.2	<i>In vivo</i> characterization of vectors via intravenous delivery .....	111
4.2.3	Vector biodistribution in systemic delivery .....	111
4.2.4	Statistical analysis .....	112
4.3	Results .....	112
4.3.1	<i>In vivo</i> transduction of skeletal muscle by local delivery of rAAVs .....	112
4.3.2	<i>In vivo</i> rAAV-mediated muscle transduction by systemic delivery .....	114
4.3.3	Biodistribution profile of peptide-modified rAAV in adult mice .....	118
4.4	Discussion .....	121
5.	OVERALL DISCUSSION .....	124
6.	FUTURE STUDIES .....	128
7.	PUBLIC HEALTH SIGNIFICANCE OF THIS STUDY .....	131
	BIBLIOGRAPHY .....	132

## LIST OF TABLES

Table 1 The primers for constructing the modified AAV2 capsids.....	50
Table 2 Neutralization of peptide-modified AAV vectors by guinea pig antiserum.....	79
Table 3 Neutralization of peptide-inserted mutants by human IVIG .....	83

## LIST OF FIGURES

Figure 1 rAAV genomic plasmids for vector production .....	52
Figure 2 Schematic representation of modified AAV2 capsid amino acid sequences .....	57
Figure 3 Topology of the AAV2 capsid with inserted muscle-specific peptide.....	58
Figure 4 Ribbon drawing of the wild-type AAV2 VP3 subunit .....	60
Figure 5 Ribbon representation of a 587 TG MTP VP3 monomer.....	61
Figure 6 Ribbon representation of a 588 HB MTP VP3 monomer .....	62
Figure 7 The electrostatic surface potential of VP3 monomers.....	63
Figure 8 Capsid protein analysis of modified rAAV2 vectors by Western blot.....	65
Figure 9 Efficiency of modified rAAV-mediated gene transfer to C2C12 myotubes .....	67
Figure 10 Examination of rAAV vectors in myotube transduction by fluorescent microscopy ..	69
Figure 11 Effect of capsid modification on rAAV-mediated gene transfer in C2C12 myoblasts.	71
Figure 12 Peptide-modified rAAV vectors in gene delivery of human liver-derived cell line ....	73
Figure 13 Infection of rAAV vectors in human cervix epithelioid carcinoma HeLa cells.....	75
Figure 14 Gene delivery mediated by rAAV vectors in human embryonic kidney 293 cells .....	76
Figure 15 Luciferase expression in human glioblastoma tumor U-87MG cells with rAAV transductions .....	77
Figure 16 Effect of guinea pig anti-AAV2 serum on peptide-modified rAAV infection of C2C12 myotubes.....	80

Figure 17 Neutralizing activity against peptide-modified rAAVs in guinea pig antiserum .....	81
Figure 18 Characterization of rAAV neutralizing profile to human IVIG in C2C12 myotubes ..	84
Figure 19 Quantification of HSPG-independence of peptide-modified mutants.....	98
Figure 20 Heparin-affinity column analysis coupling with DNA dot-blot assay .....	100
Figure 21 Western blot applied for the heparin-affinity column analysis .....	101
Figure 22 Competitive inhibition in myotube transduction of peptide-inserted rAAVs by the cognate peptide.....	103
Figure 23 Ribbon representations of VP3 subunits from unmodified, 587 TG MTP, and 588 HB MTP rAAVs .....	108
Figure 24 Intramuscular delivery of peptide-modified rAAV vectors in mice.....	113
Figure 25 Luciferase activities in muscles after systemic rAAV administration .....	115
Figure 26 Luciferase activities in mouse hearts after systemic delivery of peptide-modified vectors.....	116
Figure 27 Luciferase activities in non-muscle organs after systemic delivery of peptide-modified vectors.....	117
Figure 28 rAAV genome distribution after intravenous delivery.....	119
Figure 29 Quantify hepatic rAAV genomes after intravenous delivery.....	120

## **ACKNOWLEDGMENTS**

I would like to gratefully acknowledge my dissertation advisor, Dr. Xiao Xiao, for his guidance, encouragement, and patience throughout my PhD training. I would like to express my gratitude to my committee chair and dissertation co-advisor, Dr. Phalguni Gupta, for his enormous help and support during my graduate years. I would also like to thank my committee members, Drs. Paula R. Clemens, Frank J. Jenkins, and Simon M. Barratt-Boyes for their insightful advice in my research project and writing.

Finally, I would like to give thanks to my friends and family for their love and care over the years. I would like to extend a special appreciation to my dear parents, Lung-Fang Yu and Lai A-Chuan Yu, who have always stood by me in difficult times.

## **1. INTRODUCTION**

### **1.1 Muscular dystrophy**

#### **1.1.1 Clinical definition and classification**

Muscular dystrophies (MDs) are a heterogeneous group of hereditary disorders characterized by progressive muscle wasting and weakness. Typical features of dystrophic muscle include variation in myofiber size, infiltration of fat and connective tissue, areas of muscle necrosis, and centrally located nuclei. Dystrophic myofiber membranes are fragile, so extensive damage occurs and causes muscle necrosis and wasting. MD often affects multiple systems. Death is usually due to respiratory insufficiency or cardiac failure in patients with MD. Although MD presents a vast clinical variability regarding age of onset, pattern of skeletal muscle involvement, degree of severity, and rate of disease progression, the original classification of MD depends on the distribution of predominant muscle weakness and the mode of inheritance (1). According to the basis of classification, several major groups have been defined. Three identified principal types of MD are a) Duchenne and Becker muscular dystrophies (DMD and BMD), b) limb girdle muscular dystrophy (LGMD), and c) facioscapulohumeral muscular dystrophy (FSHD). Myotonic dystrophy (DM) is the most common adult MD. Emery-Dreifuss muscular dystrophy (EDMD) is delineated as a rare form of MD. Congenital muscular dystrophy (CMD), distal muscular dystrophy, and oculopharyngeal muscular dystrophy (OPMD) are relatively uncommon

groups. Clinical signs and symptoms are important for the physical examination, but immunohistochemistry and DNA based mutation analysis have made it feasible to establish precise diagnosis of the dystrophies.

### **1.1.2 Epidemiology**

Since DMD has been clearly characterized for many years, its distribution and incidence are well established. DMD patients are present all over the world. The prevalence of DMD has been repeatedly evaluated in many countries. The study shows that DMD affects 1 in every 3,500 live male births, regardless of race or nationality (2). Most DMD patients have a family history of MD, but *de novo* mutations of the dystrophin gene occur in one-third of cases (3).

In contrast to DMD, some types of dystrophy are especially frequent in certain populations. For example, the incidences of several autosomal recessive LGMDs in Brazil, North America, and the Middle East are frequent, but they are rare elsewhere. Fukuyama CMD is often found in Japan, while the autosomal dominant distal muscular dystrophy is most common in Scandinavia. OPMD usually exists in French Canadian families (4).

### **1.1.3 Pathogenesis**

The genetic basis of more than 30 different dystrophies has been explored. The defective gene in MD results in the dysfunction of muscle proteins, including cytoskeletal proteins, basement membrane proteins, transmembrane proteins, proteases, and nuclear envelop proteins. The molecular studies of these mutations lead to insights into the pathogenesis of MD. MDs often impair multiple system functions. In addition to the skeletal muscle weakness, cardiac complications are symptomatic of many MD disorders. The understanding of the pathogenesis

for cardiac involvement in different MDs allows us to develop more effective management and treatment for MD patients. Certain dystrophies possess successive cycles of degeneration and regeneration of muscle fibers. Muscle necrosis triggers local inflammation with subsequent infiltration of mononuclear cells into necrotic lesions. Inflammatory changes in the muscle may enhance muscle damage and accelerate the pathogenic progression.

DMD is the most severe and common form of dystrophy. It is a lethal X-linked recessive disorder and predominantly affects boys. DMD patients typically lack clinical symptoms at birth. Initial signs of muscle weakness in the DMD patient generally present at the age of 2~5 years. Twenty percent of affected boys have intellectual impairment. Progressive muscle wasting is persistent and mainly affects proximal muscle function with a decrease in lower limb strength (5). Because of continuous muscle wasting, most DMD boys lose their ambulation and become wheelchair-bound by age 12. Death usually occurs in the teens or early twenties from respiratory or cardiac failure (6).

In 1987, the gene responsible for DMD was cloned and the gene product was subsequently named dystrophin (7-9). The human dystrophin gene is identified on chromosome Xp21 (10, 11). The dystrophin gene is the largest gene in association with a disease and encodes a 427 kDa cytoskeletal protein. Dystrophin protein is predominantly expressed in smooth, cardiac, and skeletal muscle (12). It also can be detected in brain at a lower level (13). Dystrophin comprises four structural domains: a) the amino-terminal actin-binding domain, b) a central rod domain, c) a cysteine-rich domain, and d) a carboxy-terminal domain (14, 15). The dystrophin-glycoprotein complex (DGC) is a transmembrane protein complex and its primary function is to maintain muscle membrane integrity. In addition to dystrophin, the DGC contains the dystroglycan (DG) complex of  $\alpha$  and  $\beta$ -DG, the sarcoglycans ( $\alpha$ ,  $\beta$ ,  $\gamma$ , and  $\delta$ -SG), sarcospan, a pair of syntrophins,



and dystrobrevin. The amino acid terminus of dystrophin binds to actin filaments (F-actin) of the intracellular cytoskeleton (16, 17). The carboxy-terminal of dystrophin inside the muscle cell interacts with  $\beta$ -DG, a transmembrane protein that associates with  $\alpha$ -DG in the extracellular matrix (ECM). Extracellular  $\alpha$ -DG binds to laminin-2 of the basal lamina and thus links the internal cytoskeleton to the ECM (18). Mutations in genes encoding the DGC components lead to 12 distinct dystrophies; therefore, the DGC complex has its fundamental importance in the pathogenesis of MD.

55-65% of DMD cases are caused by deletions of one or more exons of dystrophin gene. No functional dystrophin protein is produced in DMD patient although a few “revertant” fibers expressing dystrophin are occasionally seen due to the possible frame-restoring exon-skipping (19). Absence of dystrophin expression hampers the DGC formation and further causes membrane destabilization during muscle contraction. The loss of membrane integrity induces the presence of necrotic myofibers, so necrosis elicits repeated cycles of degeneration and regeneration on muscle. Eventually the regenerative capacity of muscle satellite cells is no longer effective, and muscle mass is gradually replaced by fat and connective tissue. This myopathic process gives rise to the progressive muscle wasting and severe systemic muscle dysfunction in DMD.

BMD and DMD are termed dystrophinopathy because both diseases are caused by a variety of defects in the dystrophin gene (20). In BMD, the aberrant changes of dystrophin gene are “missense” mutations or deletions that preserve the reading frame and allow the synthesis of a truncated or semifunctional dystrophin molecule (21). The distributions of muscle weakness and wasting among BMD and DMD patients are similar; however, BMD patients have a milder disease course because they have partly functional dystrophin. The age of onset in BMD patients

is usually in the teenage years and some of them do not present the clinical symptoms until a much later age. Most of BMD patient are alive at the age of twenty and usually die in their forties or fifties. Some BMD patients still remain mobile until old age. DMD and BMD carriers are at risk of developing dilated cardiomyopathy (DCM). In BMD, the severity of cardiac diseases does not depend on the progression of skeletal muscle weakness. BMD patients can suffer from severe DCM with relatively well-preserved skeletal muscle function.

LGMDs are characterized by the predominant muscle weakness and wasting of the pelvic or shoulder girdle musculature with normal intelligence. These diseases have a great variability of age of onset. Milder forms have adult onset with slower progression. Conversely, severe forms exhibit childhood onset and an aggressive course. So far, at least 17 LGMDs have been defined and 13 genetic loci are identified for these disorders (22, 23). LGMDs can be divided into two groups. Less than 10% of patients have an inherited autosomal dominant trait (type 1) and are comparatively mild. The rest of LGMD cases display an inherited autosomal recessive trait (type 2) which affects both males and females. The type 2 LGMD diseases are often more severe.

Five different genes have been associated with autosomal dominant LGMDs. LGMD1A has the mutation in myotilin gene, a protein component of sarcomere (24). The sarcomere is the smallest functional unit of the striated muscle contraction apparatus and the actin/myosin movement takes place in the sarcomere. Mutations in sarcomeric protein components disrupt muscle contractile function, causing MD. Thus, they give rise to MD. LGMD1B is a rare autosomal dominant form of MD with cardiac involvement (25). The gene responsible for LGMD1B, an allelic disorder of EDMD, is lamin A/C. Lamin A/C is a nuclear envelope protein and the mutation of lamin A/C leads to an increase of nuclear fragility during mechanical stress.

The locus for LGMD1C is caveolin-3. Caveolin-3 is a muscle specific membrane protein (26). Caveolin-3 is expressed upon muscle differentiation and may be involved in the regulation of glycolysis in muscles through the binding to the muscle-specific isoform of phosphofructokinase (PFK-M) (27). The mechanism of caveolin-3 disruption resulting in MD remains speculative; however, it may be the failure of proper signal transduction events.

In autosomal recessive LGMDs, LGMD2A is the most prevalent form of LGMD and is the first case of progressive MD resulting from an enzymatic defect. LGMD2A patients have a mutation in the calpain-3 gene (28). Calpain-3 is an intracellular calcium-activated cysteine protease and it has the ability to regulate NF- $\kappa$ B activity via proteolysis. Patients exhibit a failure of nuclear localization of the cell survival mediator, NF- $\kappa$ B, and they have more apoptotic nuclei in their muscles. This suggests that the calpain-3 deficiency may block expression of cell survival genes in MD. LGMD2B arises from mutations in the dysferlin gene (29). Dysferlin is a plasma membrane protein involved in the membrane repair machinery of skeletal muscle. The role of dysferlin is to accumulate and to fuse vesicles near the site of membrane disruption to effect membrane repair. Loss of the membrane repair component further impairs the survival of muscle cells after extrinsic or intrinsic damages. LGMD 2C, 2D, 2E, and 2F associate with the mutations in genes encoding  $\gamma$ -,  $\alpha$ -,  $\beta$ -, and  $\delta$ -SG, respectively (30-33). The SGs are integral components of the DGC and seem to have a critical role in the stabilization of the DGC. A primary mutation in any one of the SGs may cause the destabilization of entire DGC complex and have substantial disruption of the plasma membrane. In striated muscle,  $\beta$ - and  $\delta$ -SG form a core and then  $\alpha$ - and  $\gamma$ -SG bind to this core before sarcoglycan complex maturation and targeting to the sarcolemma (34). LGMD2E and LGMD2F are severe clinical phenotypes of LGMD and they are associated with cardiomyopathy. Analysis of muscle from LGMD2G patients indicates

mutation of the telethonin gene (35). Telethonin is the sarcomeric protein that interacts with titin. Mutations of telethonin do not disrupt the sarcomeric architecture. This finding suggests that muscle degeneration in LGMD2G patients is more likely due to a functional defect than to disruption of sarcomeric structure. LGMD2H is caused by a “missense” mutation in the *TRIM32* gene. TRIM32 may be an E3-ubiquitin ligase that contributes to the ubiquitin-proteasome pathway (36). The TRIM32 deficiency could dysregulate protein degradation in the muscle. The fukutin-related protein (FKRP) mutation is identified in LGMD2I patients (37). FKRP localizes to the Golgi apparatus and it plays a role in modification of cell surface glycoproteins and glycolipids. LGMD2I patients show a variable reduction of  $\alpha$ -DG on sarcolemma. The unusual expression of  $\alpha$ -DG is a consequence of its abnormal glycosylation, which is the pathogenetic mechanism of LGMD2I. LGMD2I patients frequently develop DCM. Titin gene mutations cause LGMD2J, a severe form of LGMD. Titin is a central sarcomeric myofilament that is expressed in heart and skeletal muscle (38). Titin has an important role for the assembly of actin and myosin in the sarcomere. One of the principal effects of titin is to keep myosin centrally located in the sarcomere during cycles of contraction. Mutations in titin affect the development of balanced force in the sarcomere and may cause continuous mechanical muscle damage resulting in MD.

FSHD is inherited as an autosomal dominant trait. The deletion of a tandemly repeated 3.3 kb sequence on chromosome 4q35 is highly associated with FSHD dystrophy (39). However, a single gene defect causing FSHD has not been identified. FSHD patients initially have facial muscle weakness and develop lower limb weakness in the later disease course. The uncommon symptoms, such as retinal vascular diseases, hearing loss, and abnormalities in the central

nervous system (CNS), may occur. Many patients are mildly affected by FSHD, but some patients are more severe and may become wheelchair-confined.

DM most commonly occurs in adolescence or adult life and is usually caused by an unstable CTG trinucleotide repeat at chromosome 19q13.3. Two types of DM have been characterized. DM type 1 is caused by an expansion of this CTG repeat at the three prime untranslated region (3' UTR) of the myotonic dystrophy protein kinase (DMPK) gene. DM type 2 is involved in a CCTG expansion located in an intron of the zinc finger protein 9 (ZNF9) gene (23). Myotonia with muscle weakness and wasting occurs in DM patients.

At least three EDMD diseases have been reported and all of them are caused by mutations in genes coding for nuclear envelope proteins. A mutation in the emerin gene causes X-linked EDMD (40). The less common autosomal dominant and recessive forms of EDMD have mutations in the lamin A/C gene (41). Emerin interacts with lamin A and lamin C in the nucleus (42). It is predicted that mutations in emerin or lamin A/C locus perturb the integrity of the nuclear membrane and increase the cell susceptibility to apoptosis. Some reports also indicate that these mutations disturb the regulation of gene expression by abnormal control of nuclear mRNA release (43). EDMD predominantly presents with contractures of the spine, elbows, and Achilles tendons with mild muscle weakness in a humeroperoneal distribution. All individuals with EDMD, irrespective of the mode of inheritance, have the serious risk of cardiac conduction defects.

CMD is a relatively uncommon autosomal recessive group of myogenic disorders. The clinical features present at birth or in the first few months of life. CMD patients have hypotonia, generalized muscle weakness, contractures, and motor development delay. Some types of CMD may lead to mental retardation due to structural defects within brain. Based on the expression of

laminin  $\alpha 2$  (also known as merosin), CMD is divided into merosin-negative and merosin-positive groups. Compared to the merosin-positive group, the merosin-negative cases of CMD are more severe and they often develop serious respiratory problems. MDC1A (muscular dystrophy, congenital, type 1A) is associated with mutations in the *LAMA2* gene located on chromosome 6q2 and contributes to 40% of CMD cases (44). MDC1A individuals present a primary total or partial deficiency of laminin  $\alpha 2$  (45, 46). Laminin  $\alpha 2$  is the extracellular muscle protein that bridges the interaction between  $\alpha$ -DG and the basal lamina. In MDC1A patients, laminin  $\alpha 2$ -deficiency disrupts the basal lamina resulting in a loss of the stability of muscle cytoskeletal network. MDC1C and LGMD2I are allelic disorders, due to mutations in the FKRPF gene (47). Both types have a variable reduction of  $\alpha$ -DG, but not  $\beta$ -DG. The amount of  $\alpha$ -DG expression is associated with the clinical severity. Individuals with the severe disease course of MDC1C present a profound depletion of  $\alpha$ -DG resulting from abnormal glycosylation. As in LGMD2I, DCM is also common in MDC1C individuals. Muscle biopsies from MDC1C patients typically show a secondary deficiency of laminin  $\alpha 2$ , while a secondary reduction of calpain-3 and laminin  $\beta 1$  is observed in the muscle biopsy of LGMD2I. Defects in a number of glycosyltransferases are responsible for several CMDs, such as MDC1D, muscle-eye-brain disease (MEB), Walker Warburg syndrome (WWS), and Fukuyama congenital muscular dystrophy (FMDC). These types of CMD are characterized by severe muscle weakness and mental retardation. They cause aberrant hypoglycosylation of  $\alpha$ -DG leading to the dystrophic phenotype (48). The *LARGE* gene encoding a putative glycosyltransferase is associated with MDC1D (49). POMGnT1 is an *O*-linked mannose  $\beta 1, 2$  *N*-acetylglucosaminyltransferase and MEB patients have mutations in the *POMGnT1* gene (50). Mutations in POMT1, a mannosyltransferase, only account for 20% of WWS cases. The severe “nonsense” mutations in

the fukutin gene also display WWS (51, 52). In Japan, FMDC is the second most common form of MD and is caused by mutations in the fukutin gene. The enzymatic activity of fukutin protein probably controls the modification of cell surface glycoproteins. Fukutin protein is located in the Golgi body and secretory granules. Moreover, it is involved in neuronal migration (53, 54). The loss of fukutin protein in FMDC also elicits the secondary protein deficit of merosin and the DGC complex. Collagen VI is an extracellular matrix protein and its expression has been found in a wide variety of tissues (55). It consists of three polypeptide chains. These chains are  $\alpha 1$ ,  $\alpha 2$ , and  $\alpha 3$  encoded, respectively, by the *COL6A1* and *COL6A2* genes on chromosome 21q22.3 and the *COL6A3* gene on chromosome 2q37. Collagen VI plays a role in anchoring the muscle fiber basement membrane to the extracellular matrix (56-59). Additionally, collagen VI seems to transmit signals from the extracellular to the intracellular space through the binding to cellular transmembrane receptors, such as integrins (60). In this way, collagen VI induces cell proliferation and inhibits apoptosis (61, 62). Mutations in all three collagen VI genes lead to two types of CMD, the more severe Ullrich muscular dystrophy (UMDC) and the milder Bethlem myopathy (63, 64). The deficiency of collagen VI results in the unexpected apoptosis due to the presence of aberrant structure alterations in mitochondria and sarcoplasmic reticulum (SR) (65). RSMD1 (or rigid spine syndrome) is a selenoprotein N (SEPN1) deficient CMD due to mutations in the *SEPN1* gene (66). SEPN1 protein is a membrane-bound glycoprotein in the rough endoplasmic reticulum and the function of SEPN1 protein may regulate protein trafficking and processing (67). The expression level of SEPN1 protein is high in the diaphragm, which explains the severe restrictive respiratory syndrome in RSMD1 patients. Integrins are transmembrane glycoproteins expressed in skeletal muscle, especially at the sarcolemma, neuromuscular junction and myotendinous junction. They act as the cell surface receptors and

provide a link between the actin cytoskeleton and the extracellular matrix. In addition, integrins play an essential role in muscle differentiation during embryonic development. The major laminin receptor in skeletal, cardiac, and smooth muscle is integrin  $\alpha7\beta1$  (68-70). Mutations in the integrin  $\alpha7$  gene cause the destruction of the myotendinous junction and lead to a mild form of CMD in humans (71-73).

Distal muscular dystrophy is divided into autosomal recessive inheritance leading to early onset (less than 30 years of age) and autosomal dominant inheritance with late onset (over 40 years of age). The autosomal recessive form, Miyoshi myopathy (MM), and LGMD2B are allelic disorders. Both diseases have mutations in the gene encoding dysferlin, but they differ in the distribution of muscle weakness at onset (74-76). Tibial muscular dystrophy (TMD) is an autosomal dominant distal myopathy. TMD and LGMD2J have the same mutation in the titin gene. If the mutation in the titin gene appears in homozygous form, it can cause LGMD2J. Otherwise, a heterozygous mutation in the titin gene presents as TMD (77-79). The difference between LGMDs and distal muscular dystrophies is that distal myopathies primarily attack the distal musculature without conspicuous involvement of other muscle group while LGMDs display predominant muscle weakness and wasting of the pelvic or shoulder girdle musculature.

OPMD is characterized by extraocular muscle weakness, ptosis, dysphagia, and weakness in neck and proximal upper limb muscles (80). The first exon of the *PABP2* gene encoding the poly-(A)-binding protein normally contains a (GCG)<sub>6</sub> triplet repeat. However, there is an addition of two to seven (GCG) repeats in OPMD individuals. The triplet repeat expansion impedes normal transport of mRNA from the nucleus (81).

The discovery of the dystrophin gene and its role in causing DMD has facilitated the development of research on the elucidation of MD pathogenesis. Many types of MD are caused



by muscle membrane instability due to the loss of a network between the intracellular cytoskeleton and the extracellular matrix. Nevertheless, the pathogenesis of MD appears to be more complicated. Future studies should also focus on the signaling pathways controlling MD.

#### **1.1.4 Therapeutic approaches**

MD patients need effective therapy to improve their quality of life by ameliorating the dystrophic condition since these disorders can cause disability and death. Although the underlying molecular defects of MD have been known for many years, progress toward MD treatments is still far from the clinical stage. There are two major reasons for the difficulty in treating MD. One barrier is that skeletal muscle is the largest tissue of the body accounting for approximately 40% of body mass. The other fact is that muscle myofibers have no ability to divide. However, the studies accumulated in the last few years have opened new avenues for all developing treatments.

Any effective treatment of MD must allow the therapeutic agent to reach most of the diseased muscles in the body. The development of useful therapeutic strategies also requires a rational understanding of dystrophic pathology. So far, therapeutic approaches in MD treatment can be divided into two categories: approaches that attempt to improve the dystrophic condition through pharmacologic therapy, and approaches that aim to overcome the gene defect by cell-based therapy or gene therapy. Recent advances have uncovered various possible therapeutic strategies, from pharmacological interventions, cell-mediated therapy with newly isolated stem cells, to gene therapy. A combination of these approaches may successfully enhance their therapeutic effects.

#### **1.1.4.1 Pharmacological therapy**

Several pharmacological strategies have been designed to restore, maintain, or improve muscle function and strength. Slowing the rate of muscle loss and increasing muscle mass could potentially be achieved with use of protease inhibitors and growth factors. Myofiber degeneration is followed by a persistent inflammation that induces macrophages to secrete tumor necrosis factor-alpha (TNF- $\alpha$ ) and transforming growth factor beta (TGF- $\beta$ ), promoting muscle wasting and fibrosis in dystrophic muscle (82-87). Therefore, anti-inflammatory molecules have beneficial effects in delaying the pathogenic course of dystrophic muscle (88).

Glucocorticoids, such as prednisone and deflazacort, can delay the disease progression of DMD (89-91). Several studies show that glucocorticoid treatment in DMD boys can prolong independent ambulation for at least two years, slow the development of skeletal muscle defects, and delay the occurrence of respiratory and cardiac failure. These therapeutic benefits are due to their ability to preserve existing muscle fibers, to enhance myogenesis, and to suppress inflammatory responses. Unfortunately, these drugs have their side effects including decreased bone density and weight gain. In contrast to prednisone, deflazacort, the prednisone derivative, provides an effective alternative treatment with less severe side effects (92, 93). Besides the consideration of side effects, deflazacort has been shown to stimulate utrophin expression via the calcineurin/NFAT signaling pathway (94). The expression of utrophin can functionally compensate for dystrophin (95, 96).

The balance between muscle anabolic and catabolic processes is required for supporting normal muscle function. The fundamental principle has been recently applied to the new treatment of MD. It is suggested that stimulating anabolic processes can overcome, or slow muscle wasting in MD individuals since anabolic processes are able to proliferate and recruit the

muscle progenitor cells. This thought has been performed by the treatment of insulin growth factor 1 (IGF-1). IGF-1 acts as a potent anabolic agent in skeletal muscle and thus, it increases the synthesis of protein and nucleic acid as well as prohibits protein degradation. IGF-1 treatment improved the muscle maximum force in laminin-deficient *dy/dy* mice and attenuated pathologic changes of muscle dystrophy in *mdx* mice (97, 98). Unlike IGF-1, myostatin is a negative regulator of muscle growth. When *mdx* mice were given neutralizing antibodies to myostatin, muscle mass and strength were increased (99).

Recent evidence has shown that the majority of the muscle protein breakdown relies on the ATP-ubiquitin-dependent pathway (100). Compared to healthy individuals, DMD and other neuromuscular disorders abnormally increase proteasomes and ubiquitin in dystrophic muscle (100). In *mdx* mice, the proteasome inhibitor approach has revealed its ability to restore the membrane localization of dystrophin-associated proteins by blocking the ubiquitin pathway (101). Several cytokines have been associated with anabolic effects on skeletal muscle. Interleukin-15 (IL-15) is identified as a highly expressed growth factor in skeletal muscle. Notably, IL-15 appeared to ameliorate muscle wasting in tumor-bearing rats via the inhibition of the ATP-ubiquitin-dependent pathway (102). This finding could make IL-15 as a potent treatment for the muscle wasting involved in MD.

About 5%~15% of DMD cases are caused by premature stop codon in the dystrophin gene. Interestingly, the use of gentamicin suppressed the stop codon and led to the expression of functional dystrophin offering some level of strength against damage in *mdx* mice (103). However, the long-term effect of gentamicin treatment is still required to be determined. Finally, several new treatments have been carried out. Muscle protein synthesis directly associates with free amino acid glutamine concentration. DMD patients with administration of L-glutamine

appeared to reduce protein breakdown (104). Other approaches, such as calcium channel blockers, growth hormone inhibitors, and vitamin E, have been proved unsuccessful in MD treatment.

So far, the use of steroids and anabolic agents still remains the only available treatment in humans and provides the improvement of dystrophy.

#### **1.1.4.2 Cell-based therapy**

Cell-based therapies are carried out by implantation of functionally healthy myogenic cells into dystrophic muscle. A cell-mediated approach potentially provides two beneficial actions in dystrophy. The normal or genetically corrected donor myogenic cells not only fuse with dystrophic myofibers to allow the expression of a therapeutic protein deficient in the diseased myofibers (105, 106), but also give rise to a source of muscle precursor cells in myopathic muscle (107-109).

A pilot study converted *mdx* myofibers from dystrophin-negative to dystrophin-positive by the injection of wild-type myoblasts in 1989 (110). This study faced several challenges when this approach was applied to human studies. First, the injected donor cells had very limited migratory capacity. Second, the donor myoblasts exhibited poor survival. Third, immune responses against delivered myoblasts or newly synthesized therapeutic protein were induced by transplantation. *Ex vivo* mediated-transfer has been developed to improve the efficiency of myoblast transfer. In this strategy, myoblasts isolated from DMD boys were genetically modified by transduction of the dystrophin gene and then they were reintroduced into the patient (111). The *Ex vivo* based approach revealed some level of improvement in myoblast transfer, but its ability to circumvent the host immune response still needed to be optimized.

To resolve the lack of dispersion of donor cells in the host muscle, the use of blood-borne stem or progenitor cells might counteract this obstacle. Systemic delivery of circulating stem cells possessing myogenic potential is a feasible choice over myoblasts which remain in the area of injection. A successful report indicated that a fraction of bone marrow cells, referred to as side population (SP) cells, led to dystrophin expression in *mdx* mice after transplantation (112). In a related study, SP cells from a dystrophic mouse transduced with lentiviral vector expressing human micro-dystrophin were shown to express transgene in dystrophic myofibers following intravascular delivery (113). Recent findings have discovered that except SP cells, CD45 negative cells, such as multipotent adult progenitors (MAPs) (114), mesoangioblasts (115), muscle-derived stem cells (116), and synovial membrane-derived mesenchymal stem cells (SM-MSCs) (117), enable differentiation into skeletal myotubes in *vitro* and *in vivo*. In immunosuppressed *mdx* mice, human SM-MSCs not only restored the expression of dystrophin at the sarcolemma of muscle fibers, but also reduced central nucleation after local transplantation (118). The ability of human SM-MSCs to rescue systemic dystrophic myopathy via intravenous delivery has not been tested.

The extension of donor cell survival can be modulated by immunosuppressants. The use of tacrolimus (FK506) was efficient for the myoblast transplantation in monkeys, but it displayed long-term adverse effects (119). The development of immune tolerance is another potential application to reduce the immunogenicity of donor cells. Myoblasts expressing human lymphocyte antigen-G (HLA-G), a key mediator of maternal tolerance to the fetus, showed the resistance to cell lysis by alloreactive lymphocytes (120).

Currently, myoblast transplantation through intramuscular injection is the only cell-based therapy that has provided promising results at the site of injection in the non-human primate. The

next milestone should continue the attempt to achieve sufficient therapeutic effects systemically without immune complication.

### **1.1.4.3 Gene therapy**

MDs are mostly caused by single-gene blemishes. Gene therapy amends a genetic defect by the replacement or modification of a gene. When transgenic *mdx* mice expressing full-length dystrophin displayed no sign of the myopathy (121), gene therapy seems to be a promising approach to restore proper muscle function by reintroduction of a well acting gene into dystrophic muscle. Development of gene therapy for DMD provides a model for pursuing genetic therapies in other types of dystrophies.

The simplest approach of gene therapy is the injection of naked plasmid DNA encoding dystrophin into muscle. In 1990, Jon Wolff and his colleagues proved that mouse skeletal muscle could uptake and express plasmid DNA via intramuscular administration (122). Although the plasmid DNA delivery held the long-term gene expression, the gene delivery efficiency of naked plasmid was very low following intramuscular injection (123). A possible reason for the inefficiency of plasmid DNA delivery would be due to nuclease activity in the body. However, the methods including *in vivo* electroporation and hydrodynamic vascular delivery have improved the efficiency of plasmid-based gene delivery over the last several years (124-126).

The use of viral vectors for gene delivery is an alternative approach to gene therapy. GFP expression of up to 50% of the muscle fibers at the site of injection can be achieved through lentiviral vector delivery (127). Because lentiviral vectors raise concerns about insertional oncogenesis and enveloped vector particles have less stability, most current studies have occupied nonenveloped adenovirus (Ad) or AAV for delivery of therapeutic gene.

Early region 1 (E1)-deleted Ad vector was the first successful viral vector system to deliver a 6.3 kilobase pair (kbp) truncated dystrophin cDNA to skeletal muscle of *mdx* mice (128). However, this Ad vector caused a strong immune reaction to the expression of rest viral proteins (129). The Ad vector induced inflammatory process can exacerbate muscle weakness. In order to counteract problems of undesirable Ad vector immunogenicity, a newer generation of Ad vector, gutted (or helper-dependent) Ad vector, has been developed. Gutted vectors do not carry any viral coding sequence producing viral proteins and thus they can accommodate the full-length dystrophin cDNA. These helper-dependent Ad vectors expressing full-length dystrophin functionally corrected *mdx* muscle in adult mouse and induced a weaker immune response (130, 131).

Compared to Ad vectors, AAV vectors have less immunological and inflammatory response *in vivo* and they are more efficient for transducing adult muscle fibers due to their smaller size (132, 133). The AAV genome capacity is only about 4.7 kilobases (kbs), so they can not deliver full-length dystrophin. To date, a truncated mini- or micro-dystrophin gene can be packaged in AAV capsid and the expression of mini-dystrophin via AAV delivery retains good functional rescue in transgenic *mdx* mice (134).

Exon skipping has recently been used to direct a restoration of the translational reading frame of the dystrophin mRNA. A 2'-*O*-methyl antisense oligonucleotide has been engineered by removing mutated exon from the *mdx* dystrophin mRNA in cultured primary muscle cells (135). Besides, an extended study was achieved by targeting the donor and acceptor sites of mutated exon 23 with a modified antisense U7 small nuclear (sn) RNA (136). The removal of mutated exon 23 on the dystrophin mRNA of *mdx* mice produced functional dystrophin at the physiological level and led to the correction of MD.

Gene repair has been established by the utility of chimeric RNA/DNA oligonucleotides. These designed chimeric oligonucleotides are homologous to a targeted mutant gene and contain only one mismatched base. A binding between the chimeric oligonucleotide and the defective gene triggers the cell to repair the mutated gene based on the correct sequence of oligonucleotides. Rando *et al.* reported that RNA/DNA chimeric oligonucleotides mediate dystrophin expression at *mdx* muscles via the correction of a point mutation occurring in the dystrophin gene (137, 138).

Researchers have exploited a different method of gene therapy, the expression of “booster genes,” instead of replacement or modification of a defect gene. The delivery of booster genes tries to help muscle resist degeneration by alleviating the different damaging events. For example, expression of integrin  $\alpha 7$ , GalNac (*N*-acetyl galactosamine) transferase, or ADAM12 (a disintegrin and metalloprotease), enhanced cell adhesion and muscle stability while dystrophin was missing (139-141). Mini-agrin expression promoted basement membrane formation in the absence of laminin  $\alpha 2$  (142, 143). Overexpression of calpastatin reduced *mdx* muscle necrosis (144). Neuronal nitric oxide synthase (nNOS) expression showed anti-inflammation in *mdx* mice (145). Gene delivery of IGF-1, myostatin blockage, or ADAM12 accelerated muscle regeneration and decreased fibrosis (98, 99, 141). Gene transfer of an utrophin minigene prevented the dystrophic phenotype and restored DGC complex localization at the muscle membrane (146). Transgene-mediated utrophin upregulation is also an exciting avenue for MD gene therapy.

Investigators have explored a way to achieve functional restoration of dystrophic muscle and prevention of MD in human for years. Beyond doubt, the best approach is to deliver the therapeutic gene through the circulation. Like cell-based therapy, gene therapy faces a



formidable difficulty in systemic delivery. A study indicated that the coadministration of vascular endothelium growth factor (VEGF) with AAV6 vector reached the whole-body muscle transduction after systemic intravenous delivery (147). AAV8 also showed the persistent transduction of heart and skeletal muscle when injected intravenously (148). Unfortunately, both deliveries result in unwanted transduction in other tissues, such as the liver and gonads. This unspecific targeting causes serious concern about vector security and countable therapeutic effects in humans. To improve the safety and efficiency of gene therapy in clinical applications of MD, we ultimately need to develop a novel vector which specifically targets the heart and skeletal muscle without undesirable cell transduction and immunogenicity after systemic administration.

## **1.2 Adeno-associated virus**

### **1.2.1 Discovery**

In the middle 1960's, AAV was discovered as a contaminant of Ad preparations in the laboratories of Robert Atchison at University of Pittsburgh and Wallace Rowe at NIH. AAV virions were first characterized by electron microscopy during examination of human and simian Ad preparations (149-151). Immediately after AAV discovery, it was demonstrated that AAV infections have never been associated with any known diseases even though most humans have been exposed to AAV. Therefore, AAV did not receive much attention from virologists due to the absence of pathogenicity at the beginning.

By 1980, and in the early development of gene delivery for therapeutic applications, there were clear reasons to develop AAV vectors as gene transfer vehicles because AAV is not a pathogen and it appears to have a mechanism for persistence. To date, AAV has been regarded as

a dark horse among vector systems which are commonly developed for human gene therapy. Valuable data from preclinical and recent clinical evaluations have shown that the AAV vectors achieve the therapeutic effects in humans.

So far eleven AAV serotypes have been isolated. Among these serotypes, AAV serotype 2 (AAV2) isolated from humans is the most extensively characterized serotype. The basic information of AAV biology mostly covers the studies done on AAV2.

### **1.2.2 AAV genome**

AAV is a nonenveloped virus that has been assigned to the dependovirus genus of the parvovirus family. The AAV particle possesses a diameter about 22 nm and contains a linear single-stranded DNA genome of approximately 4.7 kbs with either plus or minus polarity. The AAV genome consists of two open reading frames (ORFs) termed *rep* and *cap*. The ends of the viral genome are flanked by the inverted terminal repeat sequences (ITRs). Viral transcripts produced from all promoters on the AAV genome have the same intron and they share a common polyadenylation signal.

The *rep* gene is transcribed from the p5 and p19 promoters (152). Both spliced and unspliced *rep* mRNAs are translated into four proteins. Rep proteins are non-structural proteins and they were originally thought to serve functions necessary for regulation of AAV promoters as well as for DNA replication of AAV. The p5 promoter directs expression of the larger rep proteins, Rep78 and Rep68. Rep78 is translated from the unspliced transcript while Rep68 is synthesized from the spliced mRNA. Rep78 and Rep68 can bind to the p5, p19, and p40 promoters of viral genome to regulate the AAV gene expression (153). Besides, Rep78 and Rep68 are associated with helicase and ATPase activity to participate in DNA replication

process of AAV. Through the interaction of Rep78/68 with Rep-binding element (*RBE*) in AAV ITRs (154), Rep78 and Rep 68 introduce a nick at the terminal resolution site (*trs*) of ITR by their ATP-dependent DNA helicase activities. This nicking site provides a new priming 3'OH group to allow continuous DNA synthesis during AAV replication (155, 156). Rep78 and Rep 68 are also involved in AAV genome integration into the *AAVSI* site of human chromosome 19 (157-159). The unspliced transcript from the p19 promoter produces Rep52 protein, and the spliced mRNA from the p19 promoter generates Rep40 protein. Rep52 and Rep40 are important for AAV package. The initial step of AAV encapsidation is operated by the interaction between preformed empty capsids and a complex of Rep78 or Rep68 with the/a viral genome. Thus, the helicase domains of capsid-occupied Rep52 and Rep40 are responsible for transferring newly synthesized viral genomic DNA into empty particles via the pores created at the fivefold symmetry axes (160, 161).

The *cap* gene of AAV encodes three capsid proteins, VP1, VP2, and VP3, from transcripts initiating at the p40 promoter (162). Two distinct mRNAs are synthesized from the p40 promoter for cap protein translations. VP1 is translated from an AUG start codon on the 2.4-kb mRNA. VP2 and VP3 come from the same transcript, the 2.3-kb mRNA. Interestingly, VP2 uses a weaker ACG start codon for its protein synthesis, while VP3 employs the next available AUG codon for its production on the same mRNA. VP1, VP2, and VP3 proteins possess molecular masses of 87, 73, and 62 kDa, respectively. In purified virions, VP1, VP2, and VP3 have a molar ratio of 1:1:10. These capsid proteins share overlapping sequences and they only differ at their amino termini. VP3 is 65 residues less than VP2. Compared to VP2, VP1 is extended at its N terminus by 137 amino acids. It has been identified that VP1 contains a phospholipase A2

(PLA2) domain and this domain is essential for AAV infectivity. VP3 is also required for AAV production, but VP2 is totally negligible for efficient viral packaging and infection (163).

AAV ITR is 145 bp in length and locates at both ends of viral genome. The ITRs on AAV genome are only *cis*-acting elements necessary for viral DNA replication, packaging, host chromosomal integration, as well as provirus rescue of AAV. Although ITR is not essential for high yield of Rep and Cap expression during virus production, it has been indicated that ITR contains enhancer activity on AAV promoters. Each ITR consists of an outer 125-nucleotide palindrome and a 20-nucleotide internal sequence named the *D* sequence. The outer 125 bases of ITR form a “T”-shaped palindromic hairpin structure via self-complementarity (164). The sequence segments of “T”-shaped hairpin are represented as *A*, *B*, *C* and their reverse complementary segments are termed as *A'*, *B'*, *C'*. So the typical hairpin of each ITR at the ends of AAV genome is constructed as *ABB'CC'A'-D* in sequence order. The *D* sequence is appeared only once at each end of the viral genome and remains single-stranded. ITR serves as the *origin* of AAV DNA replication due to its ideal template-primer hairpin structure for cellular DNA polymerases. The *D* sequence is further divided into two sequence stretches. The 10-nucleotide area adjacent to the hairpin is required for viral replication, packaging, and rescue (165). The next 10-nucleotide region of *D* sequence contains the binding motif of the single-stranded *D*-binding protein, a host protein FKBP52 (166). Phosphorylated FKBP52 interacting with the *D* sequence inhibits the conversion from single-stranded AAV (ssAAV) genome to the active double-stranded DNA state via the blocking of viral second-strand DNA synthesis (167). Moreover, there is a transcription initiator element in the *D* sequence. This element does not present any function in AAV life cycle. But it has been utilized as the basal promoter in the application of gene therapy (168).

### 1.2.3 AAV life cycle

AAV is described as a “defective” virus because AAV typically requires coinfection with a helper virus in order to efficiently replicate in a host cell. The helper virus is usually Ad or herpes simplex virus 1 (HSV1) (169). The helper function can also be provided from vaccinia virus, cytomegalovirus (CMV), and human herpesvirus type 6 (170, 171). E1, E2A, E4, and VA proteins of Ad or HSV1 UL5, UL8, UL29, and UL52 genes are capable of providing the helper function for AAV replication (172, 173). It is presumed that the helper virus creates the proper cellular environment and it is not directly involved in AAV propagation. In the presence of a helper virus, AAV enters into the productive phase and results in the release of newly assembled AAV virions from cells upon helper virus-induced cell lysis.

In the absence of a helper virus, the AAV gene expression program is suppressed and viral latency ensues by the integration of the virus genome into human chromosome 19 (174). This is the reason that AAV establishes a persistent infection when AAVs infect mammalian cells alone. In addition, AAV genes integrated in the host genome can be activated to lead to the AAV Rep-mediated excision of provirus DNA from cellular chromosome when a latently AAV infected cell has super-infection of a helper virus. Then, the rescued AAV provirus turns into the productive life cycle and completes AAV propagation. The introduction of the productive phase of AAV life cycle from a latent integrated provirus can also be observed by non-viral stimulations with a lower efficiency. The limited replication occurs in a latently infected cell after ultraviolet irradiation, heat shock, carcinogens, or treatment of cells with genotoxic agents such as hydroxyureas (170, 175, 176).

#### 1.2.4 AAV receptor

A successful AAV infection initiates from the attachment of a virion to the cell surface followed by viral absorption, intracellular trafficking, nuclear transport, and localization or replication of the viral genome in the cell nucleus. AAV infection relies on the expression of a specific cellular receptor allowing viral binding and entry into the target cell. The primary attachment receptor for AAV2 is identified to be cellular membrane-associated heparan sulfate proteoglycan (HSPG) and AAV2 transduction is efficiently competed with heparin (177). In addition, AAV2 has also been determined to utilize  $\alpha V\beta 5$  integrin, fibroblast growth factor receptor-1 (FGFR1), and hepatocyte growth factor receptor (c-Met) as coreceptors providing cellular internalization (178-180). More recently,  $\alpha 5\beta 1$  integrin has been shown to be an alternative coreceptor of AAV2 in human embryonic kidney 293 cells (HEK 293 cell) which lack the expression of  $\alpha V\beta 5$  integrin (181). AAV3 shows the ability to bind heparin, but the AAV3 capsid residues involved in heparin binding remain undetermined.

The cellular receptor for AAV4 and AAV5 is identified to be sialic acids with different linkage forms. AAV4 uses *O*-linked sialic acid,  $\alpha 2,3$  *O*-linked sialic acid, for viral entry while AAV5 binds to *N*-linked sialic acids,  $\alpha 2,3$  *N*-linked sialic acid and  $\alpha 2,6$  *N*-linked sialic acid, during viral infection (182, 183). AAV5 also utilizes platelet-derived growth factor receptor (PDGFR) to mediate the viral binding and internalization (184).

According to the viral capsid sequence, AAV1 differs from AAV6 by only six amino acids. So it is not surprising that both viruses share some common cellular receptors or that they interact with the same receptor for viral transduction. By using cell-based assays, it has been shown that  $\alpha 2,3$  and  $\alpha 2,6$  sialic acids appeared on *N*-linked glycoproteins facilitate AAV1 and AAV6 infections (185). However, AAV6 has more efficient liver transduction compared to

AAV1 (186). This phenomenon gives rise to the question of how this difference could exist if AAV1 and AAV6 use the same receptors. Wu *et al.* showed that AAV6 transduction relies on sialic acid more than AAV1 although the binding ability of AAV6 to sialic acid is not better than that of AAV1 (185).

AAV8 currently appears to be a powerful gene delivery vector because it can efficiently cross the blood vessel barrier. In a recent study, the 37/67 kDa laminin receptor (LamR) is demonstrated to be a cellular receptor for AAV8 by conducting a yeast two-hybrid screen (187). Two separate AAV8 capsid subdomains have been proved to mediate the LamR binding. The overexpression of LamR or the siRNA-mediated LamR inhibition determined that LamR is also important for the transductions of AAV2, AAV3, and AAV9.

### **1.2.5 AAV intracellular trafficking**

The increasing development of AAV as a gene therapy vector has expedited the discovery of events affecting the efficiency of AAV transduction. In general, the biological process of AAV transduction can be divided into seven stages. These stages include: 1) viral binding to cell surface through the interaction with the cellular receptor and coreceptor, 2) receptor-mediated endocytosis of virus for viral entry, 3) viral trafficking via the endosomal compartment, 4) viral escape from endosome, 5) viral nuclear translocation, 6) virus uncoating, and 7) viral genome conversion from a single-stranded to a double-stranded molecule capable of gene expression. Except the binding affinity of the viral particle to the cell membrane, the pace of viral uncoating, and the viral genome conversion, the intracellular trafficking is also a rate-limiting factor in AAV transduction (188). The intracellular trafficking of AAVs is used to describe a process involving the movement of virus from cellular membrane to the cell nucleus (stage 3 to stage 5)

and it is influenced by cell types. At present, the knowledge of AAV trafficking is based on AAV2 and AAV5. The realization of intracellular trafficking among other serotypes is relatively limited.

Receptor-mediated endocytosis controlling AAV cell entry has been shown in AAV2 and AAV5. For AAV2, it was indicated that virus binding to HSPG enters cells through clathrin-coated pits in a dynamin-dependent manner. The introduction of a mutated dynamin led to the decrease of AAV2 transduction (189). AAV5 uses a different primary attachment receptor; however, it also conducts viral endocytosis via clathrin-coated pits (190). In addition, AAV binding to cell receptors can initiate intracellular signaling pathways and subsequently stimulate receptor-mediated endocytosis. For example, the binding of AAV2 to the integrin coreceptor during internalization activates Rac1, a small GTP-binding protein. The activation of Rac1 results in triggering the phosphatidylinositol-3 kinase (PI3K) pathway that facilitates the rearrangement of cellular microtubules and microfilaments for movement of AAV2 particles to the nucleus (191).

Rab proteins belong to a family of small GTPases that are involved in the process of endosomal budding, sorting, movement, and fusion in the cell. Following endocytosis, AAV virus appears to enter into early endosome which is characterized by containing the small GTPase Rab5. At low multiplicities of infection (MOI) of recombinant AAV2 (rAAV2), Rab5 early endosome is predominantly routed to Rab7 late endosome (192). In contrast, rAAV2 at high MOI preferentially traffics from Rab5 early endosomal compartment to perinuclear recycling endosome (PNRE), a Rab11-positive compartment. The late endosomal compartment can be further transported to either the lysosome or the trans-Golgi. Rab7 directs the movement of late endosome to the lysosome while Rab9 mediates the late endosomal movement to the



trans-Golgi (193). Similarly, PNRE can be translocated in the trans-Golgi through a Rab11 dependent mechanism (194).

Several studies have proven that rAAV2 transduction is remarkably decreased when acidification of the endosomal compartment is impeded by the treatment of bafilomycin A1 (195). This indicates that a low endosomal pH is required for rAAV2 to escape from the endosome and is likely to promote conformational changes of key viral capsid proteins essential for AAV endosomal release and nuclear translocation. Certainly, the inactivating point mutations of the PLA2 domain of AAV2 VP1 do not hamper viral capsid assembly, packaging, and cell entry, but decrease the amount of gene expression (196). Therefore, PLA2 domain in VP1 may play a role for the viral release from the endosome and the transfer of the viral DNA to the nucleus. Another interesting finding of AAV is that proteasome inhibitors appear to enhance the viral transduction of AAV2 and AAV5. The enhanced viral transduction is not due to the blocking of viral genome degradation or the modulation of second-stranded genome synthesis. The inhibition of proteasome increases the nuclear uptake of viruses and viral gene expression in different cell systems (197, 198). Since both rAAV2 and rAAV5 capsids are able to be modified by ubiquitination *in vivo* and *in vitro* (199) and the blocking of proteasome activity increases capsid ubiquitination following the enhanced viral transduction, it suggests that the ubiquitin-proteasome pathway has a significant role in regulating capsid disassociation and nuclear transport of AAV during AAV infection. The priming of AAV capsid for ubiquitination may be taken inside the endosomes.

The intracellular processes underlying viral uncoating and nuclear translocation are mostly unclear. It is presumed that AAV particles enable to be translocated into the nucleus prior to uncoating because florescent-labeled AAV virions were observed in the nucleus (200). Since the

diameter of an AAV particle is almost the same size as the nuclear pore, the nuclear translocation of intact virion may be due to diffusion. Unfortunately, the nuclear transport of intact AAV virus presents a slow and inefficient process, so that most AAV virions accumulate in a perinuclear area. Therefore, it gives rise to the hypothesis that AAV can also become uncoated before or during nuclear translocation.

### **1.2.6 AAV capsid structure**

Tissue tropism and immunogenicity of AAV gene transfer vector are determined by specific interactions between viral capsid and host cellular components. Therefore, an understanding of the structural and functional correspondence of AAV capsid is required for engineering AAV tissue tropism in gene delivery as well as designing the nonimmunogenic vector in long-term gene expression.

To date, several AAV capsid structures have been solved by using X-ray crystallography or cryoelectron microscopy (cryo-EM) coupling image reconstruction. The atomic structure of AAV2 has been demonstrated at a 3 Å resolution by X-ray crystallography (201). The capsid structures of AAV4 and AAV5 have been determined by using cryo-EM and image reconstruction at a resolution of 13 Å and 16Å, separately (202, 203). Preliminary X-ray crystallographic analysis of AAV8 capsid has also been reported recently (204). AAV virus can generate VP1, VP2, and VP3 proteins as capsid subunits. The common feature of AAV capsid structures among all AAV serotypes is that the viral shell comprises 60 capsid protein subunits arranged with T=1 icosahedral symmetry. In all AAV viruses, the capsid protein subunit possesses a highly conserved  $\beta$ -barrel core comprised of eight strands from two antiparallel  $\beta$ -sheets. The  $\beta$ -barrel core is on the inner surface of the viral capsid. In contrast to the strands of

the  $\beta$ -barrel, the large interstrand loops located between the strands of the  $\beta$ -barrel have quite variable structures in the different AAV serotypes and are the regions responsible for antibody recognition and cellular receptor binding since these loops can be exposed on AAV surface. For example, the most prominent feature of AAV2 surface topology is the cluster of the threefold-proximal peaks. Each of threefold-related peaks on the capsid is an association of loops from two neighboring subunits. Mutations near the positively charged side of each peak affected the HSPG binding of AAV2. In addition, the basic patches on AAV2 threefold axis peaks controlling HSPG binding are missing from AAV5. This shows that the variety of AAV capsid surface structures direct specific cellular receptor binding and results in AAV's unique tissue tropism.

### **1.2.7 rAAV production in gene therapy**

The AAV ITRs are only *cis*-acting elements required for vector production and transduction. The AAV coding sequences can be replaced by the transgene of interest because both the *rep* and *cap* gene products together with helper virus proteins can be supplied in *trans* to manufacture infectious rAAV virion as a therapeutic tool. The production of rAAV initially requires the use of Ad virus. Undoubtedly, it raises safety concerns about incomplete elimination of Ad viral activity and host immune response against Ad capsid proteins existing in rAAV preparation even after the heat inactivation of rAAV stocks for human treatment. Thus, the present method for rAAV production makes use of a three-component plasmid system (205). The three plasmids in this AAV production system are a) AAV plasmid vector bearing the desired transgene flanked by AAV ITRs, b) AAV helper plasmid offering AAV Cap and Rep proteins in *trans*, and c) Ad helper plasmid providing Ad E2, E4, and VA proteins necessary for efficient AAV genome replication and gene expression. The cotransfection of these three plasmids into HEK 293 cells

stably expressing Ad E1A and E1B proteins results in the production of rAAV vectors. In the presence of helper functions from supplied Ad genes, the rAAV genome is submitted to the lytic productive phase of wild-type AAV life cycle by being rescued from the plasmid backbone. The rescued rAAV genome is then replicated and packaged into preformed empty capsid as single-stranded DNA molecule. After cotransfection, the virus can be purified by CsCl density gradient ultracentrifugation or through various chromatographies. Although the three-component plasmid system produces the Ad-free rAAV stocks without heat inactivation and it is perhaps the most robust and versatile way for vector preparation, this method is unwieldy for large-scale vector production in clinical human gene therapy. The infection of stable AAV Rep and Cap producing cells with adenovirus carrying rAAV vector genome has presented a way for scale-up (206). Furthermore, the transduction of proviral cell lines with Ad or HSV1 containing a Rep and Cap expression cassette has shown high-titer rAAV production (207, 208). However, these approaches for increasing rAAV titers still require the complete elimination of the helper virus during viral stock preparations. So recent work in the development of baculovirus expression system for rAAV production in insect SF9 cells has shown promise for future large-scale production (209). The helper functions from Ad can be provided by baculovirus. However, the baculovirus helpers tend to have passage-dependent loss-of-function deletions leading to a decrease of rAAV titer (210). The modification of AAV *rep* gene in baculoviral helpers increased the passaging stability of baculovirus vector system. Nevertheless, the use of a baculovirus system at a passage number of two or less is suggested for sufficient large-scale rAAV production.

When designing and cloning a rAAV vector plasmid, it should be considered that the two AAV ITRs occupy approximately 300 bps. To ensure efficient rAAV encapsidation, the

transgene expression cassette should not be more than 4.5 kbps. This small packaging capacity of AAV particles becomes one of the major limitations in rAAV vector applications. To overcome the limited packaging capacity of AAV, a strategy has been developed based on the heterodimerization of two AAV vectors through the formation of concatamers from either integrated or episomal viral DNA (211). Therefore, a large gene can be split and packaged into two separate rAAV vectors. One vector contains a promoter, the 5' portion of the transgene, and a splice donor sequence (SD) while the second vector carries a splice acceptor sequence (SA), the 3' portion of the transgene, and a poly A sequence. The coinfection of these two AAV vectors into target cells produces head-to-tail heterodimers via intermolecular recombination at the identical sequence homology of the ITRs. Rejoining the split gene into one continuous DNA molecule then occurs. The presence of SD and SA in this united DNA molecule allows the fused ITR sequence to be removed from synthesized mRNA and subsequently saves the expression of the intact desired protein. Although this split delivery strategy permits expression of almost double-sized transgenes in rAAV-mediated gene transfer, the efficiency of head-to-tail heterodimerization is consistently low. Finally, a study showed that the ratio of head-to-tail recombination could be efficiently increased by using vectors carrying hybrid ITRs of AAV serotype 2 and 5 (212).

The conversion from single-stranded genome to double-stranded DNA molecule, conducted by host-cell DNA synthesis machinery, is one of the main limiting steps for the efficiency of rAAV transduction. To date, self-complementary AAV (scAAV) vectors, and named double-stranded AAV (dsAAV) vectors, have been generated to bypass the rate-limiting step of second strand synthesis. Several designs showed deletion of *D* sequence or mutation of the *trs* site of one ITR produces high percentages of scAAV vectors (213, 214). The scAAV

vectors can achieve more rapid and efficient gene expression than ssAAV does. The counterpart to this enhanced transduction efficiency is an even more limited packaging capacity retaining about 2.3 kbps. The small therapeutic agents, such as antisense oligonucleotide and siRNA, are suitable for scAAV gene delivery. It is worth mentioning that this modified scAAV vector may make poorly AAV-transduced tissues more eligible for rAAV gene therapy.

Tissue-specific transgene expression is considered as the basic requirement for secure clinical applications in humans. Since rAAV vectors have a broad tissue tropism, the organ-restricted transgene expression has been managed by the use of a tissue-specific promoter. The advantages of employing a tissue-specific promoter are the alleviation of immune response and the prolonging of transgene expression. As described, substitution of an MCK promoter/enhancer for a ubiquitous CMV promoter/enhancer in a rAAV vector producing  $\gamma$ -sarcoglycan mitigated the immune response and enhanced levels of transgene expression in  $\gamma$ -sarcoglycan-deficient mice (215). It suggested that a tissue-specific promoter minimizes immune response due to its avoidance of non-specific transgene expression in antigen-presenting cells (APCs). Although natural muscle-specific promoters generally diminish levels of transgene expression compared to non-specific viral promoters, such as CMV promoter, efforts have been made to enhance the strength of muscle-specific promoters by combinations of several myogenic regulatory elements. Several synthetic promoters containing E-box, MFE-2, TEF-1 or SRE myogenic regulatory *cis*-elements have been characterized to possess transcriptional potencies exceed those of natural myogenic promoters and viral gene promoters in muscle.

### 1.2.8 rAAV integration

The preferred site for wild-type AAV integration is located on human chromosome 19q13.3-qter, named *AAVSI*. Rep78 and Rep 68 have the ability to bridge the interaction between the wild-type AAV ITR and *AAVSI* site on chromosome. Cellular high mobility group chromosomal protein 1 (HMG-1) has been proved to stimulate AAV Rep activity at low Rep concentration when AAV infection lacks the helper virus. The binding of HMG-1 to Rep protein may promote Rep-mediated site-specific chromosome integration by increasing Rep ATPase activity (216). However, it is not surprising that rAAV vectors display a different integration pattern on host DNA since rAAV genomes, only composed of AAV ITRs and transgene, do not encode Rep protein.

After rAAV genomes successfully translocate into the nucleus following infection, single-stranded rAAV DNA needs to be transformed into a transcriptionally functional double-stranded template in order to express transgene. Duplex rAAV DNA molecules can then form circular episomes or linear concatemers. These extrachromosomal double-stranded DNA forms are transcription-competent agents. An interesting work has been postulated that free double-stranded rAAV genomic ends are substrates for the cellular DNA repair machinery (217). The involved cellular double-stranded break repair machinery dedicates to remove free ended DNA molecule through non-homologous end-joining (NHEJ). A complex containing DNA-dependent protein kinase (DNA-PK) from this repair machinery regulates the balance between linear versus circular forms of double-stranded rAAV genomes. This regulation might be mediated by the binding of DNA-PK complex to linear rAAV DNA. Taken together, these results predict that free ended double-stranded rAAV genomes can be processed to not only circular episomes but also integrated proviruses due to cellular DNA repair systems responsible for cleanness of free

ended duplex DNA. As expected, subsequent study has shown that rAAV vectors appear to randomly integrate at chromosomal double-strand breaks. (218). Furthermore, rAAV vectors integrate at the existing chromosome breakage sites rather than self-causing breaks. The integration rate of double-stranded rAAV genomes is about 10% in the liver (219). The emerging consensus is that rAAV vectors generally persist as non-integrated episomes and they integrate at only low frequencies.

Chromosomal integration of rAAV vector DNA is a double-edged sword. It provides a foundation for persistent transgene expression over the long-term. On the other hand, it raises the safety issue about insertional mutagenesis. Because rAAV vectors do not create sites for chromosomal integration, concerns about insertional oncogenesis for rAAV vectors are much less than those for lentiviral vectors. Recent research has shed some light on this issue; by examining the tumor formation in rAAV-treated mice, Bell *et al.* has determined that rAAV vectors do not have tumorigenic properties in a large-scale study (220).

### **1.2.9 Immune responses to rAAV**

rAAV-mediated gene delivery can be limited by host humoral and cell-mediated immune responses against viral vector. Since rAAV vectors do not carry any viral genes, the primary target of the immune response is the viral capsid of vector particles. Several works have determined that the neutralizing antibodies against rAAV capsids are generated and could cause the failure of rAAV readministration in gene delivery. Interestingly, a study has revealed that over 80% of normal human subjects are seropositive for AAV antibody and 18% of them have neutralizing antibody. Because humans are natural hosts for AAV, the presence of pre-existing neutralizing antibodies may severely impair the application of rAAV in human gene therapy



(221). Mechanisms for antibody-triggered neutralization of viral infection include aggregation of viral particles, induction of capsid conformational changes, interruption of cellular receptor attachment, and inhibition of viral uncoating. As mentioned, the large loop insertions between the strands of the capsid  $\beta$ -barrel core constitute the majority of the capsid surface and are responsible for the interaction with antibodies. Compared to unmodified AAV2, AAV2 capsid mutants harboring peptide insertions in surface exposed loop regions have been shown to reduce up to 70% the affinity for AAV antibodies in human serum samples (222). Although the homology of amino acid sequence between AAV2 and AAV8 capsids is up to 83%, it has been proposed that AAV8 may have less concern about its preexisting immunity in humans. Because AAV8 is originally isolated from nonhuman primates, it does not have prevalence in humans.

Extensive investigation into rAAV directed cytotoxic T lymphocyte (CTL) response has shown that the cellular immune response to rAAV vector is also dependent on AAV capsid. Specific T-cell responses to the capsid of rAAV2 vectors have been associated with liver toxicity in human gene therapy trial of hemophilia B (223). A recent work clearly demonstrated that AAV2 capsid elicits T-cell response against capsid, and AAV8 does not lead to activation of capsid-specific T cells in mice and cynomolgus macaques (224).

Notwithstanding the existence of rAAV capsid-induced immune response in human gene therapy, this obstacle may be overcome by the use of alternative serotypes and selective modifications of rAAV capsid protein. In practical applications, the transgene product of rAAV sometimes may act as an immunogenic antigen. This immune complication depends on the route of administration, the status of target tissue, and the nature of transgene product. The immune response derived from transgene expression can be adjusted by alteration of transgene epitopes without losing the physiological function of the delivered gene.

### 1.3 Engineering AAV tropisms

The success of rAAV-mediated gene delivery in humans is associated with efficient tissue-specific transgene expression. Except deployment of tissue-specific promoters, cell-restricted transgene expressions require the ability of the vector to bind to the desired target cells. In the past years, a number of AAV serotypes and over 100 AAV variants have been isolated from cultured Ad stocks, human tissues, and nonhuman primate sources. The benefits of diverse AAV serotypes in human gene therapy include the potential to evade preexisting immune responses and the ideal targeting due to their variety of native tropisms. The mechanism underlying diverse tissue tropisms of AAV serotypes is primarily associated with the usage of different cellular receptors.

Despite of AAV5, AA1 to AAV6 were found as contaminants in laboratory Ad stocks at the beginning. AAV5 was identified from a human penile condylomatous wart (225). Particularly, AAV2 and AAV3 are believed to originate from human due to their prevalence of neutralizing antibodies in humans (226). On the contrary, AAV4 appears to stem from monkeys because antibodies against AAV4 are present in nonhuman primates (227). The origin of AAV1 remains unclear since AAV1 antibodies have been found in monkeys and AAV1 genomes have been discovered in human tissues (228). In theory, AAV6 is considered as a hybrid between AAV1 and AAV2. AAV6 left ITR and p5 promoter sequences are almost identical to those of AAV2 and the rest of AAV6 genome displays a similar composition to that of AAV1 (229). AAV 7 and AAV8 have been identified as originating in monkeys by a novel PCR-based strategy (230). By using the same PCR-spanning method, AAV9 is isolated from human tissues (228) while AAV10 and AAV11 have recently been confirmed to come from cynomolgus monkeys (231). AAV DNAs are not only isolated from primates but also are found in other

species, such as snakes, horses, cows, goats, chickens, and lizards. Among these AAV strains, avian and bovine AAVs have contributed to gene delivery studies (232, 233).

The different AAV serotypes reveal sequence variation within the capsid domain, which is responsible for host ranges and tissue tropism among the serotypes. In general, each AAV serotype has its preferential tropism when delivered locally. Gene transfer with AAV2 vectors in the central nervous system (CNS) shows efficient, non-toxic and long-time transgene expression (234). Compared to AAV2, AAV5 results in a more widespread infection in the brain (235, 236). While AAV5 and AAV4 are the best serotypes for retina infection, AAV1, 5, and 6 hold significant advantages over AAV2 for gene therapy in airway epithelial cells (237, 238). AAV 8 is the most efficient vector in liver and pancreas targetings (230, 239, 240). However, AAV3 has not been found to offer noticeable advantages in gene delivery. AAV9 has appeared to transduce murine lung and skeletal muscle better than AAV8 (228). AAV10 and AAV11 are used for gene delivery in individuals having a preexisting immunity to AAV2.

In muscular transduction, AAV1 and AAV6 show much more efficient gene deliveries in skeletal muscle and in cardiomyocytes compared to other AAV serotypes (241, 242). AAV7 vector has an efficiency of gene transfer in skeletal muscle equivalent to that demonstrated by AAV1 (230).

However, all AAV serotypes result predominantly in transduction of the liver and display their tropisms in a wide range of tissue types with much lower efficiency after systemic delivery. It makes AAV difficult to perform efficient gene delivery specifically to certain tissues, which are either embedded in the deep places of body or distributed throughout the whole body, without invasive procedures. Thus, the purpose of creating new AAV vectors is to enable the transfer of therapeutic genes into cell types which are poorly transduced by current AAV vectors

and restrict AAV tropism to specific tissues via desired systemic delivery. So far, several outstanding approaches have been explored to manipulate the endogenous tissue tropisms of AAV vectors. The following methods have been developed to engineer novel tropisms derived from different AAV serotypes.

### **1.3.1 Ligand-directed targeting**

Ligand-directed targeting of gene delivery rAAV vectors is a method to insert receptor-targeting peptides into viral capsids for achieving the proper surface display of ligand in presentation of the ligand to its receptor. Specific tissue-restricted transgene delivery is an important goal of gene therapy due to some critical considerations. First, current AAV vectors can be inefficient in acquiring entrance to the cell types needing treatment. Second, therapeutic transgenes may be harmful if delivered into unintended tissues. Based on these concerns, ligand-directed targeting provides the potential advantage of improving the safety and efficacy of gene transfer via rAAV treatment.

Phage display peptide libraries have been widely used to isolate ligands binding to desired cell types. At present, several groups have successfully redirected AAV targeting by incorporating the specific peptide identified by phage display into AAV capsid. For example, Work *et al.* identified peptides homing to the lung and brain by *in vivo* phage display from rats and then inserted these isolated targeting peptides after position 587 in the AAV2 capsid to retarget virus to the expected organs in a preferential manner (243). Although such incorporation of peptides isolated by phage display into the AAV capsid can be an ideal approach for specific gene delivery, the peptide conformation may be changed in viral capsid protein context and thus, the specific ligand-receptor interaction may be lost or diminished. The insertion of peptides

selected by phage display into AAV capsid may also interrupt functions necessary for the viral life cycle in viral production and could prohibit producing sufficient viral titers required for gene therapy. In order to counteract these limitations, Müller *et al.* selected appropriate ligand-inserted AAV mutants from a large library presenting random peptides at position 588 in the viral capsid (244). This successful work allows us to efficiently select ligand-displayed rAAV clones for high-affinity targeting to a specific receptor.

### **1.3.2 Combinatorial AAV library**

Library-based approaches through DNA shuffling or error-prone polymerase chain reaction (PCR) are powerful ways to generate vector diversity for directed evolution. DNA shuffling, also named *in vitro* recombination involves digesting a set of functionally related genes with DNase I to a pool of random DNA fragments. These DNA fragments then can be reassembled into a full-length gene by repeated annealing cycles in the presence of DNA polymerase. This reaction promotes the fragments to prime each other depending on sequence homology. Therefore, recombination takes place when fragments from one copy of a gene prime on another copy to cause template switching (245). This recombination strategy intends to extend the diversity of a library for evolution processes. Similarly, error-prone PCR technique is able to produce extensive vector variety for the selection of evolution. However, the error-prone PCR creates a library of mutants with random point mutations by PCR-based mutagenesis of a start sequence (246). Moreover, DNA shuffling and error-prone PCR can be combined to provide a large viral library diversity on specific purpose. Reiterative cycles of shuffling and controllable mutagenesis rate of error-prone PCR followed by screening or selection has proved to be a useful approach for the evolution of single-gene products with enhanced activity.

More recently, a study has generated an AAV library on AAV2 *cap* gene with error-prone PCR-based mutagenesis and a staggered extension process analogous to DNA shuffling (247). Novel AAV2 variants with different heparin sulfate-binding affinities were identified by subjecting the viral library to heparin affinity column chromatography. Neutralizing-antibody escape clones were isolated by selection and amplification of infectious mutants in the presence of antiserum against wild-type AAV2 capsid. Furthermore, Perabo *et al.* have exploited error-prone PCR to efficiently obtain the selected AAV vectors that escape neutralization by human antibodies (248).

The generation of AAV libraries with enhanced diversity for further directed evolution is not only to acquire novel tissue-specific AAV tropism, but also to enable mapping the structural and functional capsid domains of native targetings on various serotypes.

### **1.3.3 Chimeric AAV vectors**

Chimeric vectors refer to the AAV virions composed of capsid proteins with domain or amino acid swapping between different serotypes. Rational swapping and marker rescue strategies have been involved in the production of chimeric rAAV vectors with different cellular receptor binding affinity. Domain swapping implies the transfer of specific capsid protein domains from one serotype to similar regions on another serotype. The swapped capsid domains range from single to multiple amino acids and can be surface loops or specific residues of viral particles. This strategy can provide vital information to identify capsid regions which are determinants for driving tissue tropism. By using domain swapping, a study has identified that the residue 350-430 region of AAV1 VP1 capsid protein is critical for AAV1 muscle tropism (249). Nevertheless, it has been noticed that simply swapping domains may not always make chimeric

vectors gain desired specific tropism. For example, substitution of the heparin-binding motif from AAV2 onto a similar region of AAV5 capsid protein generated chimeric viral particles at good yields and conferred heparin-sulfate binding ability to these newly produced chimeric vectors. However, the resultant chimeric viruses were noninfectious on cells normally susceptible for AAV2 transduction (250).

The marker rescue approach is developed to take advantage of the sequence homology of *cap* gene between AAV serotypes for serving as crossover points for recombination initiated by cellular machinery (251). The recombination of *cap* sequences can lead to the rescue of infectious or targeted phenotypes in generated AAV mutants via directed selection of functional capsid domains assembled into mutated viable virions. A work has demonstrated that three AAV2 capsid mutant sequences identified as noninfectious and unable to bind heparin are rescued after cotransfection with AAV3 capsid DNA sequences.

Domain swapping and marker rescue techniques hold tremendous potential for the generation of chimeric rAAV vectors with newly acquired tropisms. Besides, these strategies can also contribute to establish structure-function correlates of AAV serotype capsids along with crystal structure data.

#### **1.3.4 Mosaic AAV vectors**

Mosaic AAV vectors can be defined as capsid structures composed of mixtures of complete capsid proteins from different serotypes or wild type and mutant capsid proteins from the same serotype. Theoretically, the ratio of capsid subunits from various sources or different serotypes in mosaic virions generally reflects the input ratio of cotransfected plasmids carrying different *cap* genes during viral production. Recently, Rabinowitz *et al.* manufactured a panel of mosaic

vectors by the transfection of pairwise combinations of AAV serotype 1 to 5 cap-expressing plasmids at several input ratio (252). Interestingly, mosaic viruses composed of AAV3 and AAV5 capsid mixtures at the 3:1 ratio exhibited duality in receptor binding. This AAV3-AAV5 mosaic vectors displayed a phenotype combination from their parental viruses, AAV3 and AAV5, so they not only bind to heparin sulfate but also interact with mucin. In this method, new properties different from either parental virus have also been observed in some “cross-dressed” AAV virions. As described, AAV1 and AAV2 do not transduce Chinese hamster ovary K1 cells (CHO K1) efficiently in culture. Nevertheless, mosaic AAV1/2 virus, generated by transfection of AAV1 and AAV2 capsid protein-expressing constructs at a ratio of 1:3, exhibited dramatically increased transduction in CHO K1 cells. The new viral property derived from generated mosaic AAV vectors may be due to alterations in cellular receptor usage and intracellular trafficking of mosaic AAV1/2 virions in CHO K1 cells.

The mosaic approach may also furnish insight into capsid assembly in AAV biology. The generation of mosaic virions supplying combinations of AAV1 and AAV2 capsids all led to virion production at high titer, whereas mixing of AAV5 capsid subunits with other AAV serotypes displayed viral yields at moderate titers. Increase of AAV4 capsid subunits in the combination of other serotype capsids provided the lowest yields of mosaic viruses (252). These outcomes emphasize the importance of capsid subunit compatibility in viral assembly of hybrid virions for creating new tropisms.

By involving altered cellular receptor usage, mosaic strategies are a useful tool to generate novel tissue-specific tropism in a simple way. The unique advantage of this mosaic application is that it is able to combine selected characteristics from various capsid subunit sources that synergistically contribute to synthesize a novel tropism.



### 1.3.5 Two-component system

The two-component system utilizes a bifunctional adaptor or bridging molecule that binds to AAV vectors and interacts with a target cellular receptor. In contrast to ligand-directed targeting, this method does not change the sequence of the *cap* genes nor does it force serious constraints on the size or types of used ligands.

The use of a two-component system to target AAV2 to a nonpermissive cell line has been carried out (253). A bispecific F(ab' $\gamma$ )<sub>2</sub> antibody was constituted with the binding specificity for AAV2 virion and the cell surface receptor  $\alpha_{IIb}\beta_3$  integrin. This bispecific antibody mediated a novel interaction between AAV2 vector and the cellular receptor  $\alpha_{IIb}\beta_3$  integrin expressed on the nonpermissive human megakaryocytes. Although this technique successfully directed AAV2 vectors to interact with integrin and epidermal growth factor (EGF) *in vitro* (254), the stability of these conjugated vectors in *in vivo* targeting remains to be determined.

Two-component systems do not require information about the crystal structure of AAV capsids or capsid surface-displayed domains, but they involve in constructing the bispecific molecules and the determination of cell-specific receptors that mediate viral attachment and internalization. The potential of this strategy is limited in that the inclusion of the additional protein adaptor may raise the number of hurdles in the transfer of the two-component system into clinical and commercial applications.

## 1.4 Specific aims

Non-viral and viral vectors can accomplish gene delivery to the targeted tissues. Among these vectors, AAV has been emerged as a powerful vector for gene transfer due to its nonpathogenicity and long-term gene expression. Although recombinant AAV vectors can readily saturate individual muscles following direct injection, a single injection into muscle restrictively transduces the cells localized around the injection site. Skeletal muscle accounts for approximately 40% of the whole body in weight. To successfully correct the disorders affecting the heart and skeletal muscle, systemic delivery of AAV vectors through the circulation by a single intravenous administration is the best way to reach the whole-body transduction of muscle. Unfortunately, AAV vectors primarily transduce in the liver and have the broad tropism after systemic intravenous delivery. Gene transfer into unwanted nonmuscular tissues decreases the efficacy of AAV-mediated transgene expression and raises safety concerns about the potential increase of germline transmission. To overcome this challenge in the treatment of muscle diseases, the **goal** of this thesis project is to develop a muscle-specific AAV vector for systemic delivery.

Compared to other AAV serotypes, AAV2 was the first primate AAV genome to be cloned into plasmid in 1980s (255) and has therefore been the best characterized. So AAV2 has been chosen as the object in this study. The research of AAV2 tropism modification might build for the development of novel tropism on other AAV serotypes. HSPG is the primary receptor of AAV2. The residues, R585 and R588 on AAV2 capsid, are primarily involved in heparin binding. In contrast, the mutations on R484, R487, or K532 of AAV2 capsid yielded an intermediate heparin-binding (250). A study showed the mutations of R484 and R585 from basic amino acids to acidic glutamate residues markedly detargeted AAV2 vectors from the liver, and

this AAV2 mutant is predominantly retargeted to the heart through systemic delivery in mice (256). It appears the possibility that the muscular transduction can be increased by AAV2 with mutations on HSPG binding sites due to the reduced vector retention by the liver. Recently, White *et al.* (257) also determined the insertion of endothelial cell-targeting peptide, MTPFPTSNEANL, into AAV2 capsid following amino acid 587 could increase its efficiency and selectivity for vascular targeting. However, peptide-engineered AAV for muscle targeting has not been developed.

Based on these findings, the **hypothesis** in this study is that either the mutations on HSPG binding sites of AAV2 capsid or an insertion of the muscle-specific peptide ASSLNIA, isolated by phage display (258), on AAV2 capsid could enhance the ability of AAV2 on specific muscle targeting and avoid non-specific vector uptake by undesirable tissues.

**The specific aims of this study are:**

1. To characterize and evaluate the muscle-targeting effects, selectivities, and neutralizing antibody-evasions of modified AAV2 vectors *in vitro*
2. To address the primary pathway of modified AAV2 vectors during viral cell entry
3. To demonstrate the muscle-targeting abilities of modified AAV2 vectors by local and systemic deliveries after a single administered dose *in vivo*

## **2. MODIFICATIONS OF AAV2 CAPSID MEDIATE SELECTIVE VECTOR TARGETING TO MYOTUBES AND CONFER VIRAL RESISTANCE TO NEUTRALIZATION**

### **2.1 Introduction**

Normal muscle activity is essential for maintaining individual ambulation, respiratory, and cardiac function. Undoubtedly, diseases of the striated muscle significantly impair human mortality and life quality. A large variety of genetic defects impede the ability of muscle to accomplish these tasks and often result in loss of ambulatory capability or heart failure. Pharmacological treatment, cell-mediated approach, and gene therapy have been used to minimize the damage from myopathy in patients. Among these strategies, gene transfer to muscle offers the greatest hope for the treatment of disorders specific to muscle, such as MD. AAVs are believed to lack pathogenicity and have shown stable gene expression over a long period. These advantages make AAV vector a promising candidate for treatment of MD among vector systems applying in human gene therapy. Direct intramuscular injection of AAV vectors evokes a high efficiency of gene transfer in the area of injected muscle. However, perfect therapy for MD will require whole-body gene transfer to the muscle to insure the patient's survival. Since all serotypes of AAV vector predominantly transduce the liver when given by intravenous delivery, the development of an efficient and muscle-specific AAV vector for systemic gene transfer needs to be pursued in order to achieve efficacious therapeutic effects without safety

concerns. In order to avoid nonmuscular targeting of AAV vectors, genetic modification of AAV tropism was conducted. AAV2 was chosen as the target for engineering the specific muscle tropism in this study because it is the best characterized among eleven AAV serotypes. AAV2 infection is initiated by the binding of the virus to cellular HSPG (177). The expression of HSPG is widely shown in various tissues. Clearly, this is the reason that AAV2 has broad tropism. Although a previous study could not elucidate effects of mutated heparin-binding vectors on skeletal muscle targeting due to undetectable reporter activity in muscle tissue, it has demonstrated that mutations in heparin-binding sites of the AAV2 capsid redirect vectors to the heart from the liver through systemic delivery (256). Based on this finding, modified AAV2 carrying R484, R585 and R588 mutations in the HSPG-binding motif of the capsid was generated and their specificities of skeletal muscle targeting was observed. Retargeting AAV vectors by the insertion of specific targeting ligands into the capsid is a feasible approach to modify AAV tropism. Samoylova *et al.* identified a muscle-specific binding ligand by screening a phage display library (258, 259). Phages were initially selected after three *in vitro* rounds on C2C12 mouse myotubes. Then, the phages obtained *in vitro* were injected to mice via tail vein injection and were rescued from skeletal muscle. After two rounds of *in vivo* selections, the clone carrying ASSLNIA peptide was isolated and purified as an individual clone. By intravenous delivery, the binding of the ASSLNIA phage to mouse skeletal muscle was increased about fivefold relative to phage with no insert. The ASSLNIA phages also showed a twofold increase in their binding to the heart compared to the control phage. The phage carrying this muscle-specific peptide also decreased its targeting in the liver, kidney, and brain. Therefore, the muscle-specific peptide ASSLNIA was genetically incorporated into AAV2 capsid after residue 587 or 588. The abilities of specific muscle targeting of peptide-inserted vectors were examined in

various cell lines. Meanwhile, the present study explored the issue concerning the practicality of rAAV2 usage. Although a number of AAV serotypes have been isolated from human and nonhuman primate tissues, rAAV2 is the only serotype that has been used in clinical trials for the treatment of hemophilia, cystic fibrosis, DMD, and other diseases. Despite the well-established safety of rAAV2 vectors for gene delivery in humans, the major obstacle to the efficacy of AAV2 vectors *in vivo* is the prevalence of preexisting neutralizing antibodies in individuals previously exposed to AAV2. Hence, the modified AAV vectors were tested for the evasion of neutralizing antibodies *in vitro*. These *in vitro* examinations have clearly demonstrated muscle-targeting efficiency, selectivity, and immune escape of modified AAV2 vectors.

## **2.2 Material and methods**

### **2.2.1 Cell culture**

C2C12 murine myoblasts (American Type Culture Collection, Rockville, Maryland), human hepatocellular carcinoma HepG2 cells, human cervical carcinoma HeLa cells, human embryonic kidney 293 cells (HEK 293 cells), and human glioblastoma tumor U-87MG cells were grown in Dulbecco's modified Eagle's medium (DMEM) containing 10% fetal bovine serum (FBS). To induce the differentiation of C2C12 myoblasts,  $1 \times 10^4$  C2C12 myoblasts per well in 24-well plates were first grown for up to 3 days in DMEM supplemented with 10% FBS and then, they were differentiated from C2C12 myoblasts to C2C12 myotubes in the presence of DMEM and 2% horse serum (HS). After 4 days of differentiation, the C2C12 myotubes were formed.

### 2.2.2 Plasmid construction

The plasmid pBSKS-AAV2Cap containing AAV2 *cap* gene was used as the template for the construction of all modified capsids. Mutagenesis was achieved by using PCR. The mutations of heparin binding sites on AAV2 capsid were introduced by the mutagenic primers which contain the desired mutation. For the peptide-modified capsid, we designed the primers encoding amino acids ASSLNIA flanked by peptide linker. This muscle-specific peptide (ASSLNIA) was then inserted into the site after residue 587 of AAV2 capsid by PCR. The synthesized PCR products were digested with *DpnI* endonuclease to eliminate the parental plasmid template and further added phosphates at 5' of oligonucleotides by T4 polynucleotide kinase (New England BioLabs) to allow subsequent ligation. The modified AAV2 containing the mutations on heparin binding sites with the peptide insertion after amino acid 587 of capsid was also generated. The sequences of primers are listed in Table 1. The modified Cap gene was then subcloned from pBSKS-AAV2Cap to pXX2 (260) by *EcoRV* and *Xcm I*.

**Table 1 The primers for constructing the modified AAV2 capsids**

Primer	Sequences
-----	
1) Primers for the mutagenesis of heparin binding sites:	
R484E+	5' AGC AGC AGC GAG TAT CAA AG 3'
R484E-	5' CGT AAC AGG GTC AGG AAG C 3'
R585A-	5' TGC CTG GAG GTT GGT AGA TAC AGA ACC AT 3'
R588A+	5' GGC AAC GCA CAA GCA GCT ACC GCA GAT GTC 3'
2) Primers for the ASSLNIA peptide insertion:	
587 TG MTP+	5' AAC ATC GCC GGA TTA AGT AGA CAA GCA GCT ACC GCA 3'
587 TG MTP-	5' GAG GGA GGA AGC TCC TGT GTT GCC TCT CTG GAG GTT 3'
588 HB MTP+	5' AAC ATC GCC GCC GCC CAA GCA GCT ACC GCA GAT 3'
588 HB MTP-	5' GAG GGA GGA GGC GCG GCG GTT GCC TCT CTG GAG GTT 3'
-----	

### **2.2.3 Molecular modeling**

The location of the inserted muscle-specific ligand on the VP3 domain of the AAV2 capsid was generated by Swiss-Model (261-264). Swiss-Model is an automated comparative protein structure modeling server provided by the Biozentrum (University Basel) and the Advanced Biomedical Computing Center (NCI Frederick, USA). The ribbon drawing of either the peptide-modified or wild-type AAV2 VP3 subunits was produced with the available coordinates of AAV2 (201) (Protein Databank accession no. 1LP3) supplied as a template. DeepView/Swiss-Pdb Viewer revealed the surface charge distribution on the VP3 subunit with or without the MTP insertion.

### **2.2.4 rAAV vector production**

To produce modified rAAV2 virus, the three-plasmid cotransfection method was applied in HEK 293 cells (205). The plasmids used in transfection were the following: i) ssAAV CMV-Luc plasmid with the luciferase (Luc) gene driven by the CMV promoter, or dsAAV CB-EGFP plasmid with the enhanced green fluorescent protein (EGFP) gene controlled by the CB promoter (CMV enhancer/chicken beta-actin promoter). Both plasmids carry the promoter-driven transgene flanked by AAV ITRs (Figure 1); ii) the pXX6 plasmid, which contains the helper genes from adenovirus; iii) the modified pXX2 plasmid, which supplies AAV2 rep protein and modified capsid protein. As a control, wild-type rAAV was also prepared with unmodified pXX2 plasmid expressing wild-type AAV2 capsid protein. These three plasmids were mixed at a 2:3:1 molar ratio. Transfections were carried out by the following procedures. HEK 293 cells were split and reached 80% confluency for transfection. Twenty 15-cm plates were transfected by using the calcium phosphate system. After 48 hours of transfection, cells were trypsinized and



harvested by centrifugation at 3,000 rpm for 10 minutes. Cell pellets were resuspended in DMEM, and the virus was released by freezing and thawing three times. The crude lysate was then treated with benzonase (Sigma), at 50 units/ml final concentration, at 37°C for two hours. The virus was further purified twice through CsCl density gradient ultracentrifugation.

rAAV genomic titers were determined by DNA dot-blot assay. Briefly, 2 µl of the purified rAAV stock was digested with DNase I (10 µg/ml) in DMEM at 37°C for one hour and then 200 µl of 2x proteinase K buffer (20 mM Tris.Cl pH 8.0, 20 mM EDTA pH 8.0, 1% SDS) was added. Next, proteinase K was added to reactions at a final concentration of 1 mg/ml and the samples were incubated at 55°C for one hour. Viral DNA was precipitated by ethanol and the DNA pellet was dissolved in an alkaline buffer (0.4 M NaOH, 10 mM EDTA pH 8.0). DNA samples were applied to Nylon membranes and probed with a horseradish-peroxidase-labeled CMV or EGFP probe. Signals were detected by the North2South<sup>®</sup> chemiluminescence kit (Pierce). In order to detect if these mutant virions were composed of three capsid proteins, 2x10<sup>10</sup> viral particles of unmodified or modified ss rAAV CMV-Luc virus were subjected to Western blot with anti-AAV2 capsid guinea pig sera provided by R. J. Samulski (University of North Carolina).

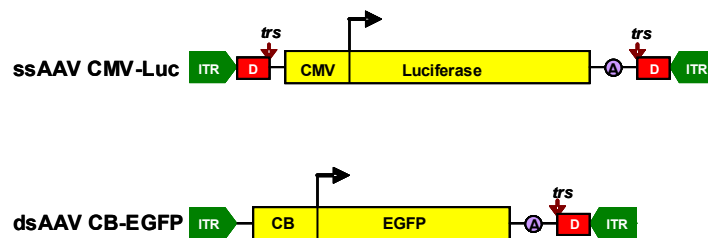


**Figure 1** rAAV genomic plasmids for vector production

The conventional ssAAV CMV-Luc plasmid (Upper) has two ITRs flanking the luciferase gene expression cassette controlled by the CMV promoter. This plasmid can produce ss rAAV virus harboring the luciferase reporter gene. For dsAAV CB-EGFP plasmid (Lower), there is a deletion of the *D* sequence together with the adjacent *trs* from one of AAV ITRs and is able to generate ds rAAV virus carrying EGFP reporter gene driven by the CB promoter (213).

### 2.2.5 *In vitro* transduction assay

C2C12 myotubes were grown in 24-well plates and infected with rAAV CMV-Luc vectors at  $2 \times 10^{10}$  genomic particles/per well. After three days of transduction, myotubes were given fresh DMEM containing 2% horse serum (HS) and subsequently incubated at 37°C for 6 days. Then, myotubes were lysed for the luciferase assay. For ds rAAV CB-EGFP virus, C2C12 myotubes were treated with ds rAAV CB-EGFP vectors at  $1 \times 10^{10}$  genomic particles/per well. EGFP expression was observed under a Nikon TE-300 inverted fluorescent microscope. Images were taken at 100x magnification at 72 hours after infection.

C2C12 myoblasts ( $2 \times 10^4$  cells/well) were grown in 12-well plates overnight. These cells were infected with rAAV CMV-Luc at  $10^4$  genomic particles/cell and adenovirus type 5 (Ad5) at an MOI of 5 plaque forming units/cell for 48 hours. Reporter gene activities were further determined by the luciferase assay.

$1 \times 10^5$  HepG2 cells per well were seeded in 12-well plates and these cells were incubated with rAAV CMV-Luc vectors at  $10^3$  genomic particles/cell in the presence of Ad5 at an MOI of 10 plaque forming units/cell for 48 hours. Cells were then harvested for the luciferase assay.

HeLa cells ( $6 \times 10^4$  cells/well) or  $3 \times 10^5$  HEK 293 cells per well were grown in 12-well plates for 24 hours. These cells were then infected with rAAV CMV-Luc at  $10^3$  genomic particles/ per cell and Ad5 at an MOI of 5 plaque forming units/cell for 48 hours. To test transduction efficiencies, luciferase activities were determined by the luciferase assay.

U-87MG cells were grown at a density of  $3 \times 10^4$  cells/well in 12-well plates overnight and then infected with rAAV at  $10^4$  genomic particles/cell for 48 hours. Reporter gene activities were determined by the luciferase assay.

rAAV-mediated *in vitro* transduction experiments were repeated independently at least two or three times in triplicate.

### **2.2.6 *In vitro* neutralization assay**

This assay was developed to determine the effect of a preexisting anti-AAV immune response on modified rAAV2 vectors *in vitro*.  $2 \times 10^{10}$  particles of ss rAAV CMV-Luc vector or  $1 \times 10^{10}$  particles of ds rAAV CB-EGFP virus were preincubated with anti-AAV2 capsid guinea pig polyclonal serum diluted in phosphate-buffered saline (PBS) for 45 minutes at room temperature in a total volume of 50  $\mu$ l. The final dilution of anti-AAV2 capsid guinea pig sera was from 1:500 to 1:2000. These virus-serum mixtures were added to C2C12 myotubes in a final volume of 450  $\mu$ l and incubated for 72 hours. For ss rAAV CMV-Luc infection, C2C12 myotubes were then changed to fresh DMEM containing 2% HS. After subsequent incubation at 37°C for 6 days, cells were collected for the luciferase assay. Myotubes transduced with the ds rAAV CB-EGFP virus were examined for EGFP expression by fluorescent microscope after incubation with the virus-serum mixture for 72 hours.

The neutralization assay also explored the issue concerning the practicality of modified rAAV2 usage in human clinical application. Pooled, purified, human intravenous immunoglobulin G (IVIG) was purchased from Sigma and solubilized by PBS to a concentration of 100 mg/ml. IVIG dilutions ranging from 1:50 to 1:500 were then made in PBS.  $2 \times 10^{10}$  ss rAAV CMV-Luc vectors were then exposed to various human IVIG dilutions at 37°C for 60 minutes. Subsequently, the ss rAAV CMV-Luc-serum mixtures were added in C2C12 myotubes for 72 hours at 37°C. Next, viruses were removed by replacing with fresh DMEM with 2% HS.

Cells were incubated for 6 days and were then harvested for the luciferase assay. The neutralizing effect of human IVIG was analyzed by examining inhibition of luciferase activity.

The neutralizing titer was determined as the dilution of antibody at which 50% of transduction was inhibited. Neutralizing experiments were performed in triplicate in two independent experiments.

### **2.2.7 Luciferase assay**

The harvested cell pellets were washed with 1x PBS and then lysed in 100  $\mu$ l of luciferase lysis buffer (0.05% Triton X-100, 0.1 M Tris-HCl pH 7.8, 2 mM EDTA). The lysate was subsequently treated by freezing and thawing three times. The lysate was centrifuged at 12,000 rpm for 15 minutes in 4°C and 20  $\mu$ l or 40  $\mu$ l of supernatant was measured for light activity using the luciferase kit (Promega) with a luminometer. Protein content in each sample was determined by Bradford protein assay (BioRad). Luciferase activities were expressed as relative light units per milligram of protein (RLU/mg protein).

### **2.2.8 Statistical analysis**

Unpaired Student's *t* test was performed by one- or two-tailed test. All *in vitro* data were tested and were considered significant when  $P < 0.05$ . Data were shown as mean $\pm$ SEM.

## 2.3 Results

### 2.3.1 Generation of AAV2 capsid mutants

A previous study used alanine substitution mutagenesis to discover that the mutation of arginine residues at positions 585 or 588 completely eliminates the heparin-binding ability of AAV2 (250). In addition, the substitution of the arginine residues at positions 484 and 585 with acidic glutamate residues resulted in significantly reduced infection of liver tissue without affecting transduction of the heart using intravenous delivery (265). For these reasons, the mutant AAV2 capsid carrying triple mutations on the heparin-binding sites of AAV2 capsid was generated. This heparin-binding mutant (HBSmut) has the mutations at positions 585 and 588 from arginine to alanine, and the substitution of the arginine at amino acid 484 with glutamate (Figure 2).

Using the insertion of a peptide containing RGD motif, a group identified that positions after residues 139, 584, and 587 are tolerant to peptide insertion with display of the ligand on the particle surface (266, 267). According to this, the insertion of heterologous peptide after residue 587 of AAV 2 capsid has received the most attention since it locates between residues R585 and R588, the primary heparin-binding motif of AAV2 capsid. Hence, it has the potential to simultaneously disrupt heparin binding of AAV2 and retarget AAV2 vectors to a desirable tissue.

The peptide ASSLNIA was selected for the targeting of murine myofibers *in vivo* (258). In the present study, this muscle-specific peptide was introduced after amino acid 587 of the capsid gene (Figure 2). Since a recent work showed that different linker sequences flanking the inserted peptide correspond to the targeting effect of the peptide (266), two MTP-inserted mutants with different peptide linkers (587 TG MTP and 588 HB MTP) were designed. 587 TG MTP virus does not retain the heparin binding motif of the capsid at the site of peptide insertion while the

insertion of exogenous peptide on 588 HB MTP capsid still remain residues primarily involved in heparin binding. The modified AAV2 vector combining the mutations on heparin binding sites with the peptide insertion after amino acid 587 of capsid (HBSmutMTP) was also constructed.

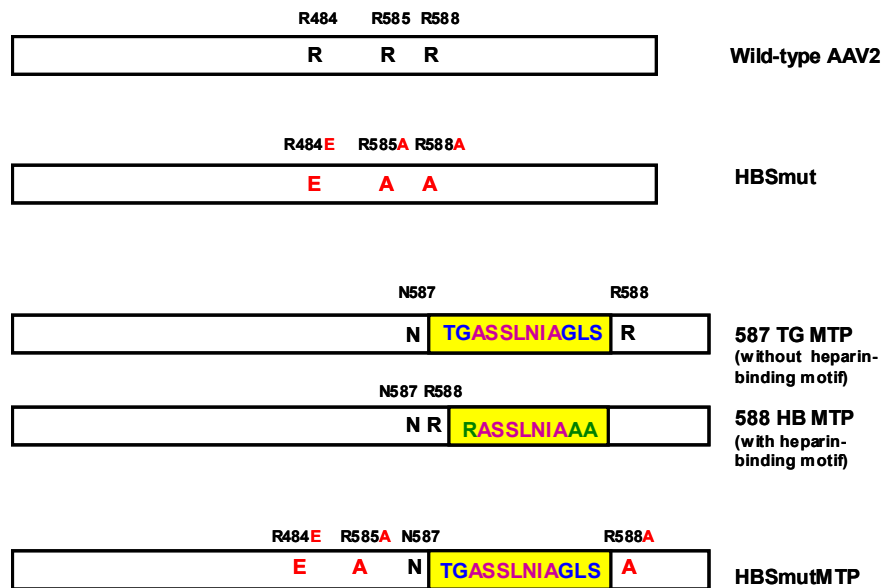


**Figure 2 Schematic representation of modified AAV2 capsid amino acid sequences**

Constructs were generated with residue mutations, MTP insertions flanked by two different linkers, or the combination of residue mutations and MTP insertion. Changes compared to the wild-type AAV2 amino acid sequence are highlighted in red letters. There are five putative loop regions (Loop I-V) within AAV2 capsid protein. Insertions of muscle-specific peptide are displayed at Loop IV, which is in a pocket conformation as a receptor anchor (268).

Sixty monomers of the VP1, VP2, and VP3 structural proteins assemble to form an intact AAV2 viral particle. Since the capsid proteins, VP1, VP2, and VP3 share overlapping sequences at their C termini including a peptide-insertion site after position 587, the small targeting peptide introduced after residue 587 is present in all 60 capsid subunits that make up the viral particle (Figure 3). Therefore, sixty muscle-specific peptides are present on a modified virion.

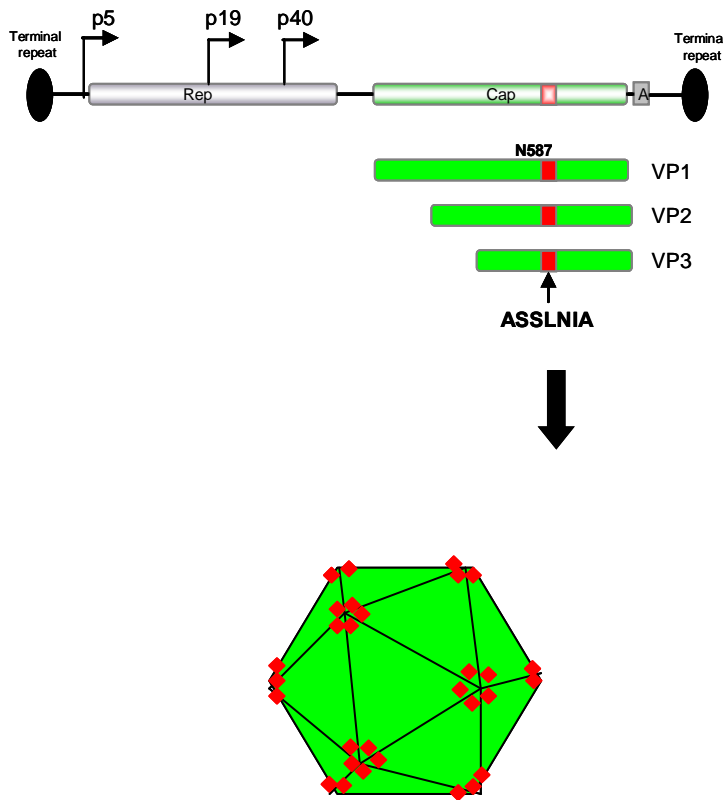


**Figure 3 Topology of the AAV2 capsid with inserted muscle-specific peptide**

**Introducing the coding sequence of MTP that directs specific muscle binding on AAV2 *cap* gene mediates the production of muscle-targeting rAAV virus. The inserted MTP (red) is displayed at the fivefold axis of symmetry of each subunit on the surface of AAV2 virion (green) (269).**

The X-ray structure of AAV2 capsid was used to analyze the peptide-inserted capsid structures at the molecular level. Compared to the structure of wild-type AAV2 VP3 monomer (Figure 4), an external loop, containing the RXXR domain (X is any amino acid), that conferred a heparin-binding phenotype was missing in the 587 TG MTP VP3 subunit (Figure 5). In contrast, 588 HB MTP retained the loop structure containing the RXXR motif similar to that of wild-type AAV2 capsid subunit (Figure 6). The insertion of MTP ligand did not destroy this loop structure which was required for heparin binding in 588 HB MTP virus. The surface charge distribution on the VP3 subunits from peptide-modified mutants was also examined. As expected, both unmodified and 588 HB MTP VP3 monomers had shown a positive charge on the loop-like structure presenting the RXXR motif (Figure 7). Although 587 TG MTP VP3 had the positively charged force at the C-terminal of the inserted peptide, this location did not have an extended loop-like structure available for heparin binding and the heparan sulfate consensus-binding sequences required at least two basic residues close to each other which were also missing at this positively charged area (270).



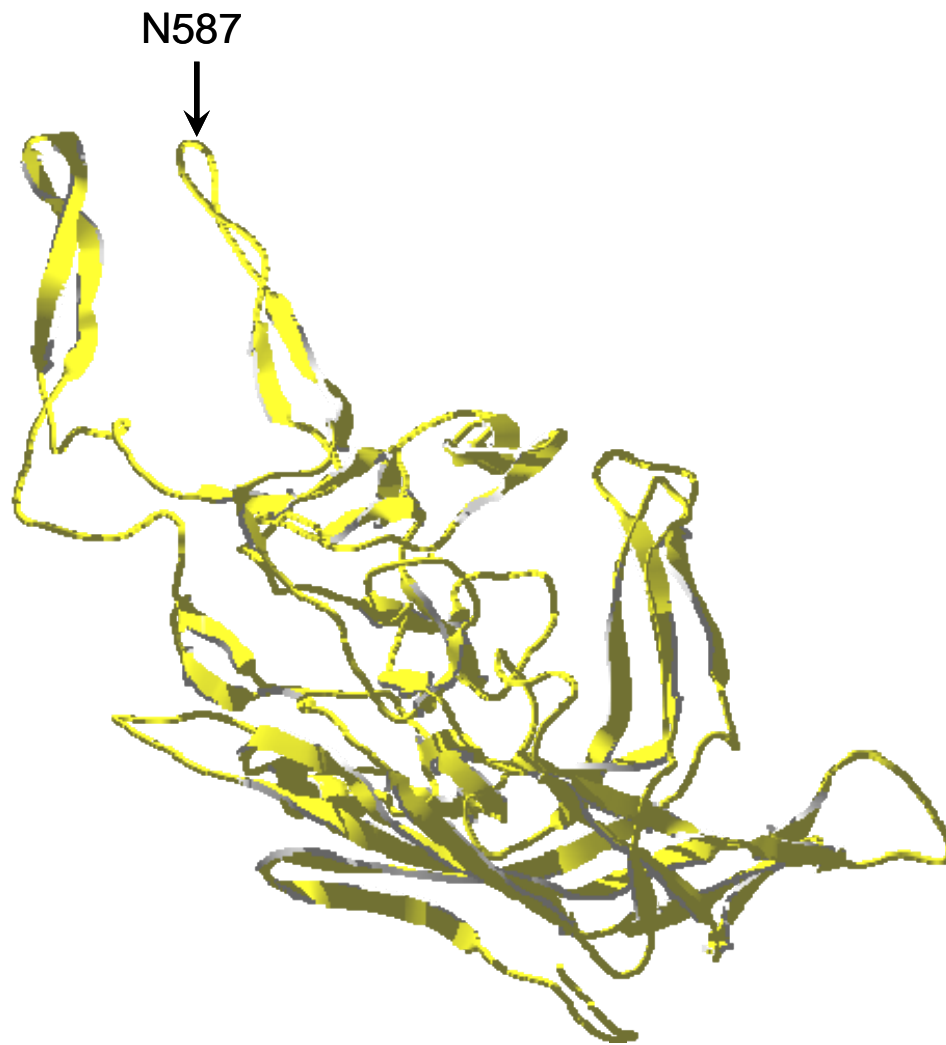


**Figure 4** Ribbon drawing of the wild-type AAV2 VP3 subunit

Small arrow indicates the location of residue 587. The molecular model was generated by Swiss-Model.



**Figure 5** Ribbon representation of a 587 TG MTP VP3 monomer

The inserted muscle-specific ligand is highlighted in red. The amino acids displayed on the unmodified rAAV2 are represented as green. This capsid monomer was generated using Swiss-Model.

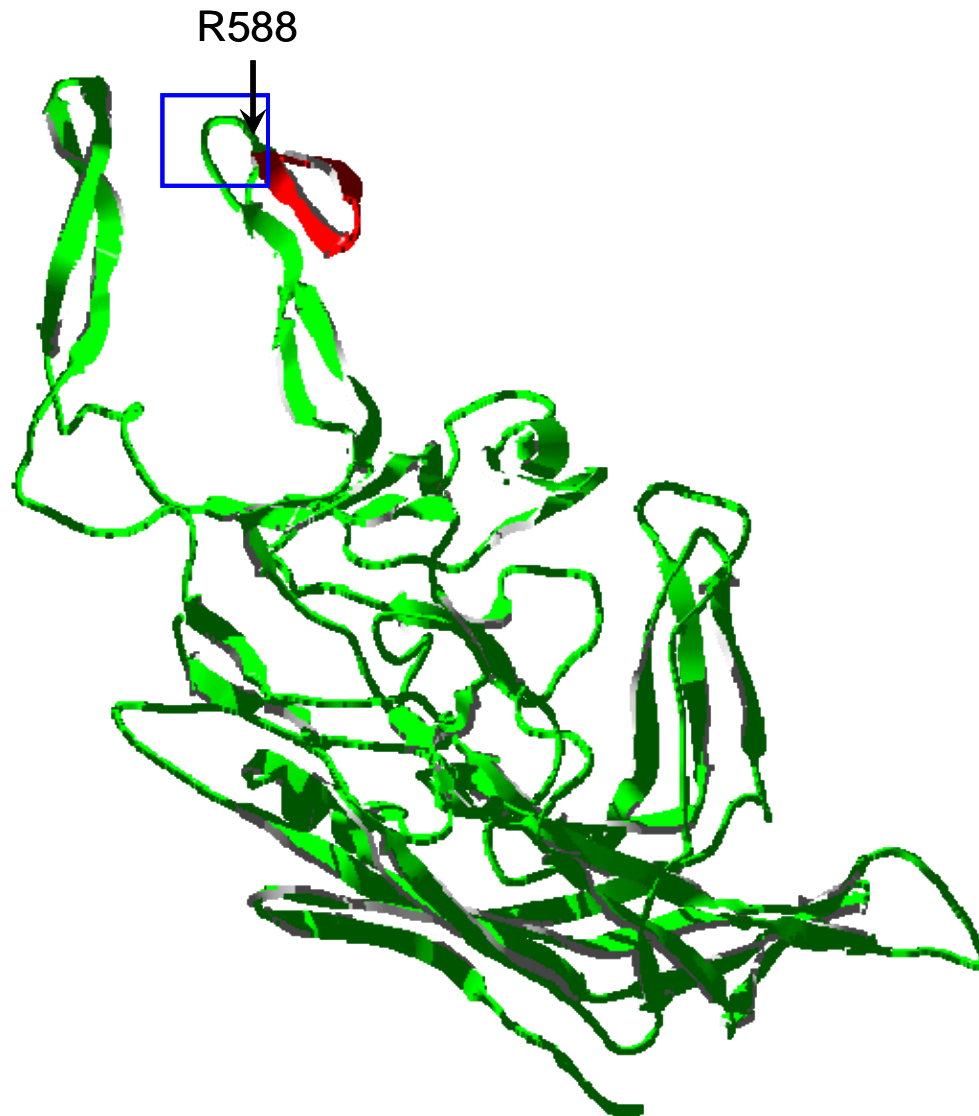
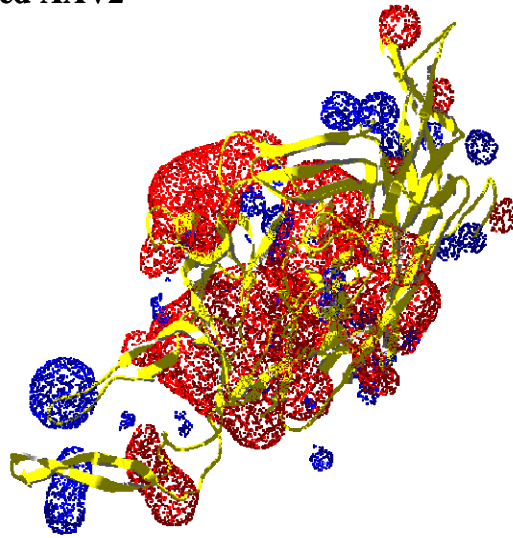


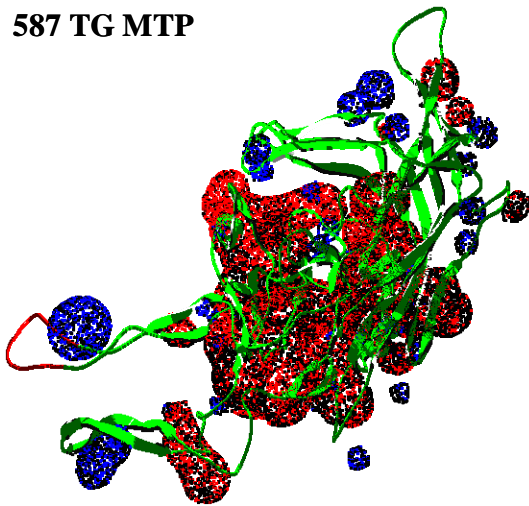
**Figure 6** Ribbon representation of a 588 HB MTP VP3 monomer

The inserted muscle-specific ligand is highlighted in red. The amino acids displayed on the unmodified rAAV2 are represented as green. Small arrow indicates the location of R588. The loop containing the heparin-binding motif, the RXXR domain, is marked by blue rectangle. This capsid monomer was generated using Swiss-Model.

### Unmodified AAV2



### 587 TG MTP



### 588 HB MTP

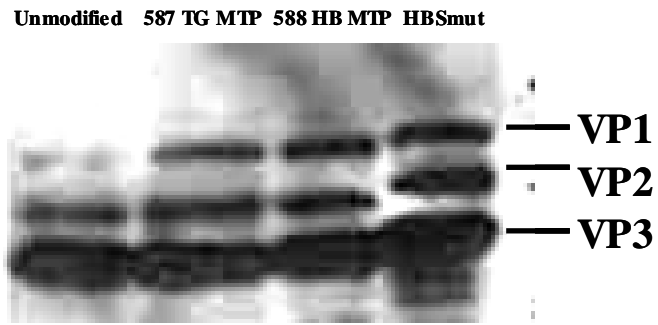


Figure 7 The electrostatic surface potential of VP3 monomers

The electrostatic surface potential of VP3 subunits were calculated with Coulomb. Red dots indicate the negatively charged regions and blue dots reveal the positively charged areas.

DNA dot-blot assays were performed to detect the viral yields of all mutant AAV vectors. The dot-blot assay examines the titer of AAV particles that contain DNase-resistant AAV genomes. The HBSmut, 587 TG MTP, and 588 HB MTP mutants created modified AAV2 vectors with titers comparable to that of wild-type AAV2. However, the HBSmutMTP mutant was tested negative by the dot-blot assay. This result implied that a combination of peptide insertion and heparin-binding mutations led to unwanted damage in viral assembly or packaging due to the creation of too many modifications within the *cap* gene. Either the mutant capsids of HBSmutMTP were unstable and no longer protected vector genomes from DNase digestion, this mutant generated empty viral particles, or the mutant produced intact AAVs at a low yield and the sensitivity of the dot-blot assay was not sufficient to detect low numbers of packaged viral genomes.

To confirm the capsid protein composition of modified rAAVs, Western blotting was utilized to determine viral proteins from virus preparations having equivalent numbers of genome-containing virions (Figure 8). The stoichiometry of the VP1, VP2, and VP3 proteins from the heparin-binding mutant (HBSmut) or peptide-modified viruses (587 TG MTP and 588 HB MTP) was similar to that of the three capsid proteins from the wild-type virion.



**Figure 8 Capsid protein analysis of modified rAAV2 vectors by Western blot**

Similar numbers of rAAV genome-containing particles ( $2 \times 10^{10}$ ) were separated on 10% SDS-PAGE and analyzed by Western blot, using anti-AAV2 capsid guinea pig sera.

### 2.3.2 Transduction efficiencies of modified vectors in cultured myotubes

Previous studies have shown that rAAV2 vectors can transduce muscle cells to result in the expression of therapeutic genes via intramuscular injection (271, 272). However, the relative infectivity of AAV2 for muscle fibers compared with other cell types, such as immortalized cell lines, or hepatocytes is low (265). The reason for this inefficiency of muscle transduction may reflect insufficient interaction between AAV capsid and the cell surface receptor of muscle. In order to validate the muscle-transduction efficiencies of these capsid mutants *in vitro*, murine C2C12 myotubes were used here because MTP incorporated into the AAV capsid was originally isolated from phage selection in C2C12 myotubes (258) and differentiated C2C12 myotubes express many of the proteins presented in adult skeletal muscle. Using ss rAAV vectors expressing the luciferase reporter gene from the CMV promoter, these modified vectors were initially tested for their abilities to infect C2C12 myotubes (Figure 9). Compared to unmodified vector, the peptide-modified ss rAAV 587 TG MTP and ss rAAV 588 HB MTP viruses with a genomic particle amount of  $2 \times 10^{10}$  were able to transduce differentiated C2C12 myotubes ( $P > 0.05$ ). In comparison to unmodified ss rAAV transduction efficiency, peptide-modified ss rAAV 588 HB MTP vector containing heparin binding motif showed a 47.47% increase in myotube transduction although ss rAAV 587 TG MTP vector transduction decreased approximately 26.28%. In marked contrast, impairment of the heparin-binding sites of capsid by mutation significantly reduced viral transduction in C2C12 myotubes. ss rAAV HBSmut was unable to achieve more than 0.038% transduction efficiency as compared to unmodified ss rAAV virions ( $P < 0.05$ ).

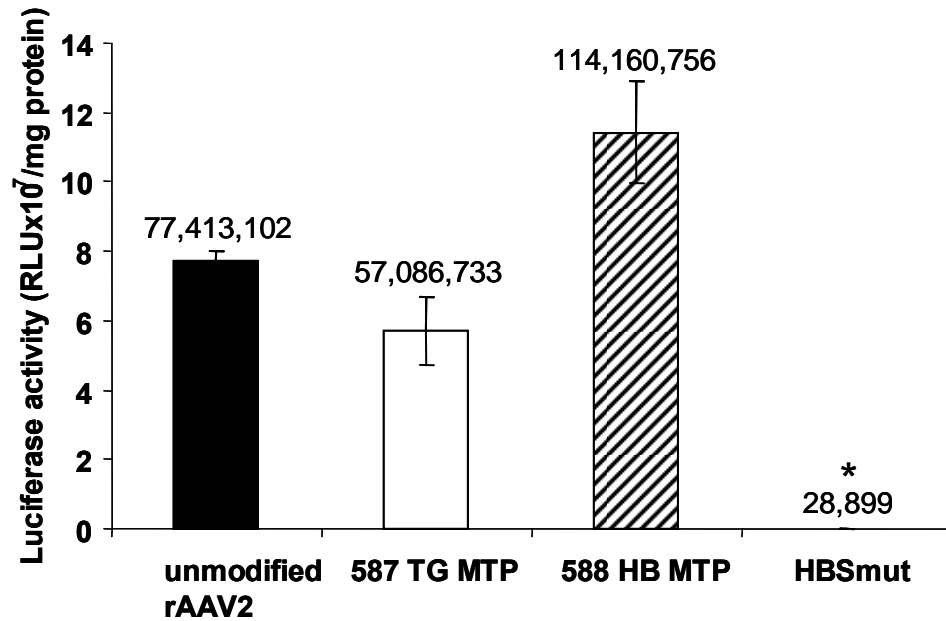


**Figure 9** Efficiency of modified rAAV-mediated gene transfer to C2C12 myotubes

Mouse C2C12 myotubes were infected with  $2 \times 10^{10}$  genomic particles/well of ss rAAV CMV-Luc vector which carries either unmodified capsid, peptide-inserted capsid, or heparin-binding mutated capsid in 24-well plates. After 3 days, myotubes were replaced by fresh DMEM containing 2% HS and subsequently incubated for 6 days. Luciferase activity was then analyzed to evaluate the transduction efficiencies of modified rAAV vectors. Compared to unmodified vector, peptide-modified vectors, 587 TG MTP and 588 HB MTP, maintained their transduction efficiencies in C2C12 myotubes ( $P > 0.05$ ) while the heparin-binding mutant (HBSmut) remarkably decreased its myotube infectivity ( $P < 0.05$ ). \* $P < 0.05$  vs unmodified rAAV2 vector.



To confirm that these muscle-targeting effects of modified rAAV vectors were exclusively due to the modification of viral capsid, an additional control experiment was performed, where the transduction assay in C2C12 myotubes was carried out with ds rAAV vectors expressing the EGFP indicator gene from the CB promoter (Figure 10). As expected, this experiment yielded similar results when myotubes were infected with  $1 \times 10^{10}$  of unmodified or modified ds rAAV CB-EGFP vectors. Based on the determination of EGFP expression, ds rAAV 587 TG MTP vector showed less effective myotube transduction than unmodified ds rAAV vector. In addition, the EGFP signal detected in ds rAAV 588 HB MTP-infected myotubes was comparable to that of myotubes infected by unmodified virus. The heparin-binding mutant dramatically eliminated luciferase activity driven by the CMV promoter in ss rAAV HBSmut-transduced C2C12 myotubes (Figure 9). Similarly, EGFP-positive myotubes were essentially undetectable in the infection of ds rAAV HBSmut vectors containing the CB-EGFP expression cassette (Figure 10).

Taken together, these results highlighted the simple insertion of MTP coding sequence in capsid is a more feasible way to manage AAV muscle tropism than the heparin-binding mutation of viral capsid. In addition, the transduction efficiencies of modified rAAV vectors in C2C12 myotubes are solely directed by their capsid modifications, since vectors with different expression cassettes yield the same results.

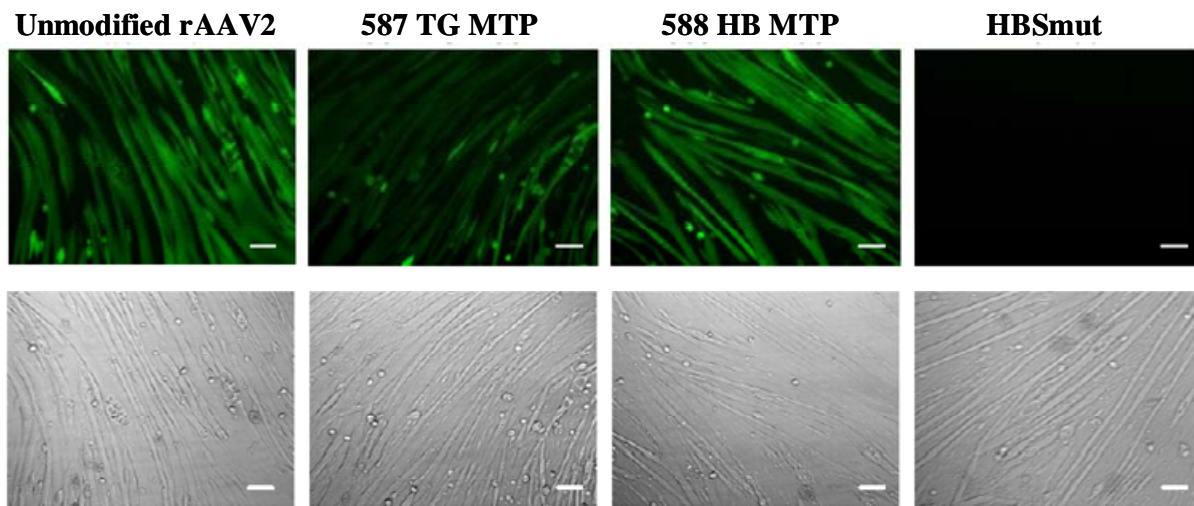


**Figure 10 Examination of rAAV vectors in myotube transduction by fluorescent microscopy**

C2C12 myotubes were transduced with ds rAAV CB-EGFP vectors at  $1 \times 10^{10}$  genomic particles/per well in 24-well plates. EGFP expression driven by the CB promoter was then observed under a Nikon TE-300 inverted fluorescent microscope. Pictures were taken at 72 hours after infection. Fluorescent photography is shown in the upper panel and the morphology of C2C12 myotubes on the same field as the fluorescent image is displayed in the lower panel. Peptide-modified vectors, 587 TG MTP and 588 HB MTP, revealed their infectivities in myotubes, but the heparin-binding mutant completely lost its ability to transduce cultured myotubes. Scale bar, 100 $\mu$ m.

### 2.3.3 Targeting selectivities of modified vectors

In addition to targeting ability to the desired cell type, safety and efficacy of retargeted AAV vectors would be further enhanced by avoiding vector uptake into non-target cells. The ultimate aim in this study is to generate a muscle-specific AAV vector for mature myotube targeting in order to cure diseased myofibers. Thus, rAAV-mediated gene transfer in myoblasts is not desired.

To evaluate the selectivity of modified vectors, undifferentiated murine C2C12 myoblasts (the progenitor cell line of differentiated C2C12 myotubes) were infected with modified rAAV CMV-Luc vectors carrying either wild-type capsid or modified capsid. In direct contrast to reporter gene expression produced in C2C12 myotubes, peptide-modified vectors, rAAV 587 TG MTP and rAAV 588 TG MTP, remarkably lowered reporter gene expression than unmodified rAAV in C2C12 myoblasts ( $P<0.05$ ) (Figure 11). rAAV 587 TG MTP vector resulted in a 92.59% decrease in gene expression in myoblasts and rAAV 588 HB MTP vector reduced its myoblast transduction by 96.95%. Similarly, rAAV HBSmut displayed extremely low infectivity in C2C12 myoblasts compared to the unmodified virus ( $P<0.05$ ).

According to these observations, there was the possibility that the cellular receptor recognized by the muscle-targeting peptide is downregulated in the undifferentiated C2C12 myoblasts (273).

## C2C12 myoblasts

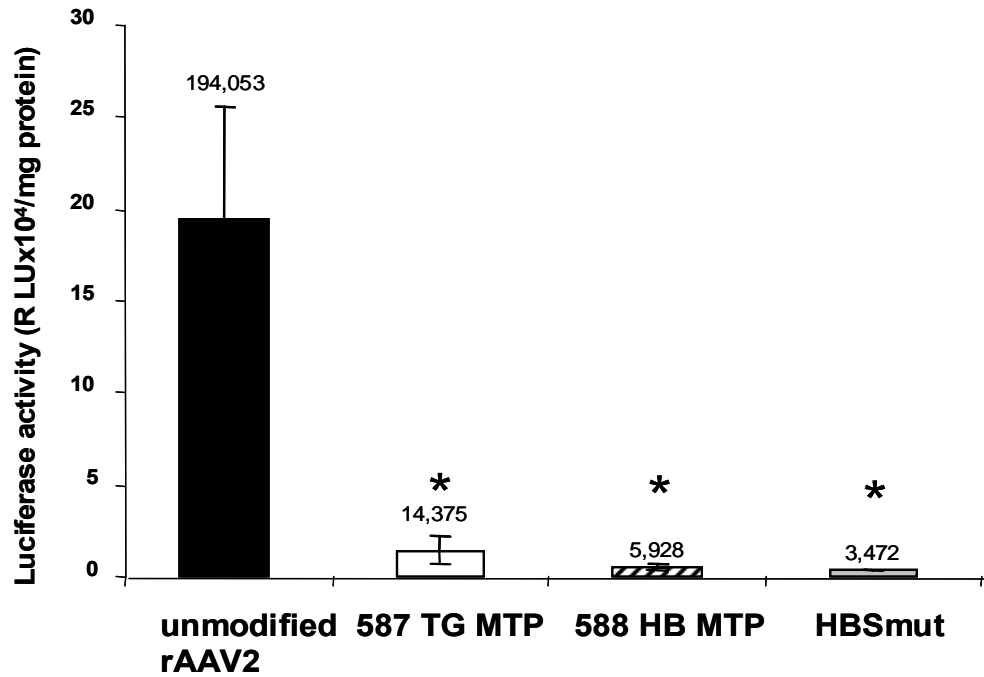


Figure 11 Effect of capsid modification on rAAV-mediated gene transfer in C2C12 myoblasts

C2C12 myoblasts were infected with rAAV vectors in the presence of Ad5 and luciferase activity was analyzed 48 hour later. Ad5 coinfection was utilized to maximize rAAV transduction by enhancement of vector second-strand synthesis (274). \* $P < 0.05$  vs unmodified rAAV2 vector.

rAAV vectors have a predominantly hepatic tropism when delivered systemically (275, 276). In neonates, vector genomes transduced in the liver are rapidly degraded when hepatocytes undergo cell division during liver growth. However, AAV vector DNA sequestered in the adult liver remains stable because the liver cells are largely quiescent in adults (148). Therefore, undesired liver targeting not only hampers transduction efficiency at the muscle, but also gives rise to safety concerns about accumulation of large amounts of vector DNA in the adult liver, where targeted viral DNA is difficult to be cleaned out by host spontaneous mechanism.

In this regard, ss rAAV CMV-Luc carrying different peptide-modified capsids was used to examine if peptide-modified rAAV vectors retained with them a native tropism of AAV2 toward the infection of HepG2 cells, a human hepatocellular carcinoma cell line. Compared to unmodified AAV2 virus, CMV-driven luciferase expression from rAAV 587 TG MTP totally abolished in transduction of HepG2 cells ( $P<0.05$ ) (Figure 12). Furthermore, rAAV 588 HB MTP represented a 10.72-fold decrease in luciferase activity of infected HepG2 cells ( $P<0.05$ ).

These results show that the insertion of the muscle-targeting peptide after residue 587 of capsid dramatically detargeted peptide-modified vectors from hepatocytes while these peptide-modified vectors maintained their ability to transduce myotubes at an acceptable level.

## HepG2 cells

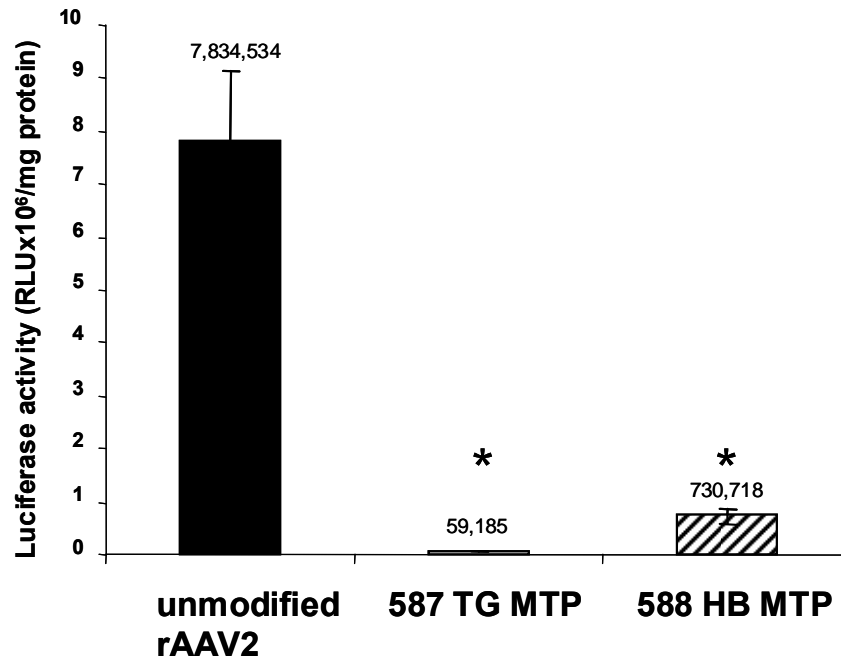


Figure 12 Peptide-modified rAAV vectors in gene delivery to a human liver-derived cell line

HepG2 cells were transduced by rAAV at  $10^3$  genomic particles/cell in the presence of Ad5. Cells were then lysed and luciferase activity was determined at 48 hours after infection. \* $P < 0.05$  vs unmodified rAAV2 vector.

Using ss rAAV vectors containing the luciferase gene under control of the CMV promoter, this study next sought to determine whether modified rAAV vectors displayed selectivity in a number of human non-muscle cell lines. For this purpose HeLa cells, the human cervix epithelioid carcinoma cell line, was first employed in testing targeting specificity of modified AAV2 vectors. As demonstrated by luciferase enzyme activity, transduction of HeLa cells with rAAV HBSmut, rAAV 587 TG MTP, or rAAV 588 HB MTP vectors resulted in a 97.96%-99.51% decrease in reporter gene activities compared to the vector carrying a wild-type capsid ( $P<0.05$ ) (Figure 13).

Moreover, HEK 293 cells, a human embryonic kidney cell line, were also infected with modified AAV2 vectors to ensure the specific targeting effect from these mutant vectors. Consistently, rAAV HBSmut, rAAV 587 TG MTP, and rAAV 588 HB MTP viruses were significantly impaired in their ability to transduce HEK 293 cells with efficiencies ranging from 0.45% to 2.69% of unmodified AAV2 transduction ( $P<0.05$ ) (Figure 14).

Finally, this study further assessed if peptide-modified vectors could alter their targeting effects in the human glioblastoma tumor U-87MG cells to decrease nonspecific targeting. The result showed that transduction efficiencies of rAAV 587 TG MTP and rAAV 588 HB MTP vectors in U-87MG cells were very poor compared to unmodified vectors ( $P<0.05$ ) (Figure 15).

These *in vitro* transduction assays demonstrated that rAAV HBSmut vector fails to mediate gene expression in all tested cells including C2C12 myotubes. In contrast, both peptide-modified vectors are capable of targeted gene delivery to myotubes and efficiently eliminate their targeting in non-target cells. It is possible that the targeted receptor of the selected muscle-targeting peptide is not ubiquitously expressed or activated on non-muscle cells.

## HeLa cells

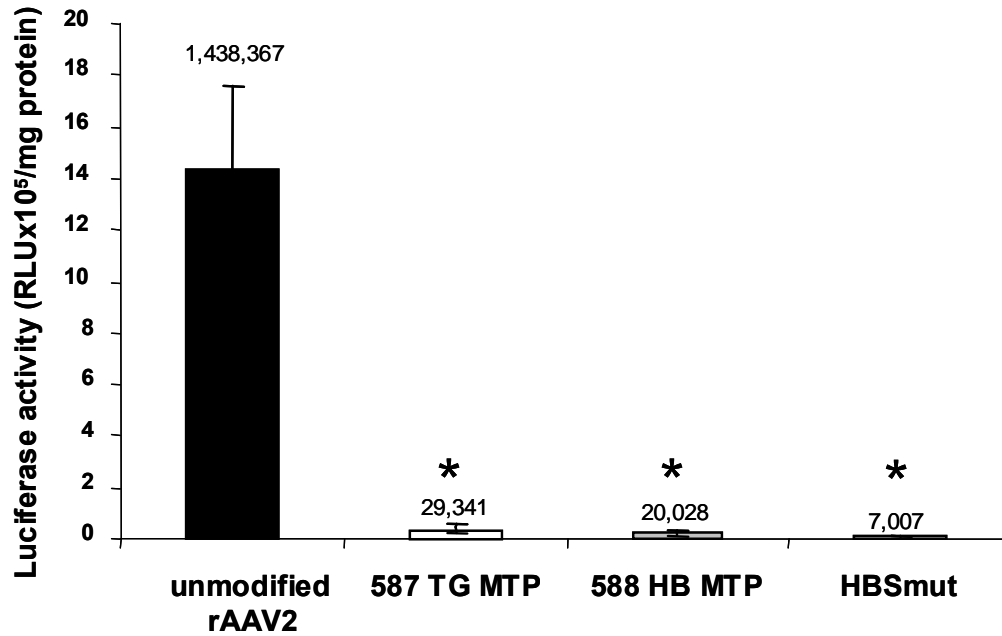


Figure 13 Infection of rAAV vectors in human cervix epithelioid carcinoma HeLa cells

HeLa cells were exposed for 48 hours to either modified or unmodified ss rAAV CMV-Luc vectors at an MOI of  $10^3$  with Ad5 coinfection. Cells were then harvested for luciferase assay. \* $P < 0.05$  vs unmodified rAAV2 vector.



## 293 cells

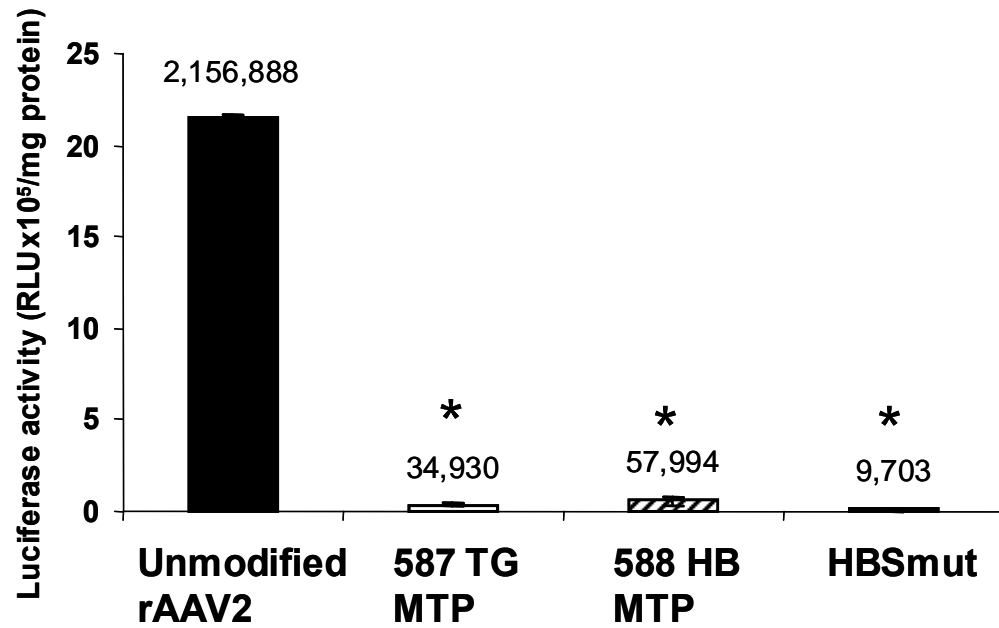


Figure 14 Gene delivery mediated by rAAV vectors in human embryonic kidney 293 cells

HEK 293 cell transduction rates were assessed after preincubation of the cells with ss rAAV CMV-Luc vector at an MOI of  $10^3$  in the presence of Ad5 for 48 hours. \* $P < 0.05$  vs unmodified rAAV2 vector.

## U-87MG cells

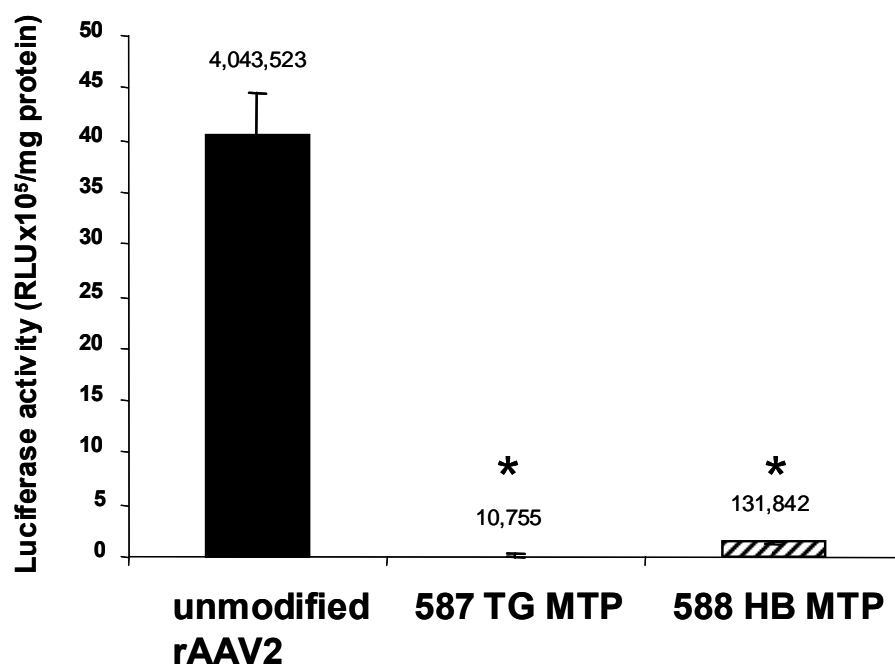


Figure 15 Luciferase expression in human glioblastoma tumor U-87MG cells with rAAV transductions

ss rAAV CMV-Luc vectors at an MOI of  $10^4$  were incubated with U-87MG cells for 48 hours at 37°C. Cells infected with either modified or unmodified rAAV vectors were then lysed and analyzed for luciferase activity. \* $P < 0.05$  vs unmodified rAAV2 vector.

### 2.3.4 Neutralization profiles of peptide-modified rAAV vectors

Humoral immunity is the predominant host immune response following either wild-type AAV infection or rAAV transduction (277-279). The presence of serum antibodies directed against AAV2 is very common in humans. For practical application of human gene therapy, this is potentially important because the preexisting immunity against vector capsid could impede *in vivo* rAAV transduction. Therefore, immune responses to AAV-based vectors need to be resolved when bringing this vector system to the clinic. Engineering of rAAV vector capsids to circumvent host antivector immune responses is an attractive approach to overcome preexisting AAV immunity and to facilitate vector readministration. A previous study has demonstrated that a 14 amino-acid peptide insertion after residue 587 of AAV2 capsid enables the vector to escape the effects of the neutralizing antibody (222). According to this, the resistance of MTP-inserted rAAV vectors to antibody-mediated neutralization was determined in here.

First, the interference of anti-AAV2 capsid guinea pig serum with unmodified or peptide-modified ss rAAV CMV-Luc transduction in C2C12 myotubes was analyzed since guinea pig serum used in this study has been performed as a positive control to characterize the presence and specificity of anti-AAV antibodies in humans (221). Neutralizing titers were defined as the antibody dilution where viral transduction was reduced by 50% ( $N_{50}$ ). The applied serum and antibody reagent acted as neutralizers when the  $N_{50}$  for unmodified AAV2 was 1:320 or higher, in agreement with previously published studies (222). At a 1:2,000 serum dilution, unmodified AAV2 vector was completely neutralized while peptide-inserted mutants, 587 TG MTP and 588 HB MTP, still retained substantial infectivity (Table 2 and Figure 16). The  $N_{50}$  of unmodified virus was determined as 1:6,315. ss rAAV 587 TG MTP produced the neutralizing titer at a dilution of 1:1,450 and ss rAAV 588 HB MTP did not reduce transduction to 50% even at a

1:500 serum dilution. Interestingly, over 10% of ss rAAV 587 TG MTP virions remained infectious and 62.75% of ss rAAV 588 HB MTP vectors possessed transduction ability when the neutralization assay was performed at the lowest serum dilution of 1:500 that totally inhibited luciferase activity from unmodified vector infection. At this dilution, 587 TG MTP and 588 HB MTP vectors demonstrated 77- and 481-fold enhanced resistance, respectively, to neutralizing antibodies compared to the unmodified vector ( $P<0.05$ ).

ds rAAV CB-EGFP vectors were also used to assess the resistance of peptide-modified vectors to neutralization by guinea pig antiserum. As described above, C2C12 myotubes infected with unmodified ds rAAV CB-EGFP virus completely lost EGFP expression in the presence of guinea pig anti-AAV2 serum at a 1:1,000 dilution (Figure 17). Transduction by ds rAAV 587 TG MTP vector yielded detectable EGFP-positive myotubes at a 1:500 dilution. In addition, ds rAAV 588 HB MTP vector was able to escape the neutralizing antibodies in guinea pig serum and enabled myotubes to display the strong EGFP signal at a serum dilution of 1:500.

Although both peptide-incorporated vectors showed resistance to guinea pig antiserum neutralization, 588 HB MTP vector was superior to 587 TG MTP vector in escaping the preexisting humoral immune responses.

**Table 2 Neutralization of peptide-modified AAV vectors by guinea pig antiserum**

rAAV vector	Neutralizing titer ( $N_{50}$ )
Unmodified rAAV2	1:6,315
rAAV 587 TG MTP	1:1,450
rAAV 588 HB MTP	< 1:500

The  $N_{50}$  was calculated by using the Reed-Muench formula (280). Data represents as the dilution of serum that completely inhibited viral transduction in 50% of the cells.

### Anti-AAV2 cap guinea pig serum

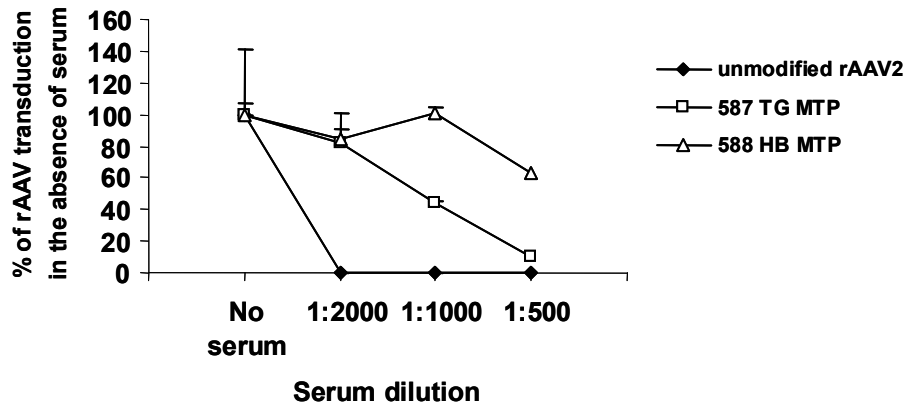
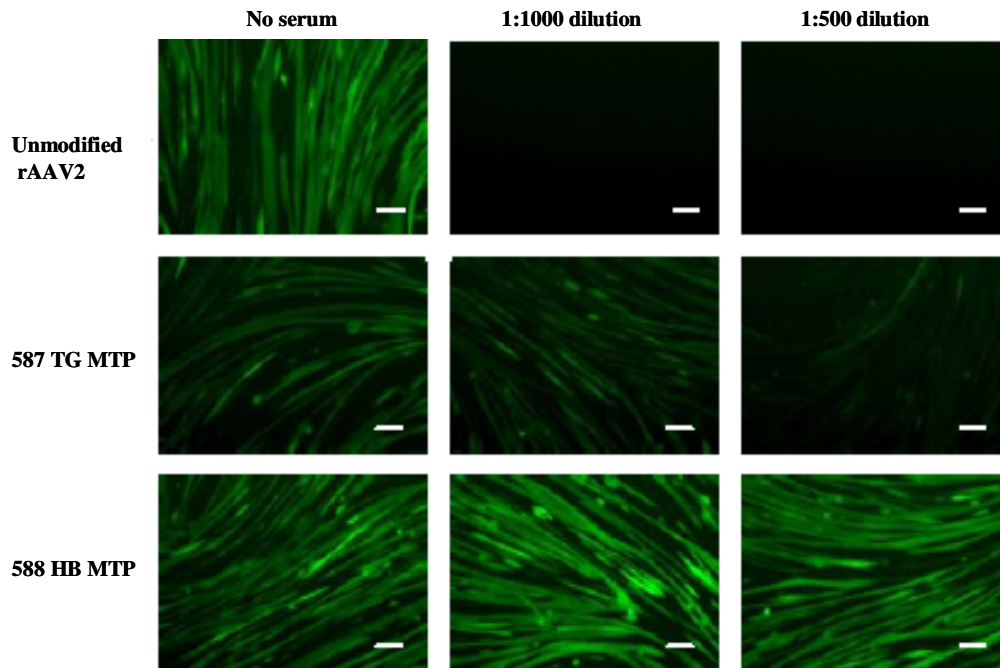


Figure 16 Effect of guinea pig anti-AAV2 serum on peptide-modified rAAV infection of C2C12 myotubes

Differentiated myotubes were infected with ss rAAV CMV-Luc vector alone or after coincubation with anti-AAV2 cap guinea pig serum at an indicated serum dilution. Myotubes were then analyzed for luciferase activity at 9 days after infection. Transduction by unmodified rAAV was completely suppressed with a serum dilution of 1:2,000 ( $P < 0.05$ ). Even at a serum dilution of 1:1,000 or 1:500 (much lower than the  $N_{50}$  of unmodified rAAV), peptide-modified vectors, 587 TG MTP and 588 HB MTP, were significantly more resistant to neutralization than unmodified rAAV ( $P < 0.05$ ).



**Figure 17 Neutralizing activity against peptide-modified rAAVs in guinea pig antiserum**

C2C12 myotubes were infected with ds rAAV CB-EGFP vector alone (left panel) or after cocubation with guinea pig antiserum at a dilution of 1:1,000 (middle panel) or 1:500 (right panel). EGFP expression was detected by fluorescence microscopy at 72 hours after transduction. Scale bar, 100 $\mu$ m. Infection of unmodified rAAV resulted in undetectable EGFP signal at a serum dilution of 1:1,000. Unlike unmodified rAAV, 587 TG MTP and 588 HB MTP vectors conferred neutralization resistance to guinea pig antiserum at a serum dilution of 1:1,000 and 1:500.

In an attempt to explore whether peptide-inserted vectors were resistant to antibody neutralization in a large portion of the human population, human IVIG was utilized in the neutralization assay. IVIG is purified human IgG and it is isolated from pooled human serum. Because IVIG is prepared from thousands of normal blood donors, it represents nearly all immune responses within the donor population. In this study, the donor population of IVIG (Sigma) is restricted to individuals in USA. All commercial sources of human IVIG have been proven to contain high AAV2 neutralizing titers ranging from 1:1,043 to 1:3,330 at an IgG concentration of 100 mg/ml (281).

When conducting the *in vitro* neutralization assay with human IgG, ss rAAV CMV-Luc vectors were preincubated with different dilutions of IVIG (100 mg/ml) before transduction of C2C12 myotubes. After 9 days of infection, luciferase activity was measured to evaluate the neutralizing resistance of peptide-modified mutants. At an IVIG dilution of 1:500, transduction by 587 TG MTP vector was severely impaired as that of unmodified AAV2 vector. Unmodified rAAV and rAAV 587 TG MTP vectors reduced their transgene expression by 76.34% and 89.62%, respectively (Table 3 and Figure 18). In contrast, 588 HB MTP vector was 2.31- to 5.26-fold more resistant to neutralization by IVIG ( $P<0.05$ ) and delivery of 588 HB MTP vector only yielded 45.35% reduction in luciferase activity at the same IVIG dilution. Even at a 1:250 IVIG dilution, 588 HB MTP vector still had an infectivity up to 53.59% while unmodified rAAV and 587 TG MTP vectors showed no more than 14% transduction ( $P<0.05$ ). Strikingly, transduction of 588 HB MTP vector exhibited a 14.68-fold improvement compared to unmodified vector ( $P<0.05$ ) when the neutralization assay was using a 1:50 IVIG dilution that completely neutralized unmodified and 587 TG MTP vectors. Moreover, unmodified rAAV and 587 TG MTP vectors generated the neutralizing titer at an IVIG dilution of 1:1,106 and 1:1,383,

respectively. The neutralizing titer of 588 HB MTP virus was determined as a 1:423 IVIG dilution.

According to these data, only 588 HB MTP vector had a significantly increased level of resistance to IVIG neutralization.

**Table 3 Neutralization of peptide-inserted mutants by human IVIG**

<b>rAAV vector</b>	<b>Neutralizing titer (<math>N_{50}</math>)</b>
<b>Unmodified rAAV2</b>	<b>1:1,106</b>
<b>rAAV 587 TG MTP</b>	<b>1:1,383</b>
<b>rAAV 588 HB MTP</b>	<b>1:423</b>

The  $N_{50}$  was calculated by using the Reed-Muench formula (280). Data represents as the dilution of serum that completely inhibited viral transduction in 50% of the cells.



### Pooled human IgG (IVIg)

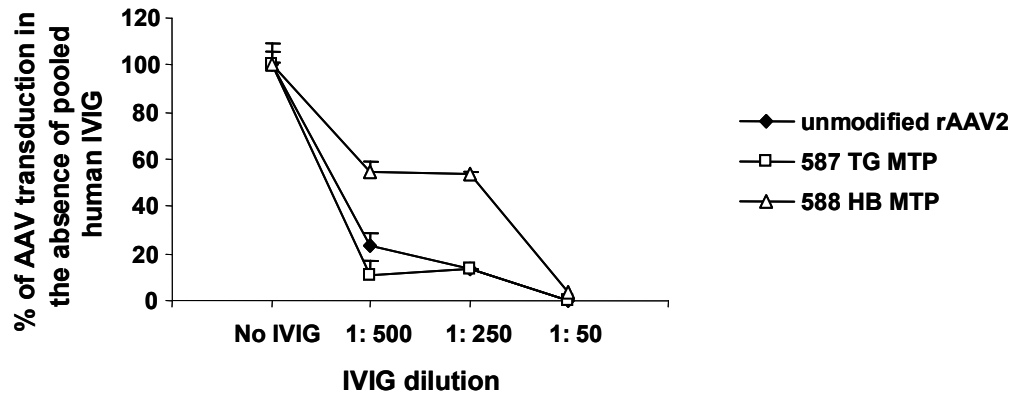


Figure 18 Characterization of rAAV neutralizing profile to human IVIG in C2C12 myotubes

Differentiated myotubes were transduced with ss rAAV CMV-Luc vector alone or after coincubation with human IVIG (100 mg/ml) at an indicated dilution. Myotubes were then measured for luciferase activity at 9 days after infection. Compared to unmodified rAAV and rAAV 587 TG MTP vectors, rAAV 588 HB MTP vector significantly increased resistance to human antibody neutralization at all tested IVIG dilutions ranging from 1:500 to 1:50 ( $P < 0.05$ ).

## 2.4 Discussion

Achieving efficient dissemination of gene delivery vectors throughout the myocardium and skeletal musculature of an adult is a prerequisite for successful treatment of striated muscle diseases because it subsequently directs sufficient expression of therapeutic genes in most, if not all, of the diseased muscles. Distribution of vectors to the muscles of an individual through the circulation by adopting a simple intravenous administration is imperative for clinical therapies. At present this is hampered by the native tropism of viral vectors, so that no available vector exists for muscle tropism without involvement of nonspecific targeting after a single injection via the intravenous route. Toward a realistic clinical goal, novel muscle-targeting vectors are required.

As the capsid is the sole mediator during viral cell entry, AAV retargeting can be accomplished by genetic modification of the capsid protein. To gain a tissue-specific rAAV vector, single-step insertion of targeting peptide into capsid is proven to remove native tropism of AAV2 in combination with provision of desired tropism. Although targeted gene delivery to specific vascular tissue (vena cava), brain, and lung have been developed by displaying a selected ligand on the surface of AAV2 (243, 257), inserting a suitable peptide into the AAV vector for augmenting muscle-specific binding has not been described. Here, the result showed that a small peptide ASSLNIA, originally selected by a random phage display library (258), can be incorporated into the capsid of AAV2 vectors and mediate enhanced specificity of targeted gene transfer to myotubes. This increased selectivity of AAV transduction did not need further capsid modification. Inclusion of the muscle homing peptide ASSLNIA not only displayed adequate vector infectivity in cultured myotubes but also exhibited an extremely low binding affinity for non-target cell types, such as undifferentiated myoblasts, hepatocyte-derived cells,

and embryonic kidney cells. Besides, both engineered peptide-modified AAV vectors were significantly more resistant to neutralization than virus carrying wild-type AAV2 capsid in guinea pig anti-AAV2 serum, albeit with a decreased level of resistance to neutralization by human IVIG. This study is the first to genetically modify AAV muscle tropism by using an insertion of a targeting peptide. The study sheds light on the solution of preexisting immunity against AAV2 vectors during clinical applications.

A good knowledge of the attachment receptors of AAVs, as well as of their crystal structures of capsid proteins, has greatly helped progress in using the system of ligand-directed targeting. At least two important parameters will shape the success of peptide-incorporated capsids for retargeting viral vectors. The first challenge is to choose the location for insertions of foreign peptides. The acceptable insertion sites must tolerate insertions without affecting either assembly or packaging of the virus capsid and these positions allow inserted ligands to be exposed on the surface of virus. Meanwhile, the insertion at the chosen site can interrupt the interaction between virus and cellular receptors in order to diminish the natural tropism of the vector. The crystallographic structure of the AAV2 capsid has been unveiled recently (201). In this model, the capsid protein subunit contains eight antiparallel  $\beta$ -strands that form a barreled structure common in the different parvovirus genres. Loops of variable length connect each strand of the  $\beta$ -barrel and extend outward to constitute the surface features of AAV. Alignments of sequences from all the parvovirus capsid proteins reveal that sequences of the  $\beta$ -barrel core are the most conserved (282). Mutations within these highly conserved regions usually abolish viral capsid formation (283). Conversely, sequence similarity of the loops is low. These variable sequence regions are allowed to present insertions. Loop GH is one of variable sequence regions and is required for binding to heparin. As mentioned, the position after residue 587 in the capsid

of AAV2 corresponding to an external loop (loop IV or GH) in the capsid could tolerate amino acid insertions without causing any deleterious effects on virus assembly or packaging (268). Consistent with previous studies, the peptide-modified vectors, 587 TG MTP and 588 HB MTP, represented viral titers comparable to that of unmodified virus (data not shown). In this study, the peptide-modified viruses were similar to the unmodified one in their ability to package a vector genome for efficient virion propagation. After an appropriate insertion site in the capsid has been chosen, the choice of targeting peptide must be made. It has been indicated that the nature of the inserted peptide may have important consequences on particle formation (284, 285). For example, peptides have fewer detrimental effects on viral yield than those containing multiple cysteine residues (286). On account of this, the chosen muscle-specific ligand did not possess any cysteines and it allowed both peptide-modified vectors to produce viral yields at reliable levels. The heparin-binding mutant (HBSmut) included three mutations (R484E, R585A, and R588A) that were located in the loop GH region, not in the  $\beta$ -barrel core. Thus, this mutant also resulted in a viral titer similar to that of unmodified vector as expected.

The *in vitro* transduction results described in this study provide proof that ligand-directed AAV muscle targeting displayed potential clinical value. The data showed a promising strategy to alter AAV2 tropism without disrupting viral replication and intracellular trafficking, since the peptide-modified vectors can be efficiently produced and retain their ability to direct transgene delivery to the nucleus of targeted C2C12 myotubes (Figure 9 and Figure 10). The insertion of a muscle-specific ligand into the viral capsid maintained the normal efficiency of the post-attachment steps of the peptide-modified vectors in myotubes. These post-attachment steps are the downstream events required for productive infection and they include escape from the endosome, migration to the nucleus, and viral uncoating by virtue of vector-mediated gene

expression. Additionally, specificity in the delivery of therapeutic genes is the next crucial issue for effective gene therapy in systemic treatment of MD. Indiscriminate gene delivery to unwanted cell types would certainly diminish the gene dose to the targeted muscle fibers and would probably be harmful. Knocking out the native tropism of AAV vectors is the best approach to achieve cellular specificity. Transduction of peptide-inserted vectors, 587 TG MTP and 588 HB MTP, on undesirable cell lines proved that these ligand-expressing viruses demonstrate a profile of gene transfer significantly different from that of virus carrying wild-type capsids. Both peptide-inserted vectors had a dramatic decrease ranging from 90.67% to 99.73% in gene transfer efficiency compared to unmodified AAV2 when they were used to infect C2C12 myoblasts, HepG2, HeLa, 293, and U-87MG cells (Figure 11~15). The decrease in effectiveness of vector-mediated gene transfer to undesired permissive cells suggests that this targeting method was both specific and restrictive. The PDB, SwissProt, nonredundant GenBank CDS translations, Spupdate and PIR data bases were used to search for the ASSLNIA sequence, but no matches were discovered in the previous study (258). Although the target receptor of the ASSLNIA peptide is not identified and it is not known whether this peptide represents a nature ligand, it seems clear that insertion of this muscle-specific peptide produced rAAV vectors with a restriction of the viral tropism to the desired myofibers. Ligand-directed muscle targeting remarkably improved the selectivity of targeted gene transfer in the *in vitro* assays. Thus, the peptide-engineered AAV vectors in this study give rise to the hope of transforming muscle-specific *in vivo* gene transfer through systemic routes from concept to reality.

Apart from cellular specificity of gene transfer vehicles, avoiding elimination and neutralization of vectors by the host immune responses is also a critical factor which can have an important effect on gene therapy. Anti-CD4 and Anti-CD40 Ligand (anti-CD40L) antibodies

have been used to suppress T-cell activation and B-cell activation through T-cell helper function, respectively while CTLA4-immunoglobulin fusion protein (CTLA4Ig) has been shown to inhibit T-cell activation by interfering with CD28-B7 costimulatory pathway between T and B cells. Therefore, these treatments would be expected to block, or at least to reduce primary host immune responses against rAAV vectors and facilitate viral delivery of therapeutic genes. Transient depletion of helper T cells with anti-CD4 antibodies at the initial rAAV2 exposure allowed successful transgene expression following vector readministration to skeletal muscle (287). Similarly, treatment with anti-CD40L antibody (MR1) and a soluble CTLA4Ig at the primary exposure to AAV permitted repeat vector delivery in mouse lung and prevented production of neutralizing antibodies (288). However, it should be noticed that these treatments do not specifically act on viral immunity but are involved in potentially detrimental general immunosuppression. Moreover, these reagents were much less effective when the individual had undergone a secondary immune response in which a high level of neutralizing antibodies against wild-type AAV2 already existed (221). In order to circumvent the above obstacles, the best way to prevent the virus from antibody binding is to genetically modify the AAV capsid based on the epitope map of the capsid protein.

Huttner *et al.* demonstrated that the insertion of an integrin-specific RGD ligand (L14, QAGTFALRGDNPQG) after position 587 of AAV2 capsid escaped the neutralizing effects exerted by 13 of the 15 neutralizing serum samples and efficiently infected targeted cell lines (222). In accordance with this finding, it is reasonable to assume that capsid modification after residue 587 is not only able to alter the AAV tropism but also to generate immune escape variants. Therefore, the ability of AAV antibodies from guinea pig antiserum or human IVIG to neutralize transduction by the peptide-modified vectors was investigated in C2C12 myotubes.

The 587 TG MTP vector without the RXXR heparin-binding domain was significantly more resistant to neutralization by guinea pig antiserum than the wild-type AAV2 capsid (Figure 16). But it had no effect on neutralization by IVIG (Figure 18). Such results could be explained by differences in the affinities or frequencies of anti-AAV2 capsid antibodies between guinea pig antiserum and IVIG. Although 587 TG MTP vector was not neutralization resistant in an *in vitro* IVIG neutralization assay, it did display some degree of immunogenic property different from unmodified vector and this acquired phenotype tended to be more resistant to preexisting antibodies since displayed a remarkable reduction of neutralization in guinea pig serum. Besides, *in vitro* neutralization occurred via direct antibody binding of viral capsids causing virus sequestration, interruption of viral attachment to cellular receptors, induction of viral aggregation, or inhibition of viral uncoating. Neutralization mechanisms *in vivo* can be more complex and are hard to mimick by an *in vitro* assay. *In vivo*, rAAV particles are also cleared by opsonization in addition to antibody-mediated direct interference of viral infectivity. Both neutralizing and non-neutralizing antibodies elicit phagocytosis and consequently enhance clearance of viral particles by coating virions with antibodies that also bind to Fc receptors on neutrophils and macrophages (289, 290). It may allow the effect of 587 TG MTP vector on IVIG neutralization to be assessed *in vivo* by the published murine model that reconstituted SCID mice with human IVIG (281).

More recently, a series of follow-up experiments was carried out in a dose-escalation clinical study of rAAV2-F.IX (Factor IX) delivered through the hepatic artery in humans with severe hemophilia B (223). The result indicated that T cell-mediated immunity, targeting the capsid of AAV2 vectors led to the destruction of transduced hepatocytes. This liver toxicity resulted in transient transaminitis and it limited the duration of therapeutic F.IX expression to a short-lived period of ~8 weeks. To further investigate this kind of cellular immune response,

Vandenberghe *et al.* evaluated activation of T cells by AAV capsids after intramuscular injection of vectors into mice and nonhuman primates (224). High level of T cells specific to AAV2 capsid was observed in the AAV2-injected macaques. T cells from mice injected with hu.13, an AAV isolate differing from wild-type AAV2 at only two residues other than in the RXXR heparin-binding domain, could not respond to AAV2 capsid antigens. It suggests that the presence of heparin binding directly correlates with activation of capsid-specific T cells. The mechanism by which heparin binding associated with the activation of T cell responses to AAV2 capsid was immediately emerged as a dendritic cell (DC) pathway. The data of binding studies showed that RXXR-containing vectors bound DCs whereas heparin-binding deficient variants did not bind as well. Since HSPG has been determined to interact with DCs and promote their activation (291, 292), it has been speculated that the binding of AAV2 capsid to HSPG shuttles the virion into a DC pathway that triggers its processing and MHC class I presentation followed by T-cell activation. Based on these findings, it is possible that the heparin-binding deficient 587 TG MTP vector will not induce T-cell immunity due to the ablated heparin-binding motif. Enzyme-linked ImmunoSPOT (ELISPOT) can evaluate mice injected with 587 TG MTP vectors for activation of T cells to AAV2 capsid proteins in the future.

Unlike the T-cell activation to AAV2 capsid, mutations that reduced neutralization by human sera or IVIG do not exclusively locate in the heparin-binding domain (293). Furthermore, the presence or absence of heparin-binding ability of AAV2 virions is not directly correlated with preventing vectors from antibody-mediated neutralization because many antibody-escape mutants in AAVs and a number of picornaviruses occur in receptor-binding sites without affecting receptor binding (247). For example, the N587A mutation of AAV2 capsid lying on the RXXR heparin-binding site evaded antibody neutralization in human sera, but had no effect on



heparin binding and maintained high infectivity (293). The same phenomenon was observed in this study. The 588 HB MTP vector retaining the heparin-binding affinity (Figure 20 and Figure 21 in chapter 3) dramatically reduced sensitivity to neutralizing antibodies in guinea pig antiserum (Figure 16) and human IVIG (Figure 18) compared to unmodified AAV2 vectors. One trait of the N587A mutant is that only one amino acid substitution was sufficient to avoid antibody neutralization. Actually, except this mutation, several single mutations, such as the R471A, T550A, and V708A mutants, have also been found to reduce neutralization by IVIG or individual human sera (293). It reveals that the precise conformational structure of capsid epitope is indeed required for neutralizing antibody recognition. Although the 588 HB MTP vector had an intact RGNR motif which did not contain any amino acid substitution, it is possible that the insertion of MTP peptide adjacent to the RXXR region caused capsid conformational change which directly interfered with neutralizing epitopes spanning residues 585 to 588 or antigenic determinants on neighboring loops within the threefold proximal peaks on the capsid surface. This induced conformational change blocked the antibody recognition and thus, conferred the neutralization resistance on the 588 HB MTP virus. Another explanation is that insertion of a targeting ligand after the RXXR motif led the 588 HB MTP vector to be able to use a different uptake route, which depended on an alternative cellular receptor rather than HSPG binding when the epitopes located in the heparin-binding motif were bound by antibodies.

Systemic gene delivery to only certain cell types is highly desirable, especially when the target cells, such as muscle fibers, are dispersed throughout the body. Taken together, these *in vitro* results indicated that the MTP-modified vectors retained their ability to transduce target myotubes and acquired cell targeting selectivity. Importantly, the MTP-incorporated vectors also exhibited the improved resistance to neutralization by antibodies against wild-type capsid. The

finding reported here provides us a starting point to create an efficient muscle-specific vector suitable for systemic delivery in human gene therapy.

### **3. DEPENDENCE OF HSPG-BINDING OF MODIFIED AAV2 VECTORS IN MYOTUBE TARGETING**

#### **3.1 Introduction**

The binding of AAVs to their target cells is the indispensable step in establishing a successful infection. A wide spectrum of cell surface molecules have been demonstrated to participate in the processes of cell-virion recognition and interaction. Numerous viruses utilize cell surface glycoproteins, glycolipids, or proteoglycans as receptors to infect target cells. The specific interaction between viruses and cell surface receptors plays a key role in determining the host range and the tissue tropism of an AAV. AAV2 is gaining attention as a promising vector system for gene transfer because of its ability to achieve long-term transgene expression. However, the wide distribution of its primary attachment receptor, HSPG, throughout the body hinders selective transduction of target tissue. Heparan sulfate is found to be associated with both plasma membranes and the extracellular matrix in large quantities. Heparan sulfate is present at the cell surface in the form of HSPGs and is a highly sulfated polysaccharide, possessing a number of negatively charged groups. These negative charges of heparan sulfate, therefore, interact with the viral proteins carrying positive charges and bridge the initial contacts between viruses and target cell (294). Vectors aiming to redirect the tropism of AAV2 have been produced by insertion of targeting peptides at the position after residue 587/or 588 of the capsid. This is likely to interfere with the HSPG binding of the RXXR motif on AAV2 capsid and thus, enables the targeting

vector to acquire novel tropism. In some cases, the HSPG binding ability of peptide-modified vectors is only partially affected (257) or is even restored (286, 295, 296). To investigate whether MTP peptide incorporation after amino acid 587/or 588 interfered with HSPG binding of modified AAV2 vectors, *in vitro* transduction assay with exogenous competing heparin and heparin-affinity column analysis were used to assess this. The competitive blocking experiment with synthesized muscle-specific ligands was further applied to examine if the transduction of myotubes by peptide-modified vectors was specifically mediated by the ASSLNIA peptide inserted at AAV capsid.

Peptide-specific effects on the tropism of the modified vectors had been proven. The results from this chapter highlighted the potential value of combined *in vivo* phage display (258) and the technology of vector capsid modification for exploitation of novel muscle targeting vectors.

## 3.2 Material and methods

### 3.2.1 *In vitro* heparin competition assay

A total of  $2 \times 10^{10}$  genomic particles of single-stranded unmodified rAAV, rAAV 587 TG MTP, or rAAV 588 HB MTP vectors expressing the luciferase gene from CMV promoter were first incubated with or without 30  $\mu\text{g/ml}$  heparin (from porcine intestinal mucosa; Sigma) in DMEM containing 2% HS for 1 h at 37°C. Then, rAAV alone or rAAV-heparin mixture was added into C2C12 myotubes for 72 hours. Cell were next given fresh DMEM with 2% HS and were subsequently incubated at 37°C until 6 days. The infected myotubes were then harvested for the luciferase assay. All targeted rAAV-mediated transduction experiments were performed in triplicate.

### **3.2.2 Heparin-binding assay**

$5 \times 10^{11}$  genomic particles of rAAV were suspended in 0.5 ml of viral suspension buffer (50 mM  $\text{NaH}_2\text{PO}_4$ , 2 mM MgCl, 2.5 mM KCl, 50 mM Hepes, 150 mM NaCl, pH 8.0) and were then loaded onto a 1-ml HiTrap heparin column (Amersham Bioscience) preequilibrated with 0.15 M NaCl and 50 mM Tris at pH 7.5. The column was further washed twice with 5 ml of binding buffer (10 mM  $\text{NaH}_2\text{PO}_4$  pH 7.0) and eluted twice with 5 ml of elution buffer (10 mM  $\text{NaH}_2\text{PO}_4$ , 1 M NaCl pH 7.0). The flowthrough, wash, and elution fractions were collected. 20  $\mu\text{l}$  of each fraction was analyzed by DNA dot-blot assay with a CMV probe and was also subjected to Western blot with guinea pig anti-AAV2 capsid sera as described in chapter 2. Heparin dependence was verified by estimating viruses present in wash or elution fraction.

### **3.2.3 *In vitro* peptide blocking experiment**

The competitive blocking experiment by the synthetic peptides was carried out in C2C12 myotubes. AAV vectors and C2C12 myotubes were preincubated with 2 mg/ml of the synthetic muscle-specific peptide (NH<sub>2</sub>-ASSLNIA-CONH<sub>2</sub>) or the nonspecific peptide (NH<sub>2</sub>-LISNSAA-CONH<sub>2</sub>) as control at 37°C for an hour. Then, AAV vectors were added into C2C12 myotubes for 24 hours. C2C12 myotubes were washed and changed to 2% HS DMEM. After 96 hours of continuous incubation, the cells were harvested and analyzed by luciferase assay.

### **3.2.4 Statistical analysis**

All data were expressed as mean $\pm$ SEM. To test for statistical significance, unpaired Student's *t* test was applied by one- or two-tailed test. All *in vitro* data were analyzed between groups and were considered significant when  $P < 0.05$ .

### 3.3 Results

#### 3.3.1 HSPG-binding dependence for peptide-modified rAAV transduction

In a recent study, it has been shown that slow muscle fibers in newborn or 6- to 8-week-old mice seemed to be preferentially transduced by AAV2 vectors, while fast myofibers appeared to be only slightly transduced (297). Since slow myofibers have a high level of HSPG at those ages, it has been suggested that the ability of AAV2 to transduce myofibers correlates with the HSPG-mediated entry pathway. However, HSPG is a molecule found on many cell types and causes the broad tropism of AAV2. This becomes a serious limitation for systemic muscle targeting of AAV2 vector. In order to provide a practical means of conquering the limitation imparted by the endogenous viral tropism of AAV2, specific muscle-targeted AAV vectors must be able to transduce muscle efficiently by adapting an alternative entry pathway without HSPG binding.

To determine if the insertion of MTP peptide had provided the peptide-modified mutants with a HSPG-independent cell entry mechanism, gene transduction assay of C2C12 myotubes was performed by ss rAAV CMV-Luc vectors in the presence of soluble heparin. The transduction of 587 TG MTP vector was not affected by heparin ( $P>0.05$ ), whereas unmodified and 588 HB MTP vectors significantly decreased their transduction efficiency by 72.03% and 42.25%, respectively, in the presence of heparin sulfate ( $P<0.05$ ) (Figure 19).

These results strongly suggested that the mutant viral particles of the 587 TG MTP vector might be directing infection via an alternative cellular receptor.

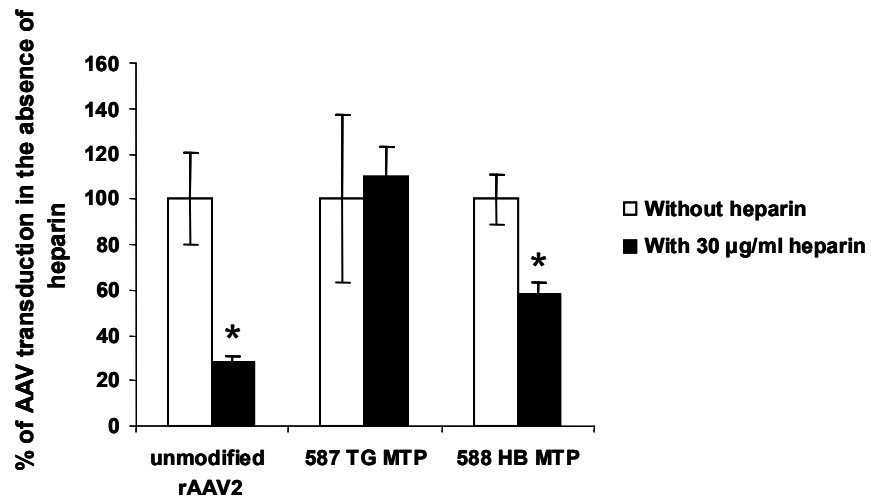


**Figure 19** Quantification of HSPG-independence of peptide-modified mutants

C2C12 myotubes were infected with ss rAAV CMV-Luc vectors carrying unmodified or peptide-inserted capsids in the absence or presence of 30 µg/ml heparin and analyzed for gene expression to examine the HSPG dependence of vectors. \*Indicates  $P < 0.05$  versus transduction in the absence of heparin.

### 3.3.2 Heparin-binding affinity of modified rAAV vectors

The previous result was able to show, that the insertion of the muscle-specific ligand after residue 587 of AAV2 capsid enabled the vector to infect myotubes in a HSPG-independent manner. Another useful way for detection of heparin-binding affinity of these mutants is by heparin column chromatography. Here, a small-scale heparin-binding assay, by loading  $5 \times 10^{11}$  of each mutant ss rAAV CMV-Luc vector onto a heparin column, was applied. After extensive washing of the heparin column, bound rAAVs were eluted in 1 M NaCl. Viruses in the collected fractions were detected by DNA-dot blot assay with CMV probe and by Western blotting using guinea pig anti- AAV2 serum.

As expected, viruses containing a wild-type capsid had a high affinity for the heparin column, and were solely found in the eluted fraction (Figure 20 and Figure 21). The 588 HB MTP rAAVs also displayed heparin-binding ability similar to unmodified vectors since the majority of the vector was found in the column elution and negligible amounts of virus were found in the unbound wash. In marked contrast to unmodified and 588 HB MTP vectors, the 587 TG MTP viruses were substantially detected in the column wash, the unbound fraction. The HBSmut vectors were essentially undetectable in the elution and some of them appeared in the flow-through.

These results were consistent with gene transduction studies in the presence of soluble heparin as competitor. The insertion of ASSLNIA targeting peptide at position 587/or 588 of the AAV2 capsid could determine the heparin-binding phenotype of vectors.



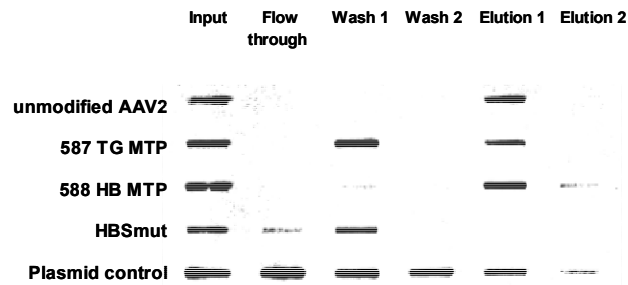


**Figure 20 Heparin-affinity column analysis coupling with DNA dot-blot assay**

$5 \times 10^{11}$  of unmodified or peptide-inserted viruses were loaded onto a prepacked and equilibrated 1 ml heparin column. Viral particles appeared in the flow-through, wash, and elution fractions were then detected by DNA dot-blot with CMV probe. Plasmid control was made by pCMV-Luc plasmid in serial two-fold dilutions.

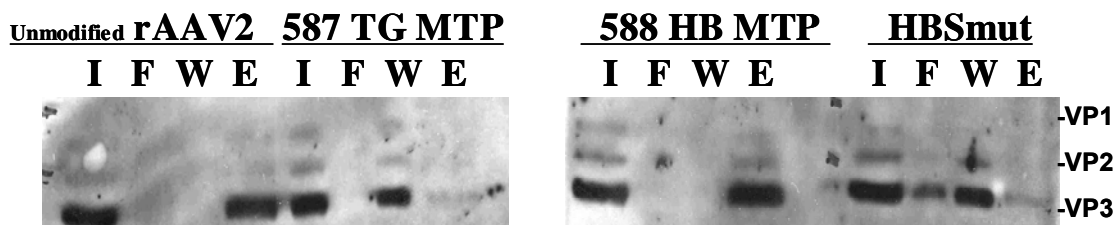


**Figure 21** Western blot applied for the heparin-affinity column analysis

The fractions from the heparin-affinity column analysis were analyzed by Western blot using guinea pig anti-AAV2 serum. The positions of VP1, VP2, and VP3 are indicated. I: Input; F: Flow-through; W: Wash step; E: Elution

### **3.3.3 Influence of synthesized blocking peptide in rAAV transduction**

After showing that 587 TG MTP mutant infected myotubes independent of heparin sulfate, it was further investigated whether the peptide-modified 587 TG MTP vector performed heparin-independent gene delivery via the introduced muscle-specific ligand. This experiment can evaluate the targeting fidelity of the chosen homing peptide for matured myofibers.

To ensure that the 587 TG MTP targeting is mediated by the ASSLNIA peptide insert, the transduction efficiency of peptide-incorporated mutants in C2C12 myotubes was determined in the presence or absence of the cognate peptide (Figure 22). Gene transduction mediated by the 587 TG MTP vectors was significantly inhibited (47.30%) in the presence of 2 mg/ml free ASSLNIA peptide ( $P<0.05$ ). Moreover, this substantial competitive inhibition by synthesized muscle-specific targeting peptide was not observed in the transduction of 587 TG MTP vector with a nonspecific control peptide containing amino acid sequence LISNSAA.

Taken together, synthesized MTP peptide exerted significant inhibition on the 587 TG MTP mutant rAAV2-mediated gene transduction and this blocking effect on viral infection could not be carried out by a nonspecific peptide. This shows that the muscle-specific ligand, ASSLNIA, ensures peptide-modified rAAV vector to gain a novel tropism that facilitates muscle targeting.

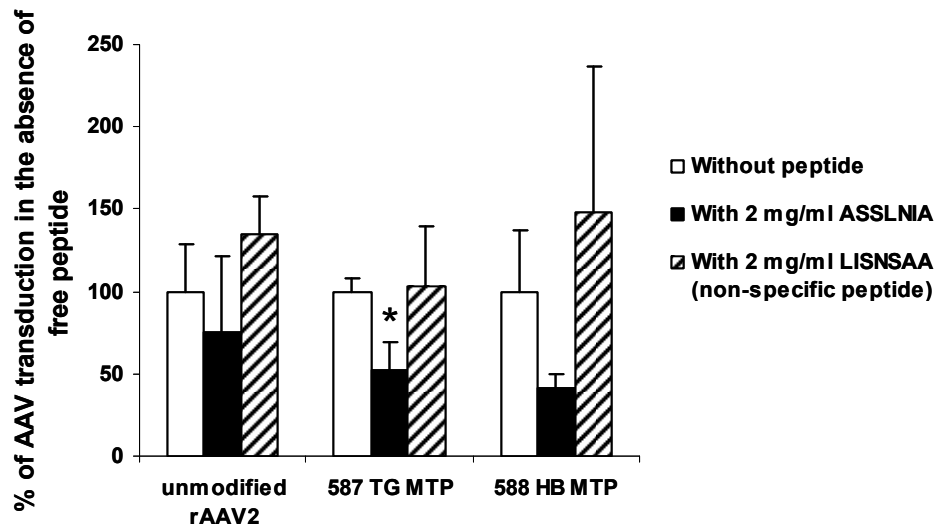


**Figure 22 Competitive inhibition in myotube transduction of peptide-inserted rAAVs by the cognate peptide**

C2C12 myotubes were infected with ss rAAV CMV-Luc vectors in the presence or absence of synthesized free peptides. Level of gene transduction efficiency of peptide-modified vector and unmodified rAAV virus were compared by evaluating luciferase expression.\*  $P < 0.05$  vs value in the absence of peptide.

### 3.4 Discussion

Heparan sulfate is present ubiquitously in the body and it can be displayed on the cell surface as HSPG. The structure of HSPG consists of a core protein and heparan sulfate polysaccharide side chains. HSPGs are required for many biological processes, including embryonic development, blood coagulation, and wound healing (298, 299). In addition to these processes, a large amount of evidence about the involvement of HSPG in assisting viral infections has emerged in recent years. More importantly, HSPG is gaining increasing attention in AAV vector delivery systems because it is the primary receptor for AAV2 cell entry and the expression of HSPG in various tissues severely impedes the efficiency and specificity of vector targeting. Therefore, incorporation of the muscle-specific ligand into a particular region of the AAV2 coat protein needs to ablate viral attachment to heparan sulfate present in the extracellular matrix and on the cell membrane.

Experimental analysis of peptide-inserted mutants in their potential capability of heparin binding was successfully performed and was a way to predict the specific muscle-targeting efficiency of modified vectors in systemic delivery prior to the *in vivo* mouse model being carried out. In gene transduction experiments, the peptide insertion after amino acid 587 of AAV2 capsid provided vector HSPG-independence in targeting gene delivery because the transduction of 587 TG MTP vector in myotubes was not suppressed by soluble heparin (Figure 19). Consistent with gene transduction data, most of the mutant viruses with ligands incorporated after position 587 were recovered in the wash fraction, albeit minor amounts of the virus contained in the eluate (Figure 20). Conversely, the peptide incorporation after residue 588 reserved the RXXR motif of the capsid and showed that the vector retained the gene transduction efficiency relying on viral attachment via HSPG (Figure 19, Figure 20, and Figure 21). It is

apparent that the HSPG dependence of 588 HB MTP vector is still less than that of unmodified rAAVs since soluble heparin enhanced its inhibition by 29.78% in unmodified rAAV2-mediated transduction (Figure 19). These findings demonstrated that the muscle-specific vector generated by the incorporation of MTP after residue 587 eliminated the endogenous tropism of AAV2 and obtained the muscle targeting specificity from introduced peptide (Figure 22).

Viral binding to HSPG is the result of electrostatic attraction between a cluster of positively charged amino acids on viral coat protein and negatively charged sulfate groups from heparan sulfate. Spatial orientation of basic residues rather than sequence proximity is considered as an important factor in determining heparin-binding affinity (300). So far, three heparan sulfate consensus-binding sequences have been identified in several receptors and viruses (270, 301). Two of them are linear binding sequences, XBBXBX and XBBBXXBX (where B is a basic amino acid, including His, Lys, or Arg, and X is any amino acid). The other one is a conformation-dependent sequence, TXXBXXTBXXXTB (T is a turn). Regions including these clusters tend to be sensitive to spacing changes. Heparin-binding domains of viral particles are usually located at the capsid surface and form a flat pocket with a positive charge. In AAV2, the basic residues K532, R484, and R487 of one subunit surround R585 and R588 from the loop of another subunit (256). A mutagenesis study identified that mutation of one of these five basic residues interfered with heparin binding and decreased viral infectivity (250). It suggests that this structure is the basic patch on AAV2 capsid required for heparin binding and its formation needs the correct subunit interaction and assembly. The peptide insertion site after amino acid 587 is part of the basic patch and is located on the capsid surface in the “finger-like” projections surrounding the threefold axis. The structure analysis data in the previous chapter were consistent with the results from gene transduction assays with the heparin competitor (Figure 19)

and provided solid evidence of the differences in heparin-binding sensitivity between 587 TG MTP vector and 588 HB MTP virus.

The insertion of peptides after residue 587 of AAV2 capsid was originally designed to disrupt the HSPG binding of AAV2 and to expose the incorporated ligand to an alternative cell receptor for viral cell entry. In fact, several reports have indicated that this insertion site did not exclusively confer the heparin-binding independence of peptide-inserted vectors (257, 286, 295, 296). A recent study has shed some light on this and shows that the amino acid content of peptides plays an important role in determining the heparin-binding affinity of modified AAVs (302). It suggested that the insertion of peptides with bulky amino acids is prone to result in the spatial separation between R585 and R588 or sterically blocks the heparin-binding ability. If the inserted peptide consists of small residues, the insertion effect could be less detrimental and the structure of the heparin-binding motif remain functional. The insertion of a peptide having basic residues could lead to the production of an HSPG binding phenotype by reconstituting a heparin-binding domain in combination with one of the original arginine from the RXXR motif or by the heparin sulfate consensus-binding sequences present at the inserted ligand. According to these findings, the inserted muscle-specific ligand with the linker sequences on 587 TG MTP mutant did not include any basic residues or the consensus heparin-binding domain. This chosen peptide sequence prevented 587 TG MTP from generating a new HSPG binding motif after peptide insertion. In addition, the inserted peptide of the 587 TG MTP virus had amino acid up to 12 which might cause the invasive effect like the damage from bulky peptide in heparin binding.

The molecular modeling data also showed that both peptide-modified vectors, 587 TG MTP and 588 HB MTP, appeared to have the inserted MTP forming the loop-like structure extending to the outside surface of VP3 monomer (Figure 23). This feature allowed the 587 TG

MTP vector to acquire specific muscle targeting from peptide insertion exposed to the surface of the capsid subunit (Figure 5). 588 HB MTP mutant is likely a better vector with the dual phenotype. Since the gene transduction of 588 HB MTP vector was not suppressed by soluble heparin as much as that of unmodified rAAVs in the presence of heparin (Figure 19), it implied that the incorporated ligand of 588 HB MTP could contribute to viral transduction which was not inhibited by heparin. Moreover, the transduction of 588 HB MTP vector in C2C12 myotubes was inhibited by the synthesized ASSLNIA peptide up to 58.75% albeit with statistical significance  $P>0.05$  (Figure 22).

In order to direct rAAV vector to a specific tissue following intravenous administration, the tropism-modified vector will require diminution of its natural tropism and it presents a ligand that will recognize a cellular receptor accessible through the circulation and selectively expressed in the organ or tissue of interest. Here, it has been shown that the 587 TG MTP vector mediated HSPG-independent muscle transduction *in vitro*. The 587 TG MTP virus is suitable for systemic gene transfer in humans.



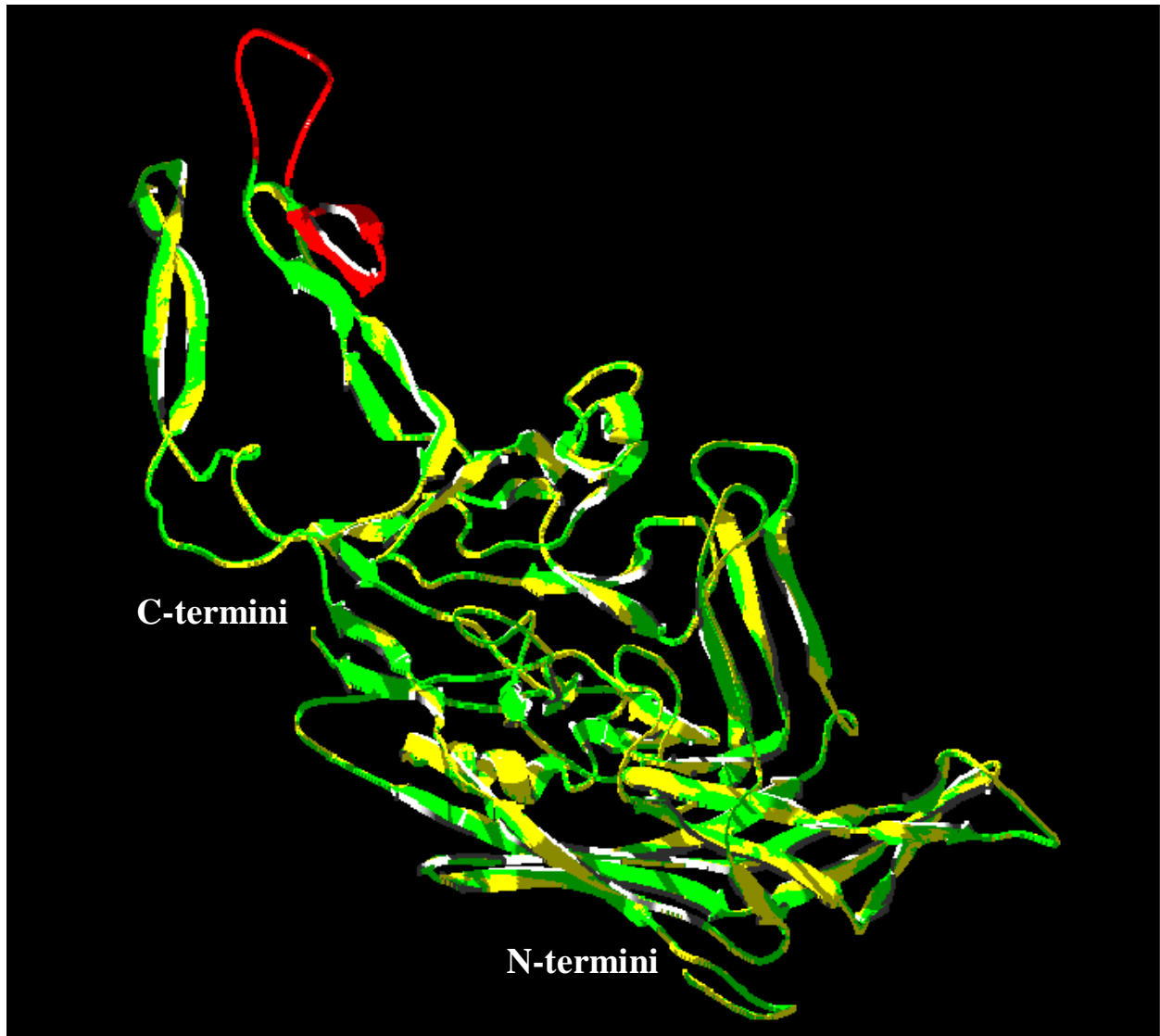


**Figure 23** Ribbon representations of VP3 subunits from unmodified, 587 TG MTP, and 588 HB MTP rAAVs  
The structures of all VP3 subunits were merged by using Swiss-Model.

## **4. INCORPORATION OF MUSCLE-SPECIFIC LIGAND INTO CAPSID RETARGETS AAV2 TO STRIATED MUSCLE AFTER SYSTEMIC DELIVERY**

### **4.1 Introduction**

The ability to target specifically the striated muscles in the body via the systemic circulation would be of great clinical significance for treatment of muscular dysfunction. Several vector systems, such as retroviruses, Ads, and AAVs, have been applied to deliver the therapeutic gene to muscle. However, viral vectors derived from retrovirus have several disadvantages, including their inability to transduce postmitotic cells (e.g., myofibers), the low gene insert capacity, and the risk of insertional mutagenesis (303-305). Ads are able to infect both mitotic myoblasts and postmitotic immature muscle fibers, but their utilizations are restricted by immunological problems and transduction of myofibers in a maturation-dependent manner (306). In contrast to Ads, AAV vectors enable conferment of sustained transgene expression for *in vivo* gene therapy to skeletal muscle as they are less immunogenic. AAV8 has been shown to be able to achieve systemic transduction of skeletal and cardiac muscles in neonatal and adult mice (148). This attributes to the capability of AAV8 in penetrating the biological barrier imposed by the blood vessel of the muscle tissue. Unfortunately, like other AAV serotypes, AAV8 possesses poor targeting selectivity as same as other AAV serotypes. Therefore, the nonspecific targeting of AAV vectors still remains a major hurdle facing the application of systemic rAAV-mediated gene transfer to skeletal muscle in humans. The modification of viral capsids to retarget vectors

has emerged as an attractive route to create ideal viral vehicles for defined applications. The results from *in vitro* studies showed the efficiency and selectivity of peptide-inserted vectors in myotube targeting. First, the data demonstrated that these peptide-modified vectors maintained their myotube transduction ability. Second, peptide-engineering AAVs decreased their transduction in non-muscular control cell lines, such as HepG2, HeLa, and 293 cells. Third, the peptide-modified AAV 587 TG MTP vector did not require the heparin-dependent mechanism for muscle targeting. These findings indicate that the muscle-targeting peptide isolated by *in vivo* phage display could be incorporated into AAV2 capsids and provide enhanced transduction selectivity *in vitro*. Thus, the targeting property of peptide-modified vectors was further evaluated through side-by-side comparison of the unmodified vector and peptide-inserted mutants by direct intramuscular and intravenous vector delivery.

## **4.2 Material and methods**

### **4.2.1 *In vivo* characterization of vectors via intramuscular delivery**

Eight-week old ICR-CD1 adult male mice were purchased from Charles River. Fifty  $\mu$ l of viral solution, containing  $2.5 \times 10^{10}$  genomic particles of ss rAAV CMV-Luc vector with unmodified capsid or peptide-modified capsid, was injected into the tibialis anterior (TA) muscle of mice. Four weeks following injection, the mice were sacrificed. The TA muscles were harvested and frozen in liquid nitrogen. After homogenization of muscle tissues, the protein concentration was determined and the luciferase assay was performed. Luciferase activity was depicted in relative light units (RLU) per milligram of protein.

#### **4.2.2 *In vivo* characterization of vectors via intravenous delivery**

Mice were injected intravenously via a tail vein with a viral solution containing  $9 \times 10^{11}$  genomic particles of ss rAAV CMV-Luc. After four weeks, the mice were sacrificed and representative organs (brain, heart, liver, skeletal muscles, kidney, testis, and spleen) were harvested for the luciferase assay. Luciferase activity was expressed as relative light units (RLU) per milligram of protein.

#### **4.2.3 Vector biodistribution in systemic delivery**

Mice were treated intravenously via a tail vein with ss rAAV CMV-Luc vectors at  $9 \times 10^{11}$  genomic particles/mouse. Mice were then sacrificed and organs (brain, heart, liver, skeletal muscles, kidney, testis and spleen) were harvested four weeks after intravenous injection. Genomic DNA was extracted from organs using DNeasy kit (Qiagen Inc). Relative numbers of vector genome were determined using real-time PCR. A luciferase quantification standard curve was generated from serial dilutions of the pAAV CMV-Luc plasmid by use of SYBR green with 100 pmol/ $\mu$ l sense 5'-GACGCCAAAAACATAAAGAAAG-3' and antisense 5'-AGGAACCAGGGCGTATCTCT-3' Luc primers. 200 ng genomic DNA was used for PCR amplification and the PCR products were quantified using TaqMan data analysis software (Applied Biosystems). All data were expressed as vector copies per  $\mu$ g genomic DNA. The following PCR reaction conditions were used: denaturation, 95°C for 2 min; 40 cycles of amplification, 95°C for 15 sec, 60°C for 1 min.

#### 4.2.4 Statistical analysis

All *in vivo* data were analyzed using the nonparametric Mann-Whitney U test. Data were shown as mean±SEM.

### 4.3 Results

#### 4.3.1 *In vivo* transduction of skeletal muscle by local delivery of rAAVs

Many gene therapy applications have used rAAV2-based vectors for gene transfer because rAAV2 has been demonstrated to lead to stable gene expression in muscle for up to several years (307, 308). To test if the peptide-modified vectors could maintain the efficiency of muscle transduction as well as unmodified rAAV2 *in vivo*, TA muscles of mice were directly injected with unmodified vectors or peptide-inserted mutants encoding luciferase from CMV promoter.

When the administered viral dose was at  $2.5 \times 10^{10}$  genomic particles per muscle, 588 HB MTP vector yielded higher transduction than rAAV vector carrying wild-type capsid (Figure 24). However, 587 TG MTP vector demonstrated decreased muscle targeting by 44% after intramuscular delivery compared to muscle transduction mediated by unmodified rAAV vectors.

These *in vivo* results from local injection were similar to the *in vitro* myotube transduction data (Figure 9).

**AAV injections in mouse tibialis anterior (TA) muscle, n=4**

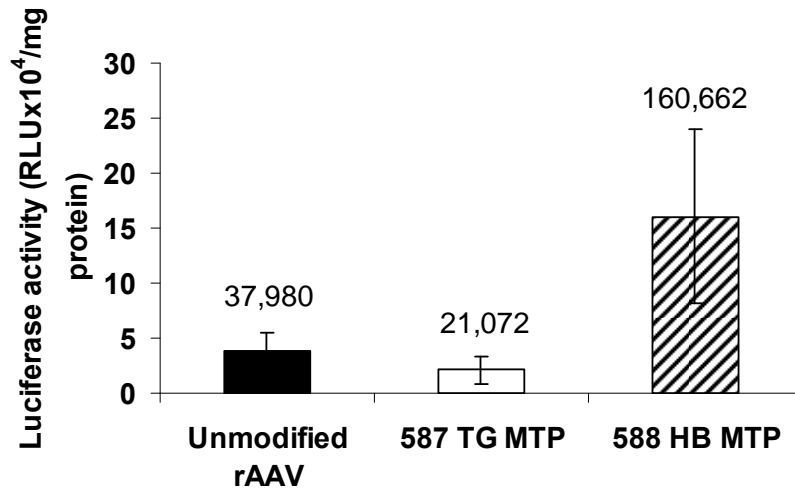


**Figure 24 Intramuscular delivery of peptide-modified rAAV vectors in mice**

Luciferase activities were obtained from the TA muscles of mice injected with  $2.5 \times 10^{10}$  genomic particles of ss rAAV CMV-Luc vector carrying wild-type or modified capsids 4 weeks before examination (n=4 TA muscles for each vector tested).

### 4.3.2 *In vivo* rAAV-mediated muscle transduction by systemic delivery

Systemic muscle targeting of peptide-modified vectors after intravenous administration was next examined at the whole-body level in eight-week old adult mice. The major organs of mice were analyzed for luciferase activity four weeks after administration through the tail vein of  $9 \times 10^{11}$  vector genomes of rAAV containing a CMV-Luc expression cassette.

rAAV 587 TG MTP demonstrated higher muscle and heart targetings than unmodified rAAV2. 587 TG MTP vector showed a 2.18-fold increased transduction compared to unmodified virus in the diaphragm (Figure 25), and increased at least 23-fold transduction of the heart (Figure 26). Peptide-modified 587 TG MTP vector provided transduction of quadriceps at levels 2.85-fold greater than that obtained using unmodified vector. Moreover, the AAV 587 TG MTP had significantly reduced transduction of lung, spleen, and brain (Figure 27). In contrast, rAAV 588 HB MTP had reduced transduction in most organs, and transduction of quadricep muscles and heart was 0.9-fold and 0.8-fold that of unmodified vector respectively (Figure 25 and Figure 26).

However, expression from the CMV promoter had shut off in the liver as was also observed in previous studies (147). The vector genomes of peptide-modified AAVs in the liver had to be determined by real-time PCR. Although CMV promoter had shut off in the liver, the luciferase activities of rAAV 587 TG MTP and rAAV 588 HB MTP in the liver were lower than that of unmodified rAAV2 (Figure 27).

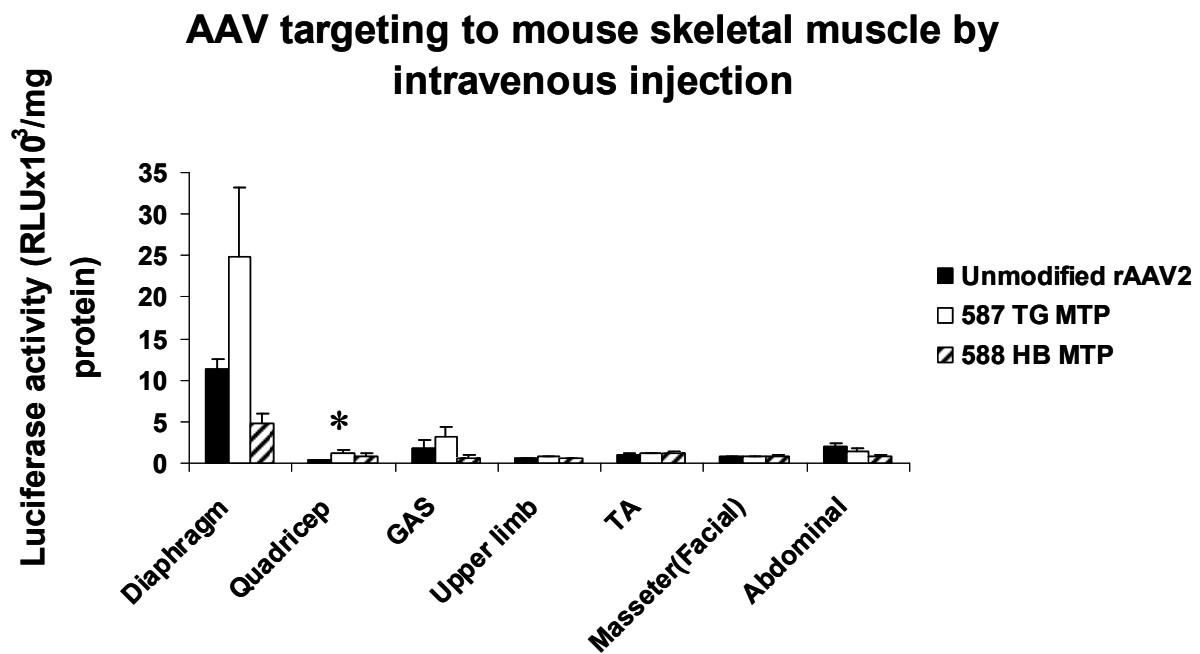


Figure 25 Luciferase activities in muscles after systemic rAAV administration

$9 \times 10^{11}$  vector genomes of ss rAAV CMV-Luc were delivered into adult mice through a tail vein injection (n=5 for unmodified rAAV2 vector, n=6 for 587 TG MTP vector, n=5 for 588 HB MTP vector). Four weeks after injection, muscle tissues were harvested for the luciferase assay. \* $P < 0.05$  vs unmodified rAAV2 vector.



### AAV targeting to mouse heart

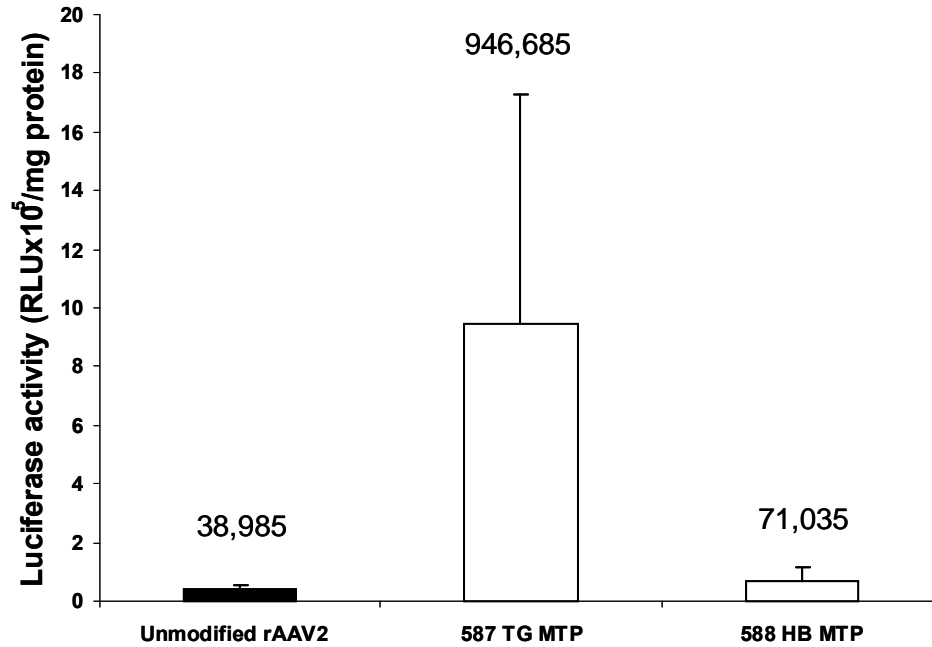


Figure 26 Luciferase activities in mouse hearts after systemic delivery of peptide-modified vectors

$9 \times 10^{11}$  vector genomes of ss rAAV CMV-Luc were delivered into adult mice through a tail vein injection (n=5 for unmodified rAAV2 vector, n=6 for 587 TG MTP vector, n=5 for 588 HB MTP vector). Four weeks after injection, mouse hearts were harvested for luciferase assay.

## AAV targeting to mouse non-muscle organs by intravenous injection

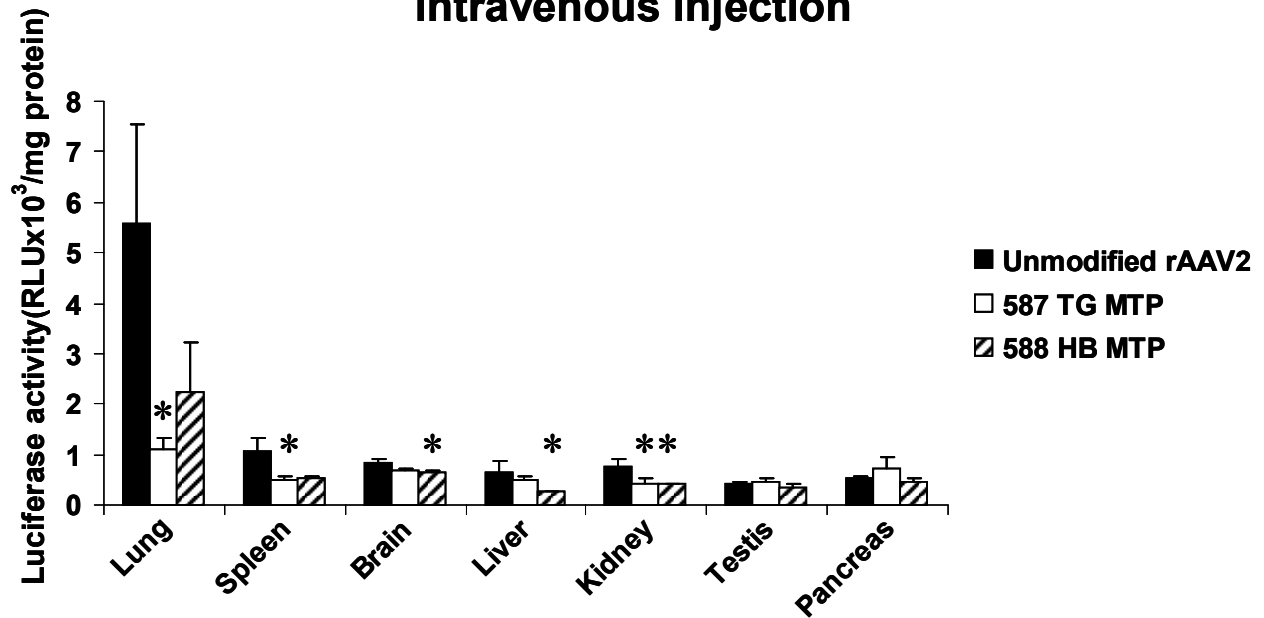


Figure 27 Luciferase activities in non-muscle organs after systemic delivery of peptide-modified vectors

$9 \times 10^{11}$  vector genomes of ss rAAV CMV-Luc were delivered to adult mice by a tail vein injection (n=5 for unmodified rAAV2 vector, n=6 for 587 TG MTP vector, n=5 for 588 HB MTP vector). Four weeks after injection, mouse hearts were harvested for the luciferase assay. \* $P < 0.05$  vs unmodified rAAV2 vector.

### 4.3.3 Biodistribution profile of peptide-modified rAAV in adult mice

In addition showing luciferase expression in the major organs of mice injected with peptide-modified vectors, the vector biodistribution in organs was further determined by real-time PCR. The SYBR green quantitative PCR was performed on these collected tissues from injected adult mice and it confirmed whether the increase of transgene expression in the heart and skeletal muscles were attributable to an increase of vector genomes in detected tissues.

As predicted, systemic infusion of unmodified rAAV vectors to adult mice resulted in accumulation in the liver of much lower levels than in other tissues (Figure 29). Quantification of copy number of virions in the liver showed that rAAV 587 TG MTP decreased its liver transduction by 44.51% compared to unmodified rAAVs (Figure 29). In addition, 587 TG MTP vector exhibited decreased transduction of the lung, spleen, and brain (Figure 28). The number of viral particles in the heart increased from  $0.96 \pm 0.45$  vector copies/ $\mu\text{g}$  tissue genomic DNA with unmodified rAAV to  $7.28 \pm 3.91$  vector copies/ $\mu\text{g}$  tissue genomic DNA with rAAV 587 TG MTP (Figure 28). rAAV 587 TG MTP-infused animals also showed the increase of vector genome in most examined skeletal muscles, including diaphragm, quadriceps, and tibialis anterior.

The real-time PCR results were quite consistent with the luciferase data. Both experiments demonstrated that peptide-modified 587 TG MTP vector simultaneously detargeted rAAV from non-muscular organs and retargeted it to striated muscles in systemic delivery.

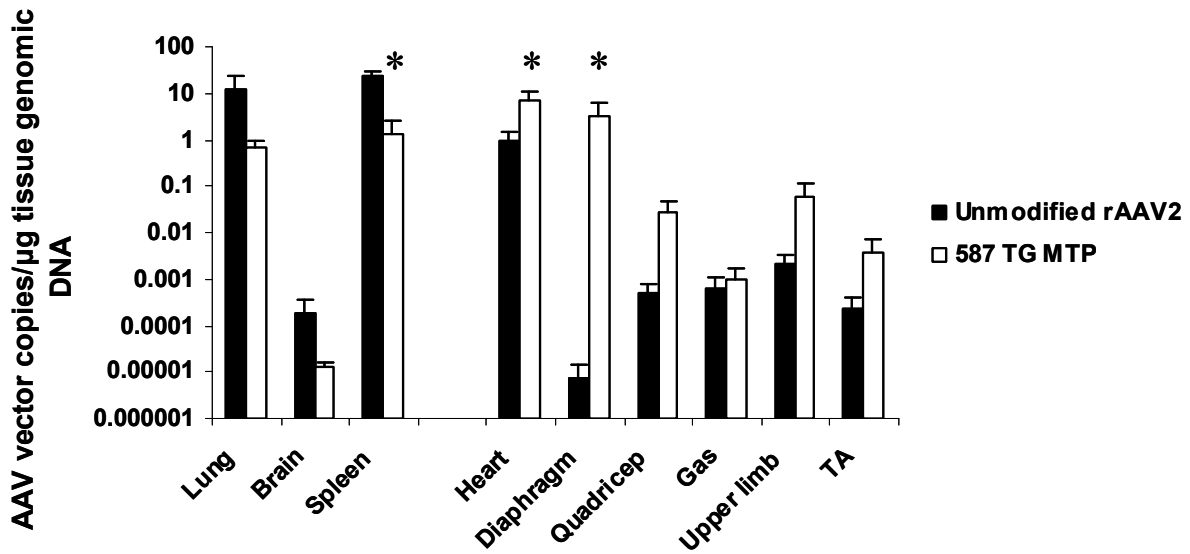


Figure 28 rAAV genome distribution after intravenous delivery

$9 \times 10^{11}$  genomic particles of rAAV were delivered to 8-week old mice via tail vein injection (n=5 for unmodified rAAV2 vector, n=6 for 587 TG MTP vector, n=5 for 588 HB MTP vector), and vector distribution was quantified by real-time PCR in all major organs one month after delivery.  $P < 0.05$  vs unmodified rAAV2 vector.

### AAV targetings in mouse liver

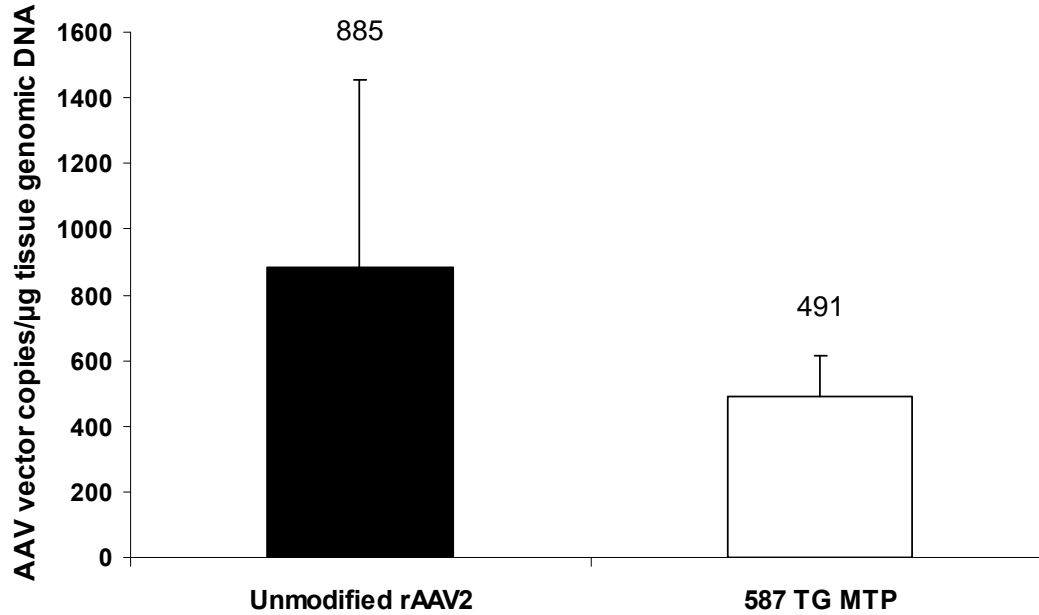


Figure 29 Quantify hepatic rAAV genomes after intravenous delivery

$9 \times 10^{11}$  genomic particles of rAAV were delivered to 8-week old mice via tail vein injection (n=5 for unmodified rAAV2 vector, n=6 for 587 TG MTP vector, n=5 for 588 HB MTP vector), and viral particles in the liver were quantified by real-time PCR one month after delivery.

#### 4.4 Discussion

The systemic delivery of therapeutic genes to striated muscle will require rAAV vector with an outstanding affinity for muscle fibers. The targeting specificity of rAAV is not only in line with the safety of gene therapy, but also is the major factor that affects the transduction efficiency of vector in the tissue of interest. A vector capable of efficiently targeting a specific tissue has important benefits in human gene therapy. One advantage is to obtain a lower established effective dose. Less viral dose could be used for therapeutic applications in humans. This is very significant since developing methods to scale up the production of rAAV vector have met with difficulty. An additional benefit is that a lower effective dose would increase the overall safety of the rAAV treatment by diminishing the amount of viral capsid protein in the body because it has been proven that viral capsid from AAV potentially elicits an immune response harmful to the therapy (224). Although integration of rAAV genomes rarely occurs in host cells (219), a decrease in the total amount of delivered vector would further reduce the chance of host genome integration and facilitate an increase of overall safety in clinical use of rAAV vectors. Therefore, the ultimate goal of this project was to develop an ideal clinical gene transfer vector for the systemic treatment of diseases affecting the heart and skeletal muscle.

This report characterized the behavior of the rAAV2 capsid incorporated with a muscle-specific ligand in its ability to transduce myofibers *in vivo* through a single intravenous administration. In contrast to the unmodified capsid, the inserted muscle-homing peptide directed rAAV2 vector to be suited for gene delivery to the heart and skeletal muscle via systemic delivery. As demonstrated in this chapter, the small differences of the insertion site on capsid and the linker sequence used in the context of the MTP insertion dramatically altered vector behavior *in vivo*.

Upon tail vein injection, the *in vivo* data clearly showed that 587 TG MTP vector was much better than 588 HB MTP vector for striated muscle transduction (Figure 25 and Figure 26). Compared to unmodified rAAV, 588 HB MTP vector only had slight increase in the heart and quadricep transduction (Figure 25 and Figure 26), but decreased its accumulation in most analyzed tissues including both muscle and non-muscle tissues (Figure 25 and Figure 27). Importantly, the capsid modification from rAAV 587 TG MTP was able to retarget the vector to the heart and most tested skeletal muscles and it simultaneously enabled the virus to detarget the liver, lungs, spleen, and brain. The CMV promoter can produce a high level of transgene expression. However, CMV promoter-driven gene expression lasts for only a few days at high levels. Moreover, CMV promoter has been shown to be inactivated in muscle tissue after implantation of primary myoblasts transduced with retroviral vectors containing CMV-canine factor IX expression cassette in mice (309). This is the reason that the luciferase activities of mouse skeletal muscles were low after intravenous delivery of rAAV vectors (Figure 25). Therefore, it would be valuable to choose a muscle-specific promoter, or sacrifice mice at 24 hours after infusion for examining systemic vector targeting.

In vector biodistribution analysis, 587 TG MTP vector produced a heart-to-liver ratio of 0.014816, and for the unmodified rAAV2 the ratio was 0.001086. Thus, there was a 13.64-fold improvement in the cardiac delivery with 587 TG MTP vector. During the respiratory cycle, diaphragm movement is an essential requirement. Since the body relies so much on the diaphragm for respiratory function, the diaphragm becomes the second most important muscle in the body after the heart. However, many disease processes ultimately cause diaphragm dysfunction. Therefore, a systemically delivered vector is necessary to efficiently target the diaphragm. The targeting ability of 587 TG MTP vector to diaphragm was assessed from the

real-time PCR results (Figure 28). The vector genome copy of 587 TG MTP vector was  $4.2 \times 10^5$ -fold improved in diaphragm compared to unmodified rAAV2 ( $P < 0.05$ ). The mechanism of the enhanced diaphragm targeting by 587 TG MTP vector is unclear.

Although 587 TG MTP vector was superior to 588 HB MTP vector in muscle transduction after systemic delivery, 588 HB MTP vector demonstrated higher infectivity in intramuscular injection compared to unmodified and 587 TG MTP rAAVs (Figure 24). Furthermore, 588 HB MTP has shown more resistance in escaping preexisting humoral immune responses (Figure 16, 17, and 18). Because muscle fibers are abundant and allow gene transfer with relatively noninvasive procedures, they have been utilized to express and secrete biologically active gene products that are normally not produced by this tissue (310, 311). The findings from this study implied that 588 HB MTP vector might be a good candidate to deliver therapeutic gene encoding secretory protein when local delivery is needed for a treatment.

All *in vivo* data has been tested for statistical significance using the Mann-Whitney test. The Mann-Whitney test (also named the rank sum test) is a nonparametric test that compares two unpaired groups. As sample numbers increase, a normal approximation is used for the hypothesis test. The approximation to the normal distribution is best when both groups have sample numbers equal to or greater than 10. In this study, the number of mice in each vector group was only five or six. This is the possibility that most *in vivo* data did not have the statistical significance with  $P < 0.05$ . However, it could be overcome by increasing the sample number of mice for the systemic delivery of rAAV.

This study has confirmed our ability to rationally design and genetically engineer tropism-modified AAV vectors for selective delivery of genes to the whole-body muscle *in vivo*.



## 5. OVERALL DISCUSSION

Gene therapy holds promise for the treatment of MDs since earlier studies have shown that expression of full-length dystrophin in muscles of transgenic *mdx* mice can eliminate the morphological and immunohistological symptoms of MD without toxicity (121). Various viral vectors have been made to deliver the therapeutic genes into the desired tissues. In the late 1990's, several reports demonstrated that AAV vectors can infect mouse muscles at surprisingly high efficiencies after a simple intramuscular injection (133, 311, 312). These findings made muscle-directed gene therapy a realistic application. Since AAV vectors allow packaging transgene less than 4.5 kbs, several approaches, such as minigene, exon-skipping, and split AAV vectors, have been developed to overcome this packaging size-limitation for the AAV-mediated delivery. However, transfer on a large amount of vector DNA into muscle by multiple intramuscular injections is impractical. Therefore, systemic delivery of AAV vectors by a single intravenous administration is the most effective method to deliver sufficient amount of therapeutic genes to muscle for the treatment of MD. Unfortunately, AAV vectors are transported poorly across vascular endothelium even when delivered by high hydrostatic pressure (313). Current techniques for gene delivery to muscle through blood transportation involve complex surgical procedures under anesthesia (255, 314, 315) and are still not feasible for whole-body vector delivery. Gregorevic *et al.* (147) showed a way to solve this problem by injecting AAV6 vector together with VEGF into the bloodstream of mice. This VEGF approach

efficiently achieved whole-body transduction of a desired gene into the heart and skeletal muscles. Wang *et al.* (148) also demonstrated that AAV8 could be utilized for efficient global muscular gene delivery by the intravascular route. But both approaches had a problem. In the systemic gene delivery through intravenous injection, AAV vectors primarily transduce in the liver with a broad tropism. Furthermore, transfer of a gene into unwanted nonmuscular tissues decreases the efficacy of the therapeutic effect of AAV-mediated transgene expression and raises the safety concerns about the potential increase of germline transmission of unwanted gene. Developing a vector that could specifically target dispersed skeletal muscles of an adult organism by systemic administration is essential for disease, like MD.

At present, at least three targeting methods are available for directing the expression of a transgene into a specific tissue. These methods include physical targeting, transcriptional targeting, and biological targeting. The physical gene delivery method is involved in injection of biodegradable microspheres or microbubbles with delivery vectors to improve the efficiency of gene transfer (316, 317). Transcriptional targeting approach involves the use of tissues-specific promoters to create vectors that express transgenes selectively (318, 319) while the biological vector targeting method utilizes modification of viral capsid proteins (320). Since the use of tissue-specific promoters is well-established for selective gene expression, explorations into capsid modification for specific gene delivery are still in their initial stage. In the study described here, the biological targeting through modification of viral coat proteins was carried out for the development of an efficient and muscle-specific targeting vector. AAV 2 was chosen for engineering its specific muscle targeting because it has been well-characterized for many years. HSPG is identified as the primary receptor of AAV2. AAV2 has been shown a broad tropism since HSPG widely exists in various tissues. Recently, several studies have shown that short

peptide sequences encoding specific receptor ligands could be incorporated into AAV capsid as a way to change vector tropism. Specific sites on AAV capsid that can tolerate the insertions of small exogenous peptides have been identified by a series of insertion mutants spanning the capsid protein of AAV vector (266). Identified positions at amino acid residues 139, 161, 459, 584, and 587 are capable of tolerating peptide insertions of up to 15 amino acids without affecting the viral yield in most cases. The insertion of the angiogenic vascular targeting motif NGR on AAV2 capsid mediated an altered tropism toward cells expressing the NGR receptor CD13 which is presented in angiogenic vascular culture and in many tumor cell lines (286). Based on the other findings, the genetic incorporation of endothelium-specific peptide SIGYPLP into the position after amino acid 587 of AAV2 capsid significantly enhanced transduction of mutated AAV in human vascular endothelial cells as compared to AAV carrying wild-type capsid (321). In contrast, SIGYPY-modified AAV2 had much lower reporter gene expression than wild-type AAV2 in both human vascular smooth muscle cells and human hepatocytes. Nicklin *et al.* (321) also indicated that the transduction of endothelial cells by SIGYPLP-modified AAV2 was independent of heparin binding. As expected, peptide-modified AAV2 vectors carrying ASSLNIA ligand enhanced the vector targeting at the heart and skeletal muscles after a single intravenous administration. Interestingly, 588 HB MTP vector retaining heparin-binding ability has significantly less enhancement of striated muscle targeting via systemic delivery as compared to 587 TG MTP vector without a heparin-binding motif (Figure 25 and 26). It is possible that 588 HB MTP vector finds it easy to be docked in the extracellular matrix since a high level of HSPG is also present in the extracellular matrix. Another possibility is that the incorporation of a specific ligand with the different linker sequences might lead AAV to enter the target cell through a different coreceptor.

Our studies have demonstrated an efficient and selective gene transfer to the heart and skeletal muscles systemically which has important implications with regard to the development of a muscle-specific AAV vector for clinical application. The unwanted hepatic tropism of AAV is the main concern for decreasing the muscle targeting efficiency after systemic delivery. Based on the data described in this study, peptide-modified 587 TG MTP vector reduced its liver targeting by 44.51% as compared to unmodified rAAV2 virus (Figure 29). In addition to preventing vectors from docking in the liver, an ideal muscle-specific AAV vector also needs to eliminate its broad tropism. In our study, ligand-inserted 587 TG MTP vector significantly decreased its targeting to other tissues, like lung, spleen, and brain (Figure 28). Unlike previous studies, the peptide-modified vector described here not only increased the muscle targeting ability but also provided a remedy for vector delivery to nonspecific tissues. Moreover, peptide-incorporated AAVs confer viral resistance to antibody neutralization for long-term gene expression (Figure 16, 17, and 18). The peptide-inserted vectors provide an important tool on the treatment of muscle diseases.

## 6. FUTURE STUDIES

Targeted efficient gene delivery specifically to muscle using a systemic route is a difficult task because muscle is an abundant tissue dispersed throughout the body. So far, this study showed specific muscle targeting in mice by ligand-directed gene delivery. Although this initial success suggests that it will be possible to apply this modified vector system for human application, a previous study indicated that a peptide isolated by phage display decreased its targeting effect when incorporated into AAV capsid (243). This might be due to the fact that peptide conformation is changed in the viral protein context. Therefore, the selection of specific ligands for muscle targeting may be more practical if the AAV display library (244, 247, 248) is established to screen the random peptide pool in primary human myotubes. In recent years, DNA shuffling and error-prone PCR have been developed to provide large viral library diversity for AAV screening for specific purposes (245, 246). These technologies not only produce the AAV clone with the desired feature, but also are a powerful way to explore the functional domain of AAV capsids from different serotypes. They should also be useful in isolating the AAV clone perfect in systemic muscle targeting.

The results from this study showed that the residual hepatic tropism was still observed in peptide-modified vectors. It will be important and essential to identify the receptor exclusively expressed in mature myotubes. New gene profiling methods, such as serial analysis of gene

expression (SAGE), will need to be performed in order to identify suitable muscle receptors for targeted gene delivery.

Before these peptide-modified vectors are applied clinically in humans, they should be tested in a mouse disease model. It would be interesting to see if this vector system still retains its targeting capability in the setting of a pathological process ongoing in muscle. The other consideration is that this MTP peptide was selected from mouse (258), not human muscle cells. Therefore, this muscle-specific ligand would need to be tested in primary human myotubes.

In this study, DNase-resistant vector genomes of HBSmutMTP mutant were not detectable by dot-blot assay. The A20 antibody performed in A20 enzyme-linked immunosorbent assay (ELISA) specifically binds to intact particles including assembled, empty or full genome-packaged, AAV2 virions, but not to single capsid proteins (322, 323) while the quantitative real-time PCR is approximately 40-fold more sensitive than the nonradioactive dot-blot assay (266). In the future, it will be interesting to address whether HBSmut MTP mutants have a defect in viral assembly or genome packaging by a combination of A20 ELISA and real-time PCR assay. For example, a mutant causing the production of empty particles will be positive for the synthesis of AAV virions by A20 ELISA and negative by real-time PCR assay. If both the A20 ELISA and quantitative real-time PCR assays show positive results, it means that the mutant vector can propagate intact viral particles containing vector genomes. It would likely indicate that the vector produced a low viral yield. To understand the mechanism causing HBSmut MTP mutant deficiency in viral production will help us to perform the more rational design for generating modified AAV vectors with specific tropism.

In contrast to the infectivity of peptide-modified vectors, the heparin-binding mutant (HBSmut) generated intact virions that protected the viral genome from DNase digestion (data

not shown), but failed to infect C2C12 myotubes and all tested non-target cell lines (Figure 9, 10, 11, 13, and 14). In an effort to determine the capsid protein composition of the HBSmut mutant, a Western blot was carried out on the cesium chloride-purified virus (Figure 8). By Western blot analysis this heparin-binding mutant appeared to assemble the virion with the same stoichiometry as wild-type virions. The unmodified and HBSmut viruses showed similar amounts of VP3. The amounts of VP1 and VP2 from HBSmut virions were also nearly equivalent to those of wild-type viral particles. The reason for turning this fully assembled mutant noninfectious is thought to be a loss of heparin binding. However, it is possible that the newly acquired tropism of HBSmut virus was not discovered in the limited number of experimental cell lines tested in *in vitro* transduction assays. Since a double mutation of the heparin-binding motif at R484 and R585 resulting in a severe defect for heparin binding strongly reduced transduction of the liver and enabled increased efficiency of cardiac gene transfer (256), it will be worthy to explore the unique tropism of HBSmut vector via *in vivo* systemic delivery.

Efficient and selective transfer of genes to the cells of interest is crucial for the success of gene therapy. Although much work is needed, studies of peptide-modified AAV vectors provide a good foundation for addressing these challenges.

## **7. PUBLIC HEALTH SIGNIFICANCE OF THIS STUDY**

MDs have a highly deleterious impact on health, affecting tens of thousands of people in the United States and they are one of the major public health problems in several countries. These diseases are a significant public health hazard because there is no effective treatment for MDs at present. Many cases of MD are new occurrences of the disease without prior family history. Although research has discovered much about genetic defects associated with many types of MD, treatment for these diseases has not been significantly improved. To provide research with respect to the development of effective treatment strategies for various forms of MD, investigators have focused on basic and clinical issues related to MD. In this study, a tropism-modified rAAV vector carried out an efficient and selective gene transfer directed to muscle via systemic delivery. The success of specific muscle targeting from peptide-incorporated AAV will lead to great advances in the treatment of patients with MD and has the potential to further reduce individual suffering and public health care spending.



## BIBLIOGRAPHY

1. Walton, J.N. & Nattrass, F.J. On the classification, natural history and treatment of the myopathies. *Brain* 77, 169-231 (1954).
2. Engel AG, Frnzzinin-Armstrong C. *Myology*. McGraw-Hill. New York (1994).
3. Emery AEH: *Duchenne muscular dystrophy*. Oxford Monographs on Medical genetics, 2<sup>nd</sup> ed. Oxford University Press, (1993).
4. Emery, A.E. Population frequencies of inherited neuromuscular diseases--a world survey. *Neuromuscul Disord* 1, 19-29 (1991).
5. Jennekens, F.G., ten Kate, L.P., de Visser, M. & Wintzen, A.R. Diagnostic criteria for Duchenne and Becker muscular dystrophy and myotonic dystrophy. *Neuromuscul Disord* 1, 389-391 (1991).
6. Samaha, F.J. & Quinlan, J.G. Dystrophinopathies: clarification and complication. *Journal of child neurology* 11, 13-20 (1996).
7. Kunkel, L.M., *et al.* Analysis of deletions in DNA from patients with Becker and Duchenne muscular dystrophy. *Nature* 322, 73-77 (1986).
8. Monaco, A.P., *et al.* Isolation of candidate cDNAs for portions of the Duchenne muscular dystrophy gene. *Nature* 323, 646-650 (1986).
9. Koenig, M., *et al.* Complete cloning of the Duchenne muscular dystrophy (DMD) cDNA and preliminary genomic organization of the DMD gene in normal and affected individuals. *Cell* 50, 509-517 (1987).
10. Monaco, A.P., Walker, A.P., Millwood, I., Larin, Z. & Lehrach, H. A yeast artificial chromosome contig containing the complete Duchenne muscular dystrophy gene. *Genomics* 12, 465-473 (1992).
11. Coffey, A.J., *et al.* Construction of a 2.6-Mb contig in yeast artificial chromosomes spanning the human dystrophin gene using an STS-based approach. *Genomics* 12, 474-484 (1992).

12. Chamberlain, J.S., et al. Expression of the murine Duchenne muscular dystrophy gene in muscle and brain. *Science* 239, 1416-1418 (1988).
13. Nudel, U., Robzyk, K. & Yaffe, D. Expression of the putative Duchenne muscular dystrophy gene in differentiated myogenic cell cultures and in the brain. *Nature* 331, 635-638 (1988).
14. Koenig, M., Monaco, A.P. & Kunkel, L.M. The complete sequence of dystrophin predicts a rod-shaped cytoskeletal protein. *Cell* 53, 219-228 (1988).
15. Davison, M.D. & Critchley, D.R. alpha-Actinins and the DMD protein contain spectrin-like repeats. *Cell* 52, 159-160 (1988).
16. Wakayama, Y. & Shibuya, S. Gold-labelled dystrophin molecule in muscle plasmalemma of mdx control mice as seen by electron microscopy of deep etching replica. *Acta neuropathologica* 82, 178-184 (1991).
17. Watkins, S.C., Hoffman, E.P., Slayter, H.S. & Kunkel, L.M. Immunoelectron microscopic localization of dystrophin in myofibres. *Nature* 333, 863-866 (1988).
18. Ervasti, J.M. & Campbell, K.P. A role for the dystrophin-glycoprotein complex as a transmembrane linker between laminin and actin. *The journal of cell biology* 122, 809-823 (1993).
19. Monaco, A.P., Bertelson, C.J., Liechti-Gallati, S., Moser, H. & Kunkel, L.M. An explanation for the phenotypic differences between patients bearing partial deletions of the DMD locus. *Genomics* 2, 90-95 (1988).
20. Monaco, A.P. & Kunkel, L.M. Cloning of the Duchenne/Becker muscular dystrophy locus. *Advances in human genetics* 17, 61-98 (1988).
21. England, S.B., et al. Very mild muscular dystrophy associated with the deletion of 46% of dystrophin. *Nature* 343, 180-182 (1990).
22. Bushby, K.M. The limb-girdle muscular dystrophies-multiple genes, multiple mechanisms. *Human molecular genetics* 8, 1875-1882 (1999).
23. Mukherjee, M. & Mittal, B. Muscular dystrophies. *Indian journal of pediatrics* 71, 161-168 (2004).
24. Speer, M.C., et al. Confirmation of genetic heterogeneity in limb-girdle muscular dystrophy: linkage of an autosomal dominant form to chromosome 5q. *American journal of human genetics* 50, 1211-1217 (1992).
25. van der Kooi, A.J., et al. Genetic localization of a newly recognized autosomal dominant limb-girdle muscular dystrophy with cardiac involvement (LGMD1B) to chromosome 1q11-21. *American journal of human genetics* 60, 891-895 (1997).

26. Minetti, C., et al. Mutations in the caveolin-3 gene cause autosomal dominant limb-girdle muscular dystrophy. *Nature genetics* 18, 365-368 (1998).
27. Song, K.S., et al. Expression of caveolin-3 in skeletal, cardiac, and smooth muscle cells. Caveolin-3 is a component of the sarcolemma and co-fractionates with dystrophin and dystrophin-associated glycoproteins. *The journal of biological chemistry* 271, 15160-15165 (1996).
28. Saenz, A., et al. LGMD2A: genotype-phenotype correlations based on a large mutational survey on the calpain 3 gene. *Brain* 128, 732-742 (2005).
29. Liu, J., et al. Dysferlin, a novel skeletal muscle gene, is mutated in Miyoshi myopathy and limb girdle muscular dystrophy. *Nature genetics* 20, 31-36 (1998).
30. Roberds, S.L., et al. Missense mutations in the adhalin gene linked to autosomal recessive muscular dystrophy. *Cell* 78, 625-633 (1994).
31. Lim, L.E., et al. Beta-sarcoglycan: characterization and role in limb-girdle muscular dystrophy linked to 4q12. *Nature genetics* 11, 257-265 (1995).
32. Noguchi, S., et al. Mutations in the dystrophin-associated protein gamma-sarcoglycan in chromosome 13 muscular dystrophy. *Science* 270, 819-822 (1995).
33. Nigro, V., et al. Autosomal recessive limb-girdle muscular dystrophy, LGMD2F, is caused by a mutation in the delta-sarcoglycan gene. *Nature genetics* 14, 195-198 (1996).
34. Holt, K.H. & Campbell, K.P. Assembly of the sarcoglycan complex. Insights for muscular dystrophy. *The journal of biological chemistry* 273, 34667-34670 (1998).
35. Vainzof, M., et al. Telethonin protein expression in neuromuscular disorders. *Biochimica et biophysica acta* 1588, 33-40 (2002).
36. Frosk, P., et al. Limb-girdle muscular dystrophy type 2H associated with mutation in TRIM32, a putative E3-ubiquitin-ligase gene. *American journal of human genetics* 70, 663-672 (2002).
37. Brockington, M., et al. Mutations in the fukutin-related protein gene (FKRP) identify limb girdle muscular dystrophy 2I as a milder allelic variant of congenital muscular dystrophy MDC1C. *Human molecular genetics* 10, 2851-2859 (2001).
38. Hackman, J.P., Vihola, A.K. & Udd, A.B. The role of titin in muscular disorders. *Annals of medicine* 35, 434-441 (2003).
39. Wijmenga, C., et al. Location of facioscapulohumeral muscular dystrophy gene on chromosome 4. *Lancet* 336, 651-653 (1990).

40. Manilal, S., et al. Mutations in Emery-Dreifuss muscular dystrophy and their effects on emerin protein expression. *Human molecular genetics* 7, 855-864 (1998).
41. Bonne, G., et al. Mutations in the gene encoding lamin A/C cause autosomal dominant Emery-Dreifuss muscular dystrophy. *Nature genetics* 21, 285-288 (1999).
42. Clements, L., Manilal, S., Love, D.R. & Morris, G.E. Direct interaction between emerin and lamin A. *Biochemical and biophysical research communications* 267, 709-714 (2000).
43. Maraldi, N.M., Lattanzi, G., Sabatelli, P., Ognibene, A. & Squarzoni, S. Functional domains of the nucleus: implications for Emery-Dreifuss muscular dystrophy. *Neuromuscul Disord* 12, 815-823 (2002).
44. Dubowitz, V. & Fardeau, M. Proceedings of the 27th ENMC sponsored workshop on congenital muscular dystrophy. 22-24 April 1994, The Netherlands. *Neuromuscul Disord* 5, 253-258 (1995).
45. Helbling-Leclerc, A., et al. Mutations in the laminin alpha 2-chain gene (LAMA2) cause merosin-deficient congenital muscular dystrophy. *Nature genetics* 11, 216-218 (1995).
46. Pegoraro, E., et al. Laminin alpha2 muscular dystrophy: genotype/phenotype studies of 22 patients. *Neurology* 51, 101-110 (1998).
47. Brockington, M., Blake, D.J., Brown, S.C. & Muntoni, F. The gene for a novel glycosyltransferase is mutated in congenital muscular dystrophy MDC1C and limb girdle muscular dystrophy 2I. *Neuromuscul Disord* 12, 233-234 (2002).
48. Muntoni, F., Brockington, M., Blake, D.J., Torelli, S. & Brown, S.C. Defective glycosylation in muscular dystrophy. *Lancet* 360, 1419-1421 (2002).
49. Grewal, P.K. & Hewitt, J.E. Mutation of Large, which encodes a putative glycosyltransferase, in an animal model of muscular dystrophy. *Biochimica et biophysica acta* 1573, 216-224 (2002).
50. Akasaka-Manyá, K., Manyá, H., Kobayashi, K., Toda, T. & Endo, T. Structure-function analysis of human protein O-linked mannose beta1,2-N-acetylglucosaminyltransferase 1, POMGnT1. *Biochemical and biophysical research communications* 320, 39-44 (2004).
51. Cormand, B., et al. Clinical and genetic distinction between Walker-Warburg syndrome and muscle-eye-brain disease. *Neurology* 56, 1059-1069 (2001).
52. De Bernabe, D.B., et al. A homozygous nonsense mutation in the fukutin gene causes a Walker-Warburg syndrome phenotype. *Journal of medical genetics* 40, 845-848 (2003).

53. Fukuyama, Y., Osawa, M. & Suzuki, H. Congenital progressive muscular dystrophy of the Fukuyama type - clinical, genetic and pathological considerations. *Brain & development* 3, 1-29 (1981).
54. Hayashi, Y.K., et al. Selective deficiency of alpha-dystroglycan in Fukuyama-type congenital muscular dystrophy. *Neurology* 57, 115-121 (2001).
55. Vitale, P., Braghetta, P., Volpin, D., Bonaldo, P. & Bressan, G.M. Mechanisms of transcriptional activation of the col6a1 gene during Schwann cell differentiation. *Mechanisms of development* 102, 145-156 (2001).
56. Kuo, H.J., Maslen, C.L., Keene, D.R. & Glanville, R.W. Type VI collagen anchors endothelial basement membranes by interacting with type IV collagen. *The journal of biological chemistry* 272, 26522-26529 (1997).
57. Tillet, E., et al. Recombinant expression and structural and binding properties of alpha 1(VI) and alpha 2(VI) chains of human collagen type VI. *European journal of biochemistry / FEBS* 221, 177-185 (1994).
58. Bidanset, D.J., et al. Binding of the proteoglycan decorin to collagen type VI. *The journal of biological chemistry* 267, 5250-5256 (1992).
59. Wiberg, C., et al. Complexes of matrilin-1 and biglycan or decorin connect collagen VI microfibrils to both collagen II and aggrecan. *The journal of biological chemistry* 278, 37698-37704 (2003).
60. Huynh-Do, U., et al. Ephrin-B1 transduces signals to activate integrin-mediated migration, attachment and angiogenesis. *Journal of cell science* 115, 3073-3081 (2002).
61. Atkinson, J.C., Ruhl, M., Becker, J., Ackermann, R. & Schuppan, D. Collagen VI regulates normal and transformed mesenchymal cell proliferation in vitro. *Experimental cell research* 228, 283-291 (1996).
62. Ruhl, M., et al. Soluble collagen VI drives serum-starved fibroblasts through S phase and prevents apoptosis via down-regulation of Bax. *The journal of biological chemistry* 274, 34361-34368 (1999).
63. Camacho Vanegas, O., et al. Ullrich scleroatonic muscular dystrophy is caused by recessive mutations in collagen type VI. *Proceedings of the National Academy of Sciences of the United States of America* 98, 7516-7521 (2001).
64. Bethlem, J. & Wijngaarden, G.K. Benign myopathy, with autosomal dominant inheritance. A report on three pedigrees. *Brain* 99, 91-100 (1976).
65. Irwin, W.A., et al. Mitochondrial dysfunction and apoptosis in myopathic mice with collagen VI deficiency. *Nature genetics* 35, 367-371 (2003).

66. Moghadaszadeh, B., et al. Mutations in SEPN1 cause congenital muscular dystrophy with spinal rigidity and restrictive respiratory syndrome. *Nature genetics* 29, 17-18 (2001).
67. Petit, N., et al. Selenoprotein N: an endoplasmic reticulum glycoprotein with an early developmental expression pattern. *Human molecular genetics* 12, 1045-1053 (2003).
68. Burkin, D.J. & Kaufman, S.J. The alpha7beta1 integrin in muscle development and disease. *Cell and tissue research* 296, 183-190 (1999).
69. Martin, P.T., Kaufman, S.J., Kramer, R.H. & Sanes, J.R. Synaptic integrins in developing, adult, and mutant muscle: selective association of alpha1, alpha7A, and alpha7B integrins with the neuromuscular junction. *Developmental biology* 174, 125-139 (1996).
70. Velling, T., et al. Distinct alpha 7A beta 1 and alpha 7B beta 1 integrin expression patterns during mouse development: alpha 7A is restricted to skeletal muscle but alpha 7B is expressed in striated muscle, vasculature, and nervous system. *Dev Dyn* 207, 355-371 (1996).
71. Hayashi, Y.K., et al. Mutations in the integrin alpha7 gene cause congenital myopathy. *Nature genetics* 19, 94-97 (1998).
72. Pegoraro, E., et al. Integrin alpha 7 beta 1 in muscular dystrophy/myopathy of unknown etiology. *The American journal of pathology* 160, 2135-2143 (2002).
73. Mayer, U., et al. Absence of integrin alpha 7 causes a novel form of muscular dystrophy. *Nature genetics* 17, 318-323 (1997).
74. Achanzar, W.E. & Ward, S. A nematode gene required for sperm vesicle fusion. *Journal of cell science* 110 ( Pt 9), 1073-1081 (1997).
75. Bashir, R., et al. A gene related to *Caenorhabditis elegans* spermatogenesis factor *fer-1* is mutated in limb-girdle muscular dystrophy type 2B. *Nature genetics* 20, 37-42 (1998).
76. Liu, J., et al. Dysferlin, a novel skeletal muscle gene, is mutated in Miyoshi myopathy and limb girdle muscular dystrophy. *Nature genetics* 20, 31-36 (1998).
77. Haravuori, H., et al. Secondary calpain3 deficiency in 2q-linked muscular dystrophy: titin is the candidate gene. *Neurology* 56, 869-877 (2001).
78. Hackman, P., et al. Tibial muscular dystrophy is a titinopathy caused by mutations in TTN, the gene encoding the giant skeletal-muscle protein titin. *American journal of human genetics* 71, 492-500 (2002).
79. Udd, B. Limb-girdle type muscular dystrophy in a large family with distal myopathy: homozygous manifestation of a dominant gene? *Journal of medical genetics* 29, 383-389 (1992).

80. Brais, B., Rouleau, G.A., Bouchard, J.P., Fardeau, M. & Tome, F.M. Oculopharyngeal muscular dystrophy. *Seminars in neurology* 19, 59-66 (1999).
81. Brais, B., et al. Short GCG expansions in the PABP2 gene cause oculopharyngeal muscular dystrophy. *Nature genetics* 18, 164-167 (1998).
82. Carbo, N., et al. TNF-alpha is involved in activating DNA fragmentation in skeletal muscle. *British journal of cancer* 86, 1012-1016 (2002).
83. Goodman, M.N. Tumor necrosis factor induces skeletal muscle protein breakdown in rats. *The American journal of physiology* 260, E727-730 (1991).
84. Li, Y.P., Schwartz, R.J., Waddell, I.D., Holloway, B.R. & Reid, M.B. Skeletal muscle myocytes undergo protein loss and reactive oxygen-mediated NF-kappaB activation in response to tumor necrosis factor alpha. *Faseb J* 12, 871-880 (1998).
85. Heino, J. & Massague, J. Cell adhesion to collagen and decreased myogenic gene expression implicated in the control of myogenesis by transforming growth factor beta. *The journal of biological chemistry* 265, 10181-10184 (1990).
86. Igotz, R.A. & Massague, J. Transforming growth factor-beta stimulates the expression of fibronectin and collagen and their incorporation into the extracellular matrix. *The journal of biological chemistry* 261, 4337-4345 (1986).
87. Roberts, A.B., et al. Transforming growth factor type beta: rapid induction of fibrosis and angiogenesis in vivo and stimulation of collagen formation in vitro. *Proceedings of the National Academy of Sciences of the United States of America* 83, 4167-4171 (1986).
88. Gosselin, L.E. & McCormick, K.M. Targeting the immune system to improve ventilatory function in muscular dystrophy. *Medicine and science in sports and exercise* 36, 44-51 (2004).
89. Mendell, J.R., et al. Randomized, double-blind six-month trial of prednisone in Duchenne's muscular dystrophy. *The New England journal of medicine* 320, 1592-1597 (1989).
90. Fenichel, G.M., et al. Long-term benefit from prednisone therapy in Duchenne muscular dystrophy. *Neurology* 41, 1874-1877 (1991).
91. Campbell, C. & Jacob, P. Deflazacort for the treatment of Duchenne Dystrophy: a systematic review. *BMC neurology* 3, 7 (2003).
92. Mesa, L.E., Dubrovsky, A.L., Corderi, J., Marco, P. & Flores, D. Steroids in Duchenne muscular dystrophy--deflazacort trial. *Neuromuscul Disord* 1, 261-266 (1991).
93. Bonifati, M.D., et al. A multicenter, double-blind, randomized trial of deflazacort versus prednisone in Duchenne muscular dystrophy. *Muscle & nerve* 23, 1344-1347 (2000).

94. St-Pierre, S.J., et al. Glucocorticoid treatment alleviates dystrophic myofiber pathology by activation of the calcineurin/NF-AT pathway. *Faseb J* 18, 1937-1939 (2004).
95. Tinsley, J.M., et al. Amelioration of the dystrophic phenotype of mdx mice using a truncated utrophin transgene. *Nature* 384, 349-353 (1996).
96. Gilbert, R., et al. Adenovirus-mediated utrophin gene transfer mitigates the dystrophic phenotype of mdx mouse muscles. *Human gene therapy* 10, 1299-1310 (1999).
97. Lynch, G.S., Cuffe, S.A., Plant, D.R. & Gregorevic, P. IGF-I treatment improves the functional properties of fast- and slow-twitch skeletal muscles from dystrophic mice. *Neuromuscul Disord* 11, 260-268 (2001).
98. Barton, E.R., Morris, L., Musaro, A., Rosenthal, N. & Sweeney, H.L. Muscle-specific expression of insulin-like growth factor I counters muscle decline in mdx mice. *The journal of cell biology* 157, 137-148 (2002).
99. Bogdanovich, S., et al. Functional improvement of dystrophic muscle by myostatin blockade. *Nature* 420, 418-421 (2002).
100. Kumamoto, T., et al. Proteasome expression in the skeletal muscles of patients with muscular dystrophy. *Acta neuropathologica* 100, 595-602 (2000).
101. Bonuccelli, G., et al. Proteasome inhibitor (MG-132) treatment of mdx mice rescues the expression and membrane localization of dystrophin and dystrophin-associated proteins. *The American journal of pathology* 163, 1663-1675 (2003).
102. Carbo, N., et al. Interleukin-15 antagonizes muscle protein waste in tumour-bearing rats. *British journal of cancer* 83, 526-531 (2000).
103. Barton-Davis, E.R., Cordier, L., Shoturma, D.I., Leland, S.E. & Sweeney, H.L. Aminoglycoside antibiotics restore dystrophin function to skeletal muscles of mdx mice. *The journal of clinical investigation* 104, 375-381 (1999).
104. Hankard, R., Mauras, N., Hammond, D., Haymond, M. & Darmaun, D. Is glutamine a 'conditionally essential' amino acid in Duchenne muscular dystrophy? *Clinical nutrition (Edinburgh, Scotland)* 18, 365-369 (1999).
105. Leriche-Guerin, K., et al. Dysferlin expression after normal myoblast transplantation in SCID and in SJL mice. *Neuromuscul Disord* 12, 167-173 (2002).
106. Vilquin, J.T., et al. Partial laminin alpha2 chain restoration in alpha2 chain-deficient dy/dy mouse by primary muscle cell culture transplantation. *The journal of cell biology* 133, 185-197 (1996).



107. Heslop, L., et al. Transplanted primary neonatal myoblasts can give rise to functional satellite cells as identified using the Myf5<sup>lacZ</sup> mouse. *Gene therapy* 8, 778-783 (2001).
108. Yao, S.N. & Kurachi, K. Implanted myoblasts not only fuse with myofibers but also survive as muscle precursor cells. *Journal of cell science* 105 ( Pt 4), 957-963 (1993).
109. Gross, J.G. & Morgan, J.E. Muscle precursor cells injected into irradiated mdx mouse muscle persist after serial injury. *Muscle & nerve* 22, 174-185 (1999).
110. Partridge, T.A., Morgan, J.E., Coulton, G.R., Hoffman, E.P. & Kunkel, L.M. Conversion of mdx myofibres from dystrophin-negative to -positive by injection of normal myoblasts. *Nature* 337, 176-179 (1989).
111. Moisset, P.A., et al. Successful transplantation of genetically corrected DMD myoblasts following ex vivo transduction with the dystrophin minigene. *Biochemical and biophysical research communications* 247, 94-99 (1998).
112. Gussoni, E., et al. Dystrophin expression in the mdx mouse restored by stem cell transplantation. *Nature* 401, 390-394 (1999).
113. Bachrach, E., et al. Systemic delivery of human microdystrophin to regenerating mouse dystrophic muscle by muscle progenitor cells. *Proceedings of the National Academy of Sciences of the United States of America* 101, 3581-3586 (2004).
114. Reyes, M., et al. Purification and ex vivo expansion of postnatal human marrow mesodermal progenitor cells. *Blood* 98, 2615-2625 (2001).
115. Minasi, M.G., et al. The meso-angioblast: a multipotent, self-renewing cell that originates from the dorsal aorta and differentiates into most mesodermal tissues. *Development (Cambridge, England)* 129, 2773-2783 (2002).
116. Cao, B., et al. Muscle stem cells differentiate into haematopoietic lineages but retain myogenic potential. *Nature cell biology* 5, 640-646 (2003).
117. De Bari, C., Dell'Accio, F., Tylzanowski, P. & Luyten, F.P. Multipotent mesenchymal stem cells from adult human synovial membrane. *Arthritis and rheumatism* 44, 1928-1942 (2001).
118. De Bari, C., et al. Skeletal muscle repair by adult human mesenchymal stem cells from synovial membrane. *The journal of cell biology* 160, 909-918 (2003).
119. Kinoshita, I., et al. Myoblast transplantation in monkeys: control of immune response by FK506. *Journal of neuropathology and experimental neurology* 55, 687-697 (1996).

120. Wiendl, H., et al. The non-classical MHC molecule HLA-G protects human muscle cells from immune-mediated lysis: implications for myoblast transplantation and gene therapy. *Brain* 126, 176-185 (2003).
121. Cox, G.A., et al. Overexpression of dystrophin in transgenic mdx mice eliminates dystrophic symptoms without toxicity. *Nature* 364, 725-729 (1993).
122. Wolff, J.A., et al. Direct gene transfer into mouse muscle in vivo. *Science* 247, 1465-1468 (1990).
123. Wolff, J.A., Ludtke, J.J., Acsadi, G., Williams, P. & Jani, A. Long-term persistence of plasmid DNA and foreign gene expression in mouse muscle. *Human molecular genetics* 1, 363-369 (1992).
124. Mir, L.M., et al. High-efficiency gene transfer into skeletal muscle mediated by electric pulses. *Proceedings of the National Academy of Sciences of the United States of America* 96, 4262-4267 (1999).
125. Zhang, G., Budker, V., Williams, P., Subbotin, V. & Wolff, J.A. Efficient expression of naked DNA delivered intraarterially to limb muscles of nonhuman primates. *Human gene therapy* 12, 427-438 (2001).
126. Liang, K.W., et al. Restoration of dystrophin expression in mdx mice by intravascular injection of naked DNA containing full-length dystrophin cDNA. *Gene therapy* 11, 901-908 (2004).
127. Kafri, T., Blomer, U., Peterson, D.A., Gage, F.H. & Verma, I.M. Sustained expression of genes delivered directly into liver and muscle by lentiviral vectors. *Nature genetics* 17, 314-317 (1997).
128. Ragot, T., et al. Efficient adenovirus-mediated transfer of a human minidystrophin gene to skeletal muscle of mdx mice. *Nature* 361, 647-650 (1993).
129. Yang, Y., et al. Cellular immunity to viral antigens limits E1-deleted adenoviruses for gene therapy. *Proceedings of the National Academy of Sciences of the United States of America* 91, 4407-4411 (1994).
130. DelloRusso, C., et al. Functional correction of adult mdx mouse muscle using gutted adenoviral vectors expressing full-length dystrophin. *Proceedings of the National Academy of Sciences of the United States of America* 99, 12979-12984 (2002).
131. Chen, H.H., et al. Persistence in muscle of an adenoviral vector that lacks all viral genes. *Proceedings of the National Academy of Sciences of the United States of America* 94, 1645-1650 (1997).

132. Herzog, R.W. AAV-mediated gene transfer to skeletal muscle. *Methods in molecular biology* Clifton, N.J 246, 179-194 (2004).
133. Xiao, X., Li, J. & Samulski, R.J. Efficient long-term gene transfer into muscle tissue of immunocompetent mice by adeno-associated virus vector. *Journal of virology* 70, 8098-8108 (1996).
134. Harper, S.Q., et al. Modular flexibility of dystrophin: implications for gene therapy of Duchenne muscular dystrophy. *Nature medicine* 8, 253-261 (2002).
135. Wilton, S.D., et al. Specific removal of the nonsense mutation from the mdx dystrophin mRNA using antisense oligonucleotides. *Neuromuscul Disord* 9, 330-338 (1999).
136. Goyenvalle, A., et al. Rescue of dystrophic muscle through U7 snRNA-mediated exon skipping. *Science* 306, 1796-1799 (2004).
137. Rando, T.A., Disatnik, M.H. & Zhou, L.Z. Rescue of dystrophin expression in mdx mouse muscle by RNA/DNA oligonucleotides. *Proceedings of the National Academy of Sciences of the United States of America* 97, 5363-5368 (2000).
138. Bertoni, C. & Rando, T.A. Dystrophin gene repair in mdx muscle precursor cells in vitro and in vivo mediated by RNA-DNA chimeric oligonucleotides. *Human gene therapy* 13, 707-718 (2002).
139. Burkin, D.J., Wallace, G.Q., Nicol, K.J., Kaufman, D.J. & Kaufman, S.J. Enhanced expression of the alpha 7 beta 1 integrin reduces muscular dystrophy and restores viability in dystrophic mice. *The journal of cell biology* 152, 1207-1218 (2001).
140. Nguyen, H.H., Jayasinha, V., Xia, B., Hoyte, K. & Martin, P.T. Overexpression of the cytotoxic T cell GalNAc transferase in skeletal muscle inhibits muscular dystrophy in mdx mice. *Proceedings of the National Academy of Sciences of the United States of America* 99, 5616-5621 (2002).
141. Kronqvist, P., et al. ADAM12 alleviates the skeletal muscle pathology in mdx dystrophic mice. *The American journal of pathology* 161, 1535-1540 (2002).
142. Moll, J., et al. An agrin minigene rescues dystrophic symptoms in a mouse model for congenital muscular dystrophy. *Nature* 413, 302-307 (2001).
143. Qiao, C., et al. Amelioration of laminin-alpha2-deficient congenital muscular dystrophy by somatic gene transfer of miniagrin. *Proceedings of the National Academy of Sciences of the United States of America* 102, 11999-12004 (2005).
144. Spencer, M.J. & Mellgren, R.L. Overexpression of a calpastatin transgene in mdx muscle reduces dystrophic pathology. *Human molecular genetics* 11, 2645-2655 (2002).

145. Wehling, M., Spencer, M.J. & Tidball, J.G. A nitric oxide synthase transgene ameliorates muscular dystrophy in mdx mice. *The journal of cell biology* 155, 123-131 (2001).
146. Wakefield, P.M., et al. Prevention of the dystrophic phenotype in dystrophin/utrophin-deficient muscle following adenovirus-mediated transfer of a utrophin minigene. *Gene therapy* 7, 201-204 (2000).
147. Gregorevic, P., et al. Systemic delivery of genes to striated muscles using adeno-associated viral vectors. *Nature medicine* 10, 828-834 (2004).
148. Wang, Z., et al. Adeno-associated virus serotype 8 efficiently delivers genes to muscle and heart. *Nature biotechnology* 23, 321-328 (2005).
149. Atchison, R.W., Casto, B.C. & Hammon, W.M. Adenovirus-associated defective virus particles. *Science* 149, 754-756 (1965).
150. Atchison, R.W., Casto, B.C. & Hammon, W.M. Electron microscopy of adenovirus-associated virus (AAV) in cell cultures. *Virology* 29, 353-357 (1966).
151. Hoggan, M.D., Blacklow, N.R. & Rowe, W.P. Studies of small DNA viruses found in various adenovirus preparations: physical, biological, and immunological characteristics. *Proceedings of the National Academy of Sciences of the United States of America* 55, 1467-1474 (1966).
152. Beaton, A., Palumbo, P. & Berns, K.I. Expression from the adeno-associated virus p5 and p19 promoters is negatively regulated in trans by the rep protein. *Journal of virology* 63, 4450-4454 (1989).
153. Pereira, D.J., McCarty, D.M. & Muzyczka, N. The adeno-associated virus (AAV) Rep protein acts as both a repressor and an activator to regulate AAV transcription during a productive infection. *Journal of virology* 71, 1079-1088 (1997).
154. Snyder, R.O., Im, D.S. & Muzyczka, N. Evidence for covalent attachment of the adeno-associated virus (AAV) rep protein to the ends of the AAV genome. *Journal of virology* 64, 6204-6213 (1990).
155. Brister, J.R. & Muzyczka, N. Mechanism of Rep-mediated adeno-associated virus origin nicking. *Journal of virology* 74, 7762-7771 (2000).
156. Snyder, R.O., et al. Features of the adeno-associated virus origin involved in substrate recognition by the viral Rep protein. *Journal of virology* 67, 6096-6104 (1993).
157. Samulski, R.J., et al. Targeted integration of adeno-associated virus (AAV) into human chromosome 19. *The EMBO journal* 10, 3941-3950 (1991).

158. Weitzman, M.D., Kyostio, S.R., Kotin, R.M. & Owens, R.A. Adeno-associated virus (AAV) Rep proteins mediate complex formation between AAV DNA and its integration site in human DNA. *Proceedings of the National Academy of Sciences of the United States of America* 91, 5808-5812 (1994).
159. Linden, R.M., Winocour, E. & Berns, K.I. The recombination signals for adeno-associated virus site-specific integration. *Proceedings of the National Academy of Sciences of the United States of America* 93, 7966-7972 (1996).
160. King, J.A., Dubielzig, R., Grimm, D. & Kleinschmidt, J.A. DNA helicase-mediated packaging of adeno-associated virus type 2 genomes into preformed capsids. *The EMBO journal* 20, 3282-3291 (2001).
161. Bleker, S., Sonntag, F. & Kleinschmidt, J.A. Mutational analysis of narrow pores at the fivefold symmetry axes of adeno-associated virus type 2 capsids reveals a dual role in genome packaging and activation of phospholipase A2 activity. *Journal of virology* 79, 2528-2540 (2005).
162. Becerra, S.P., Koczot, F., Fabisch, P. & Rose, J.A. Synthesis of adeno-associated virus structural proteins requires both alternative mRNA splicing and alternative initiations from a single transcript. *Journal of virology* 62, 2745-2754 (1988).
163. Warrington, K.H., Jr., et al. Adeno-associated virus type 2 VP2 capsid protein is nonessential and can tolerate large peptide insertions at its N terminus. *Journal of virology* 78, 6595-6609 (2004).
164. Koczot, F.J., Carter, B.J., Garon, C.F. & Rose, J.A. Self-complementarity of terminal sequences within plus or minus strands of adenovirus-associated virus DNA. *Proceedings of the National Academy of Sciences of the United States of America* 70, 215-219 (1973).
165. Gottlieb, J. & Muzyczka, N. In vitro excision of adeno-associated virus DNA from recombinant plasmids: isolation of an enzyme fraction from HeLa cells that cleaves DNA at poly(G) sequences. *Molecular and cellular biology* 8, 2513-2522 (1988).
166. Ashktorab, H. & Srivastava, A. Identification of nuclear proteins that specifically interact with adeno-associated virus type 2 inverted terminal repeat hairpin DNA. *Journal of virology* 63, 3034-3039 (1989).
167. Qing, K., et al. Adeno-associated virus type 2-mediated gene transfer: role of cellular FKBP52 protein in transgene expression. *Journal of virology* 75, 8968-8976 (2001).
168. Flotte, T.R., et al. Expression of the cystic fibrosis transmembrane conductance regulator from a novel adeno-associated virus promoter. *The journal of biological chemistry* 268, 3781-3790 (1993).

169. Handa, H. & Carter, B.J. Adeno-associated virus DNA replication complexes in herpes simplex virus or adenovirus-infected cells. *The journal of biological chemistry* 254, 6603-6610 (1979).
170. Schlehofer, J.R., Ehrbar, M. & zur Hausen, H. Vaccinia virus, herpes simplex virus, and carcinogens induce DNA amplification in a human cell line and support replication of a helpervirus dependent parvovirus. *Virology* 152, 110-117 (1986).
171. Thomson, B.J., Weindler, F.W., Gray, D., Schwaab, V. & Heilbronn, R. Human herpesvirus 6 (HHV-6) is a helper virus for adeno-associated virus type 2 (AAV-2) and the AAV-2 rep gene homologue in HHV-6 can mediate AAV-2 DNA replication and regulate gene expression. *Virology* 204, 304-311 (1994).
172. Janik, J.E., Huston, M.M. & Rose, J.A. Locations of adenovirus genes required for the replication of adenovirus-associated virus. *Proceedings of the National Academy of Sciences of the United States of America* 78, 1925-1929 (1981).
173. Weindler, F.W. & Heilbronn, R. A subset of herpes simplex virus replication genes provides helper functions for productive adeno-associated virus replication. *Journal of virology* 65, 2476-2483 (1991).
174. Kotin, R.M., et al. Site-specific integration by adeno-associated virus. *Proceedings of the National Academy of Sciences of the United States of America* 87, 2211-2215 (1990).
175. Yakobson, B., Koch, T. & Winocour, E. Replication of adeno-associated virus in synchronized cells without the addition of a helper virus. *Journal of virology* 61, 972-981 (1987).
176. Yalkinoglu, A.O., Heilbronn, R., Burkle, A., Schlehofer, J.R. & zur Hausen, H. DNA amplification of adeno-associated virus as a response to cellular genotoxic stress. *Cancer research* 48, 3123-3129 (1988).
177. Summerford, C. & Samulski, R.J. Membrane-associated heparan sulfate proteoglycan is a receptor for adeno-associated virus type 2 virions. *Journal of virology* 72, 1438-1445 (1998).
178. Summerford, C., Bartlett, J.S. & Samulski, R.J. AlphaVbeta5 integrin: a co-receptor for adeno-associated virus type 2 infection. *Nature medicine* 5, 78-82 (1999).
179. Qing, K. et al. Human fibroblast growth factor receptor 1 is a co-receptor for infection by adeno-associated virus 2. *Nature medicine* 5, 71-77 (1999).
180. Kashiwakura, Y., et al. Hepatocyte growth factor receptor is a coreceptor for adeno-associated virus type 2 infection. *Journal of virology* 79, 609-614 (2005).

181. Asokan, A., Hamra, J.B., Govindasamy, L., Agbandje-McKenna, M. & Samulski, R.J. Adeno-associated virus type 2 contains an integrin alpha5beta1 binding domain essential for viral cell entry. *Journal of virology* 80, 8961-8969 (2006).
182. Kaludov, N., Brown, K.E., Walters, R.W., Zabner, J. & Chiorini, J.A. Adeno-associated virus serotype 4 (AAV4) and AAV5 both require sialic acid binding for hemagglutination and efficient transduction but differ in sialic acid linkage specificity. *Journal of virology* 75, 6884-6893 (2001).
183. Walters, R.W., et al. Binding of adeno-associated virus type 5 to 2,3-linked sialic acid is required for gene transfer. *The journal of biological chemistry* 276, 20610-20616 (2001).
184. Di Pasquale, G., et al. Identification of PDGFR as a receptor for AAV-5 transduction. *Nature medicine* 9, 1306-1312 (2003).
185. Wu, Z., Miller, E., Agbandje-McKenna, M. & Samulski, R.J. Alpha2,3 and alpha2,6 N-linked sialic acids facilitate efficient binding and transduction by adeno-associated virus types 1 and 6. *Journal of virology* 80, 9093-9103 (2006).
186. Grimm, D., et al. Preclinical in vivo evaluation of pseudotyped adeno-associated virus vectors for liver gene therapy. *Blood* 102, 2412-2419 (2003).
187. Akache, B., et al. The 37/67-kilodalton laminin receptor is a receptor for adeno-associated virus serotypes 8, 2, 3, and 9. *Journal of virology* 80, 9831-9836 (2006).
188. Hansen, J., Qing, K., Kwon, H.J., Mah, C. & Srivastava, A. Impaired intracellular trafficking of adeno-associated virus type 2 vectors limits efficient transduction of murine fibroblasts. *Journal of virology* 74, 992-996 (2000).
189. Duan, D., et al. Dynamin is required for recombinant adeno-associated virus type 2 infection. *Journal of virology* 73, 10371-10376 (1999).
190. Bantel-Schaal, U., Hub, B. & Kartenbeck, J. Endocytosis of adeno-associated virus type 5 leads to accumulation of virus particles in the Golgi compartment. *Journal of virology* 76, 2340-2349 (2002).
191. Sanlioglu, S., et al. Endocytosis and nuclear trafficking of adeno-associated virus type 2 are controlled by rac1 and phosphatidylinositol-3 kinase activation. *Journal of virology* 74, 9184-9196 (2000).
192. Bucci, C, et al. Rab7: a key to lysosome biogenesis. *Mol. Cell. Biol.* 11, 467-480 (2000).
193. Barbero, P., Bittova, L. & Pfeffer, S.R. Visualization of Rab9-mediated vesicle transport from endosomes to the trans-Golgi in living cells. *The journal of cell biology* 156, 511-518 (2002).

194. Wilcke, M., et al. Rab11 regulates the compartmentalization of early endosomes required for efficient transport from early endosomes to the trans-golgi network. *The journal of cell biology* 151, 1207-1220 (2000).
195. Pajusola, K., et al. Cell-type-specific characteristics modulate the transduction efficiency of adeno-associated virus type 2 and restrain infection of endothelial cells. *Journal of virology* 76, 11530-11540 (2002).
196. Girod, A., et al. The VP1 capsid protein of adeno-associated virus type 2 is carrying a phospholipase A2 domain required for virus infectivity. *The journal of general virology* 83, 973-978 (2002).
197. Douar, A.M., Poulard, K., Stockholm, D. & Danos, O. Intracellular trafficking of adeno-associated virus vectors: routing to the late endosomal compartment and proteasome degradation. *Journal of virology* 75, 1824-1833 (2001).
198. Yan, Z., et al. Distinct classes of proteasome-modulating agents cooperatively augment recombinant adeno-associated virus type 2 and type 5-mediated transduction from the apical surfaces of human airway epithelia. *Journal of virology* 78, 2863-2874 (2004).
199. Yan, Z., et al. Ubiquitination of both adeno-associated virus type 2 and 5 capsid proteins affects the transduction efficiency of recombinant vectors. *Journal of virology* 76, 2043-2053 (2002).
200. Seisenberger, G., et al. Real-time single-molecule imaging of the infection pathway of an adeno-associated virus. *Science* 294, 1929-1932 (2001).
201. Xie, Q., et al. The atomic structure of adeno-associated virus (AAV-2), a vector for human gene therapy. *Proceedings of the National Academy of Sciences of the United States of America* 99, 10405-10410 (2002).
202. Padron, E., et al. Structure of adeno-associated virus type 4. *Journal of virology* 79, 5047-5058 (2005).
203. Walters, R.W., et al. Structure of adeno-associated virus serotype 5. *Journal of virology* 78, 3361-3371 (2004).
204. Lane, M.D., et al. Production, purification, crystallization and preliminary X-ray analysis of adeno-associated virus serotype 8. *Acta crystallographica* 61, 558-561 (2005).
205. Xiao, X., Li, J. & Samulski, R.J. Production of high-titer recombinant adeno-associated virus vectors in the absence of helper adenovirus. *Journal of virology* 72, 2224-2232 (1998).
206. Chadeuf, G., et al. Efficient recombinant adeno-associated virus production by a stable rep-cap HeLa cell line correlates with adenovirus-induced amplification of the integrated rep-cap genome. *The journal of gene medicine* 2, 260-268 (2000).



207. Zhang, H.G., et al. Recombinant adenovirus expressing adeno-associated virus cap and rep proteins supports production of high-titer recombinant adeno-associated virus. *Gene therapy* 8, 704-712 (2001).
208. Conway, J.E., et al. High-titer recombinant adeno-associated virus production utilizing a recombinant herpes simplex virus type I vector expressing AAV-2 Rep and Cap. *Gene therapy* 6, 986-993 (1999).
209. Meghrou, J., et al. Production of recombinant adeno-associated viral vectors using a baculovirus/insect cell suspension culture system: from shake flasks to a 20-L bioreactor. *Biotechnol Prog* 21, 154-160 (2005).
210. Kohlbrenner, E., et al. Successful production of pseudotyped rAAV vectors using a modified baculovirus expression system. *Molecular therapy* 12, 1217-1225 (2005).
211. Sun, L., Li, J. & Xiao, X. Overcoming adeno-associated virus vector size limitation through viral DNA heterodimerization. *Nature medicine* 6, 599-602 (2000).
212. Yan, Z., Zak, R., Zhang, Y. & Engelhardt, J.F. Inverted terminal repeat sequences are important for intermolecular recombination and circularization of adeno-associated virus genomes. *Journal of virology* 79, 364-379 (2005).
213. Wang, Z., et al. Rapid and highly efficient transduction by double-stranded adeno-associated virus vectors in vitro and in vivo. *Gene therapy* 10, 2105-2111 (2003).
214. McCarty, D.M., et al. Adeno-associated virus terminal repeat (TR) mutant generates self-complementary vectors to overcome the rate-limiting step to transduction in vivo. *Gene therapy* 10, 2112-2118 (2003).
215. Cordier, L., et al. Muscle-specific promoters may be necessary for adeno-associated virus-mediated gene transfer in the treatment of muscular dystrophies. *Human gene therapy* 12, 205-215 (2001).
216. Costello, E., Saudan, P., Winocour, E., Pizer, L. & Beard, P. High mobility group chromosomal protein 1 binds to the adeno-associated virus replication protein (Rep) and promotes Rep-mediated site-specific cleavage of DNA, ATPase activity and transcriptional repression. *The EMBO journal* 16, 5943-5954 (1997).
217. Song, S., Laipis, P.J., Berns, K.I. & Flotte, T.R. Effect of DNA-dependent protein kinase on the molecular fate of the rAAV2 genome in skeletal muscle. *Proceedings of the National Academy of Sciences of the United States of America* 98, 4084-4088 (2001).
218. Miller, D.G., Petek, L.M. & Russell, D.W. Adeno-associated virus vectors integrate at chromosome breakage sites. *Nature genetics* 36, 767-773 (2004).

219. Nakai, H., et al. Extrachromosomal recombinant adeno-associated virus vector genomes are primarily responsible for stable liver transduction in vivo. *Journal of virology* 75, 6969-6976 (2001).
220. Bell, P., et al. No evidence for tumorigenesis of AAV vectors in a large-scale study in mice. *Molecular therapy* 12, 299-306 (2005).
221. Moskalenko, M., et al. Epitope mapping of human anti-adeno-associated virus type 2 neutralizing antibodies: implications for gene therapy and virus structure. *Journal of virology* 74, 1761-1766 (2000).
222. Huttner, N.A., et al. Genetic modifications of the adeno-associated virus type 2 capsid reduce the affinity and the neutralizing effects of human serum antibodies. *Gene therapy* 10, 2139-2147 (2003).
223. Manno, C.S., et al. Successful transduction of liver in hemophilia by AAV-Factor IX and limitations imposed by the host immune response. *Nature medicine* 12, 342-347 (2006).
224. Vandenberghe, L.H., et al. Heparin binding directs activation of T cells against adeno-associated virus serotype 2 capsid. *Nature medicine* 12, 967-971 (2006).
225. Bantel-Schaal, U. & zur Hausen, H. Characterization of the DNA of a defective human parvovirus isolated from a genital site. *Virology* 134, 52-63 (1984).
226. Erles, K., Sebokova, P. & Schlehofer, J.R. Update on the prevalence of serum antibodies (IgG and IgM) to adeno-associated virus (AAV). *Journal of medical virology* 59, 406-411 (1999).
227. Parks, W.P., Boucher, D.W., Melnick, J.L., Taber, L.H. & Yow, M.D. Seroepidemiological and ecological studies of the adenovirus-associated satellite viruses. *Infect Immun* 2, 716-722 (1970).
228. Gao, G., et al. Clades of Adeno-associated viruses are widely disseminated in human tissues *Journal of virology* 78, 6381-6388 (2004).
229. Rutledge, E.A., Halbert, C.L. & Russell, D.W. Infectious clones and vectors derived from adeno-associated virus (AAV) serotypes other than AAV type 2. *Journal of virology* 72, 309-319 (1998).
230. Gao, G.P., et al. Novel adeno-associated viruses from rhesus monkeys as vectors for human gene therapy. *Proceedings of the National Academy of Sciences of the United States of America* 99, 11854-11859 (2002).
231. Mori, S., Wang, L., Takeuchi, T. & Kanda, T. Two novel adeno-associated viruses from cynomolgus monkey: pseudotyping characterization of capsid protein. *Virology* 330, 375-383 (2004).

232. Bossis, I. & Chiorini, J.A. Cloning of an avian adeno-associated virus (AAAV) and generation of recombinant AAAV particles. *Journal of virology* 77, 6799-6810 (2003).
233. Schmidt, M., Katano, H., Bossis, I. & Chiorini, J.A. Cloning and characterization of a bovine adeno-associated virus. *Journal of virology* 78, 6509-6516 (2004).
234. Davidson, B.L. et al. Recombinant adeno-associated virus type 2, 4, and 5 vectors: transduction of variant cell types and regions in the mammalian central nervous system. *Proceedings of the National Academy of Sciences of the United States of America* 97, 3428-3432 (2000).
235. Mastakov, M.Y., Baer, K., Kotin, R.M. & Durning, M.J. Recombinant adeno-associated virus serotypes 2- and 5-mediated gene transfer in the mammalian brain: quantitative analysis of heparin co-infusion. *Molecular therapy* 5, 371-380 (2002).
236. Kaspar, B.K. et al. Adeno-associated virus effectively mediates conditional gene modification in the brain. *Proceedings of the National Academy of Sciences of the United States of America* 99, 2320-2325 (2002).
237. Halbert, C.L., Allen, J.M. & Miller, A.D. Efficient mouse airway transduction following recombination between AAV vectors carrying parts of a larger gene. *Nature biotechnology* 20, 697-701 (2002).
238. Zabner, J. et al. Adeno-associated virus type 5 (AAV5) but not AAV2 binds to the apical surfaces of airway epithelia and facilitates gene transfer. *Journal of virology* 74, 3852-3858 (2000).
239. Loiler, S.A., et al. Localized gene expression following administration of adeno-associated viral vectors via pancreatic ducts. *Molecular therapy* 12, 519-527 (2005).
240. Wang, A.Y., Peng, P.D., Ehrhardt, A., Storm, T.A. & Kay, M.A. Comparison of adenoviral and adeno-associated viral vectors for pancreatic gene delivery in vivo. *Human gene therapy* 15, 405-413 (2004).
241. Blankinship, M.J. et al. Efficient transduction of skeletal muscle using vectors based on adeno-associated virus serotype 6. *Molecular therapy* 10, 671-678 (2004).
242. Du, L., Kido, M., Lee, D.V., Rabinowitz, J.E., Samulski R.J., Jamieson, S.W., Weitzman M.D. & Thistlethwaite, P.A. Differential myocardial gene delivery by recombinant serotype-specific adeno-associated viral vectors. *Molecular therapy* 10, 604-608 (2004).
243. Work, L.M., et al. Vascular bed-targeted in vivo gene delivery using tropism-modified adeno-associated viruses. *Molecular therapy* 13, 683-693 (2006).

244. Muller, O.J., *et al.* Random peptide libraries displayed on adeno-associated virus to select for targeted gene therapy vectors. *Nature biotechnology* 21, 1040-1046 (2003).
245. Stemmer, W.P. DNA shuffling by random fragmentation and reassembly: in vitro recombination for molecular evolution. *Proceedings of the National Academy of Sciences of the United States of America* 91, 10747-10751 (1994).
246. Wang, C., Oh, M.K. & Liao, J.C. Directed evolution of metabolically engineered *Escherichia coli* for carotenoid production. *Biotechnol Prog* 16, 922-926 (2000).
247. Maheshri, N., Koerber, J.T., Kaspar, B.K. & Schaffer, D.V. Directed evolution of adeno-associated virus yields enhanced gene delivery vectors. *Nature biotechnology* 24, 198-204 (2006).
248. Perabo, L., *et al.* Combinatorial engineering of a gene therapy vector: directed evolution of adeno-associated virus. *The journal of gene medicine* 8, 155-162 (2006).
249. Hauck, B. & Xiao, W. Characterization of tissue tropism determinants of adeno-associated virus type 1. *Journal of virology* 77, 2768-2774 (2003).
250. Opie, S.R., Warrington, K.H., Jr., Agbandje-McKenna, M., Zolotukhin, S. & Muzyczka, N. Identification of amino acid residues in the capsid proteins of adeno-associated virus type 2 that contribute to heparan sulfate proteoglycan binding. *Journal of virology* 77, 6995-7006 (2003).
251. Bowles, D.E., Rabinowitz, J.E. & Samulski, R.J. Marker rescue of adeno-associated virus (AAV) capsid mutants: a novel approach for chimeric AAV production. *Journal of virology* 77, 423-432 (2003).
252. Rabinowitz, J.E., *et al.* Cross-dressing the virion: the transcapsidation of adeno-associated virus serotypes functionally defines subgroups. *Journal of virology* 78, 4421-4432 (2004).
253. Bartlett, J.S., Kleinschmidt, J., Boucher, R.C. & Samulski, R.J. Targeted adeno-associated virus vector transduction of nonpermissive cells mediated by a bispecific F(ab' $\gamma$ )<sub>2</sub> antibody. *Nature biotechnology* 17, 181-186 (1999).
254. Ponnazhagan, S., Mahendra, G., Kumar, S., Thompson, J.A. & Castillas, M., Jr. Conjugate-based targeting of recombinant adeno-associated virus type 2 vectors by using avidin-linked ligands. *Journal of virology* 76, 12900-12907 (2002).
255. Samulski, R.J., Berns, K.I., Tan, M. & Muzyczka, N. Cloning of adeno-associated virus into pBR322: rescue of intact virus from the recombinant plasmid in human cells. *Proceedings of the National Academy of Sciences of the United States of America* 79, 2077-2081 (1982).

256. Kern, A. et al. Identification of a heparin-binding motif on adeno-associated virus type 2 capsids. *Journal of virology* 77, 11072-11081 (2003).
257. White, S.J. et al. Targeted gene delivery to vascular tissue in vivo by tropism-modified adeno-associated virus vectors. *Circulation* 109, 513-519 (2004).
258. Samoylova, T.I. & Smith, B.F. Elucidation of muscle-binding peptides by phage display screening. *Muscle & nerve* 22, 460-466 (1999).
259. Samoylov, A.M., et al. Recognition of cell-specific binding of phage display derived peptides using an acoustic wave sensor. *Biomolecular engineering* 18, 269-272 (2002).
260. Li, J., Samulski, R.J. & Xiao, X. Role for highly regulated rep gene expression in adeno-associated virus vector production. *Journal of virology* 71, 5236-5243 (1997).
261. Jürgen Kopp and Torsten Schwede. The SWISS-MODEL Repository of annotated three-dimensional protein structure homology models. *Nucleic acids research* 32, D230-D234 (2004).
262. Schwede T, Kopp J, Guex N, and Peitsch MC. SWISS-MODEL: an automated protein homology-modeling server. *Nucleic acids research* 31, 3381-3385 (2003).
263. Guex, N. and Peitsch, M. C. SWISS-MODEL and the Swiss-PdbViewer: An environment for comparative protein modelling. *Electrophoresis* 18, 2714-2723 (1997).
264. Peitsch, M. C. Protein modeling by E-mail. *Biotechnology* 13, 658-660 (1995).
265. Muller, O.J., et al. Improved cardiac gene transfer by transcriptional and transductional targeting of adeno-associated viral vectors. *Cardiovascular research* 70, 70-78 (2006).
266. Shi, W., Arnold, G.S. & Bartlett, J.S. Insertional mutagenesis of the adeno-associated virus type 2 (AAV2) capsid gene and generation of AAV2 vectors targeted to alternative cell-surface receptors. *Human gene therapy* 12, 1697-1711 (2001).
267. Shi, W. & Bartlett, J.S. RGD inclusion in VP3 provides adeno-associated virus type 2 (AAV2)-based vectors with a heparan sulfate-independent cell entry mechanism. *Molecular therapy* 7, 515-525 (2003).
268. Wu, P., et al. Mutational analysis of the adeno-associated virus type 2 (AAV2) capsid gene and construction of AAV2 vectors with altered tropism. *Journal of virology* 74, 8635-8647 (2000).
269. Rabinowitz, J.E. & Samulski, R.J. Building a better vector: the manipulation of AAV virions. *Virology* 278, 301-308 (2000).

270. Margalit, H., Fischer, N. & Ben-Sasson, S.A. Comparative analysis of structurally defined heparin binding sequences reveals a distinct spatial distribution of basic residues. *The journal of biological chemistry* 268, 19228-19231 (1993).
271. Herzog, R.W., et al. Long-term correction of canine hemophilia B by gene transfer of blood coagulation factor IX mediated by adeno-associated viral vector. *Nature medicine* 5, 56-63 (1999).
272. Herzog, R.W., et al. Stable gene transfer and expression of human blood coagulation factor IX after intramuscular injection of recombinant adeno-associated virus. *Proceedings of the National Academy of Sciences of the United States of America* 94, 5804-5809 (1997).
273. Barry, M.A., Dower, W.J. & Johnston, S.A. Toward cell-targeting gene therapy vectors: selection of cell-binding peptides from random peptide-presenting phage libraries. *Nature medicine* 2, 299-305 (1996).
274. Fisher, K.J., et al. Transduction with recombinant adeno-associated virus for gene therapy is limited by leading-strand synthesis. *Journal of virology* 70, 520-532 (1996).
275. Koeberl, D.D., Alexander, I.E., Halbert, C.L., Russell, D.W. & Miller, A.D. Persistent expression of human clotting factor IX from mouse liver after intravenous injection of adeno-associated virus vectors. *Proceedings of the National Academy of Sciences of the United States of America* 94, 1426-1431 (1997).
276. Nathwani, A.C., et al. Factors influencing in vivo transduction by recombinant adeno-associated viral vectors expressing the human factor IX cDNA. *Blood* 97, 1258-1265 (2001).
277. Chirmule, N., et al. Humoral immunity to adeno-associated virus type 2 vectors following administration to murine and nonhuman primate muscle. *Journal of virology* 74, 2420-2425 (2000).
278. Hernandez, Y.J., et al. Latent adeno-associated virus infection elicits humoral but not cell-mediated immune responses in a nonhuman primate model. *Journal of virology* 73, 8549-8558 (1999).
279. Sanftner, L.M., et al. Striatal delivery of rAAV-hAADC to rats with preexisting immunity to AAV. *Molecular therapy* 9, 403-409 (2004).
280. Sally E. Grimes. A basic laboratory manual for the small-scale production and testing of I-2 newcastle disease vaccine. RAP publication (2002).
281. Scallan, C.D., et al. Human immunoglobulin inhibits liver transduction by AAV vectors at low AAV2 neutralizing titers in SCID mice. *Blood* 107, 1810-1817 (2006).

282. Chapman, M.S. & Rossmann, M.G. Structure, sequence, and function correlations among parvoviruses. *Virology* 194, 491-508 (1993).
283. Rabinowitz, J.E., Xiao, W. & Samulski, R.J. Insertional mutagenesis of AAV2 capsid and the production of recombinant virus. *Virology* 265, 274-285 (1999).
284. Yang, Q., et al. Development of novel cell surface CD34-targeted recombinant adeno-associated virus vectors for gene therapy. *Human gene therapy* 9, 1929-1937 (1998).
285. Douar, A.M., Poulard, K. & Danos, O. Deleterious effect of peptide insertions in a permissive site of the AAV2 capsid. *Virology* 309, 203-208 (2003).
286. Grifman, M. et al. Incorporation of tumor-targeting peptides into recombinant adeno-associated virus capsids. *Molecular therapy* 3, 964-975 (2001).
287. Manning, W.C., Zhou, S., Bland, M.P., Escobedo, J.A. & Dwarki, V. Transient immunosuppression allows transgene expression following readministration of adeno-associated viral vectors. *Human gene therapy* 9, 477-485 (1998).
288. Halbert, C.L., Standaert, T.A., Wilson, C.B. & Miller, A.D. Successful readministration of adeno-associated virus vectors to the mouse lung requires transient immunosuppression during the initial exposure. *Journal of virology* 72, 9795-9805 (1998).
289. McCullough, K.C., et al. Immune protection against foot-and-mouth disease virus studied using virus-neutralizing and non-neutralizing concentrations of monoclonal antibodies. *Immunology* 58, 421-428 (1986).
290. Crowe, J.E., Jr., et al. Genetic and structural determinants of virus neutralizing antibodies. *Immunologic research* 23, 135-145 (2001).
291. Kodaira, Y., Nair, S.K., Wrenshall, L.E., Gilboa, E. & Platt, J.L. Phenotypic and functional maturation of dendritic cells mediated by heparan sulfate. *J Immunol* 165, 1599-1604 (2000).
292. Shikano, S., Bonkobara, M., Zukas, P.K. & Ariizumi, K. Molecular cloning of a dendritic cell-associated transmembrane protein, DC-HIL, that promotes RGD-dependent adhesion of endothelial cells through recognition of heparan sulfate proteoglycans. *The journal of biological chemistry* 276, 8125-8134 (2001).
293. Lochrie, M.A., et al. Mutations on the external surfaces of adeno-associated virus type 2 capsids that affect transduction and neutralization. *Journal of virology* 80, 821-834 (2006).
294. Liu, J. & Thorp, S.C. Cell surface heparan sulfate and its roles in assisting viral infections. *Medicinal research reviews* 22, 1-25 (2002).

295. Perabo, L., et al. In vitro selection of viral vectors with modified tropism: the adeno-associated virus display. *Molecular therapy* 8, 151-157 (2003).
296. Work, L.M., et al. Development of efficient viral vectors selective for vascular smooth muscle cells. *Molecular therapy* 9, 198-208 (2004).
297. Pruchnic, R., et al. The use of adeno-associated virus to circumvent the maturation-dependent viral transduction of muscle fibers. *Human gene therapy* 11, 521-536 (2000).
298. Arikawa-Hirasawa, E., Watanabe, H., Takami, H., Hassell, J.R. & Yamada, Y. Perlecan is essential for cartilage and cephalic development. *Nature genetics* 23, 354-358 (1999).
299. Kainulainen, V., Wang, H., Schick, C. & Bernfield, M. Syndecans, heparan sulfate proteoglycans, maintain the proteolytic balance of acute wound fluids. *The journal of biological chemistry* 273, 11563-11569 (1998).
300. Huntington, J.A., Olson, S.T., Fan, B. & Gettins, P.G. Mechanism of heparin activation of antithrombin. Evidence for reactive center loop preinsertion with expulsion upon heparin binding. *Biochemistry* 35, 8495-8503 (1996).
301. Mulloy, B. & Linhardt, R.J. Order out of complexity--protein structures that interact with heparin. *Current opinion in structural biology* 11, 623-628 (2001).
302. Perabo, L., et al. Heparan sulfate proteoglycan binding properties of adeno-associated virus retargeting mutants and consequences for their in vivo tropism. *Journal of virology* 80, 7265-7269 (2006).
303. Miller, D.G., Adam, M.A. & Miller, A.D. Gene transfer by retrovirus vectors occurs only in cells that are actively replicating at the time of infection. *Molecular and cellular biology* 10, 4239-4242 (1990).
304. Van Deutekom, J.C., Hoffman, E.P. & Huard, J. Muscle maturation: implications for gene therapy. *Molecular medicine today* 4, 214-220 (1998).
305. Van Deutekom, J.C., et al. Implications of maturation for viral gene delivery to skeletal muscle. *Neuromuscul Disord* 8, 135-148 (1998).
306. Acsadi, G., et al. A differential efficiency of adenovirus-mediated in vivo gene transfer into skeletal muscle cells of different maturity. *Human molecular genetics* 3, 579-584 (1994).
307. Kay, M.A., et al. Evidence for gene transfer and expression of factor IX in haemophilia B patients treated with an AAV vector. *Nature genetics* 24, 257-261 (2000).
308. Snyder, R.O., et al. Correction of hemophilia B in canine and murine models using recombinant adeno-associated viral vectors. *Nature medicine* 5, 64-70 (1999).



309. Dai, Y., Roman, M., Naviaux, R.K. & Verma, I.M. Gene therapy via primary myoblasts: long-term expression of factor IX protein following transplantation in vivo. *Proceedings of the National Academy of Sciences of the United States of America* 89, 10892-10895 (1992).
310. Arruda, V.R., et al. Posttranslational modifications of recombinant myotube-synthesized human factor IX. *Blood* 97, 130-138 (2001).
311. Kessler, P.D., et al. Gene delivery to skeletal muscle results in sustained expression and systemic delivery of a therapeutic protein. *Proceedings of the National Academy of Sciences of the United States of America* 93, 14082-14087 (1996).
312. Fisher, K.J., et al. Recombinant adeno-associated virus for muscle-directed gene therapy. *Nature medicine* 3, 306-312 (1997).
313. Greelish, J.P. et al. Stable restoration of the sarcoglycan complex in dystrophic muscle perfused with histamine and a recombinant adeno-associated viral vector. *Nature medicine* 5, 439-443 (1999).
314. Huard, J. et al. The route of administration is a major determinant of the transduction efficiency of rat tissues by adenoviral recombinants. *Gene therapy* 2, 107-115 (1995).
315. Zhang, G., Budker, V., Williams, P., Hanson, K. & Wolff, J.A. Surgical procedures for intravascular delivery of plasmid DNA to organs. *Methods in enzymology* 346, 125-133 (2002).
316. Banai, S. et al. Angiogenic-induced enhancement of collateral blood flow to ischemic myocardium by vascular endothelial growth factor in dogs. *Circulation* 89, 2183-2189 (1994).
317. Villanueva, F. S. et al. Microbubbles targeted to intercellular adhesion molecule-1 bind to activated coronary artery endothelial cells. *Circulation* 98, 1-5 (1998).
318. Pang, S. et al. Identification of a positive regulatory element responsible for tissue-specific expression of prostate-specific antigen. *Cancer research* 57, 495-499 (1997).
319. Shibata, T. et al. development of a hypoxia-responsive vector for tumor-specific gene therapy. *Gene therapy* 7, 493-498 (2000).
320. Shinoura, N. et al. Highly augmented cytopathic effect of a fiber mutant E1B-defective adenovirus of gene therapy of gliomas. *Cancer research* 59, 3411-3416 (1999).
321. Nicklin, S.A. et al. Efficient and selective AAV2-mediated gene transfer directed to human vascular endothelial cells. *Molecular therapy* 4, 174-181 (2001).

322. Wistuba, A., Weger, S., Kern, A. & Kleinschmidt, J.A. Intermediates of adeno-associated virus type 2 assembly: identification of soluble complexes containing Rep and Cap proteins. *Journal of virology* 69, 5311-5319 (1995).
323. Grimm, D., et al. Titration of AAV-2 particles via a novel capsid ELISA: packaging of genomes can limit production of recombinant AAV-2. *Gene therapy* 6, 1322-1330 (1999).